Synthesis and Characterization of Benzo-2,1,3-thiadiazole Derivatives and their Metal Complexes

SATURDAY AMEDU OKEH

NCE, 91

B.Sc (ed) Chemistry, Edo State University, Nigeria, 97

A Thesis

Submitted to the School of Graduate Studies

of the University of Lethbridge

In Partial Fulfillment of the

Requirements for the Degree

MASTER OF SCIENCE

Chemistry and Biochemistry

University of Lethbridge

LETHBRIDGE, ALBERTA, CANADA

For all those who love the truth in Christ Jesus and to my wife (Mercy) and my children

(Emmanuel and Esther Okeh)

Abstract

This thesis describes the synthesis and characterization of some 2,1,3-benzothiadiazole derivatives, specifically 2,1,3-benzothiadiazole-4,7-dicarbonitrile (DCBTD) and diethyl 2,1,3-benzothiadiazole-4,7-dicarboxylate (DEBTD). The crystal structures have been determined; also both compounds exhibit two sequential one-electron reductions in square-wave and cyclic voltammetry. Stable radical anions are detected by EPR spectroscopy. In the solid-state, DEBTD displays endo/endo, exo/exo and endo/exo conformational isomerism. Silver(I) complexes of DCBTD and DEBTD have been prepared with a number of anions (BF_4, ClO_4^-, PF_6^-, and SbF_6^-) and their crystal structures are determined. All these complexes exist as coordination polymers, some of which are dry and others are solvates (benzene, water). DCBTD is found to coordinate through one or more nitrile and one or more ring N atoms. DEBTD exclusively forms bis chelate complexes using ring N and ester carbonyl O donors. Evidence from electrochemistry and ESI mass spectrometry indicates that these polymers break down on dissolving in CH_3CN. Conversion of DEBTD into 2,1,3-benzothiadiazole-4,7-dicarboxylic acid, 2,3-diaminobenzene-1,4-dicarboxylic acid and salts thereof has been substantiated by crystal structure determinations.

ACKNOWLEDGEMENTS

Words are not actually enough to express my sincere gratitude to my supervisor Prof. René T. Boeré, for all his support, patience, motivation and guidance throughout my M.Sc studies and the period of this thesis writing. The only possible thing I can say is thanks and God will forever bless you and your family.

I would like to extend my appreciation to my committee members without whom this work could have been what it is, Associate Prof. Paul Hayes, Associate Prof. Michael Gerken, their positive critiques were geared towards achieving this goal. I would also thank Associate Prof. Peter Dibble for all your assistance and advice throughout this period.

My sincere thanks to Dr. Tracey L. Roemmelle, Kris Fisher, Tony Montina, for their time and assistance. Kevin Johnson is thanked for the elemental analysis.

To Susan Hill (Secretary to the Dept.), thank you for your assistance and advice especially during the period of my ill health. To all members of the Dibble and Boeré's lab, I thank you all for the assistance and as friends.

I would also like to thank Pastor Kohl and the Faith Baptist Church, Lethbridge for all their payers and material support throughout this period of my studies.

Time and space will not permit me to mention all the wonderful people in Chemistry and Biochemistry Dept. U of L, my heartfelt desire and prayers for all, is that God in His mercy will save all and be made ready for the coming of our LORD and SAVIOR JESUS CHRIST. Thank you ALL.

Table of Contents

List of Tables

List of Figures

List of Schemes

List of Abbreviations

BBT	Benzobis(thiadiazole)
BTD	Benzothiadiazole
BTDN	Benzothiadiazole di-nitrile
CV	Cyclic voltammetry
DCBTD	Dinitrile-2,1,3-Benzothiadiazole
DEBTD	Diethyl-2,1,3-Benzothiadiazole -4,7-dicarboxylate
DFT	Density functional theory
EA	Elemental analysis
EPR	Electron paramagnetic resonance
ESI-MS	Electrospray ionization mass spectrometry
FT-IR	Fourier transform infrared
GC	Gas chromatography
HF	Hartee-Fock
HOMO	Highest occupied molecular orbital
HPLC	High performance liquid chromatography
LUMO	Lowest occupied molecular orbital
MOF	Metal organic frameworks
MS	Mass spectrometry
NBI	Non covalent bond interaction
OOP	Out of plane
RF	Radio frequency
SBI	Secondary bond interaction
SPS	Solvent purification system
SEEPR	Simultaneous electrochemical electron paramagnetic resonance

SWV	Square wave voltammetry
TCNQ	Tetracyanoquinodimethane
TLC	Thin layer chromatography

CHAPTER ONE: INTRODUCTION

1.1 Introduction

1.1.1 What are chalcogens?

Chalcogens are chemical elements of group sixteen in the periodic table with the s^2p^4 electron configuration. These elements are nonmetals for oxygen and sulfur, selenium and tellurium are metalloids, and the radioactive polonium is a metal.[1] The name of the group was proposed by Wilhelm Blitz and colleague Werner Fischer of the Institute of Inorganic Chemistry at the University of Hannover, Germany in 1932.[2] There are fundamental similarities in the characteristic properties of these elements, but they vary significantly as the atomic number, covalent and ionic radii increase.[3] The difference in oxidation states can be explained by the electronic structure of the elements. Oxygen is able to use only *s* and *p* orbitals for bonding. Other larger members of the series like S and Se can use *s*, *p* and *d* orbitals in their hybridization, this is shown in compounds and complex ions such as: SF_6, SOF_4, SF_4 , SeO_4^{2-}, TeF_8^{2-}.[4] Compounds of group 16 elements are most often defined with electron affinity (O = 1.46, S = 2.07 Se = 2.02 and Te = 1.97) eV and the electronegativity which decreases down the group (O = 3.50, S = 2.50, Se = 2.40 and Te = 2.10).[1]

1.1.2 What are Heterocycles?

Heterocyclic compounds, also known as heterocycles, are compounds with at least one ring structure and a non-carbon atom.[5] The first series of heterocyclic compounds are three member ring heterocycles containing single atoms of either, N (aziridine) in Figure 1.1(a), O (oxiridine) or S (thiirane). The four member ring is observed in heterocyclic

compounds used as antibiotics like penicillin and cephalosporins. Common examples are azetidine and dithiete in Figure 1.1(b). Thietanes are used in the production of polymers, inhibit corrosion of iron, and are also used as fungicides and bactericides. The five membered ring family represents an important segment of the heterocycles consisting of indoles, proline and hydroxyproline, which is a major constituent of collagen. The heme group related to myoglobin, hemoglobin and chlorophylls are all formed from the pyrrole units of porphyrin. Thiophene and furan in Figure 1.1(c) are examples of five membered heterocycles containing sulfur and oxygen respectively.[6] As the ring size increases, the number of derivatives increases because of the possibility of varying the location of the heteroatoms in the molecular structures. This research will make most use of the five-membered ring fused to a benzene ring.

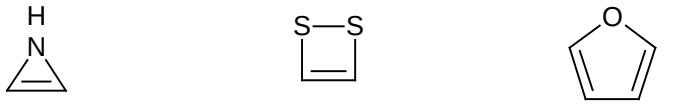

1*H*-azirene (a) 1,2-dithiete (b) furan (c)

Figure 1.1 Common examples of heterocycles

1.1.3 What are chalcogenadiazoles?

Azole is a five member ring heterocyclic compound containing at least one nitrogen atom, such as pyrazole and imidazole, a compound containing two nitrogen atoms is called diazole. Addition of a chalcogen in place of one carbon in a diazole ring results in a chalcogenadiazole. Chalcogenadiazole heterocycles containing 2N and S which are fused to a benzene ring are known as benzothiadiazoles. This thesis intends to study the chemistry of benzochalcogenadiazole derivatives, particularly those of S and, if possible,

any of Se or Te may also be included. The physical and chemical properties of these compounds are quite distinct from those of their all-carbon ring analogues. An example of such structure is shown in Figure 1.2.

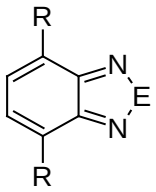

Where E = S, Se or Te

R = H, CN, $COOC_2H_5$ or COOH

Figure 1.2 Different derivatives of benzofused chalcogenadiazole rings

1.1.4 Why are they important?

The chemistry of any of S, Se or Te with nitrogen in heterocyclic compounds has been exploited greatly because of their unique conducting and superconducting properties.[7] Their availability, electrochemical reversibility and inter-convertible redox states played a significant role in their chemistry. Due to their importance,[8] more attention was given to their laboratory chemical synthesis.[9] The geometry and general characteristic properties of chalcogenadiazoles are also very interesting in the world of chemistry. Chemical bonds between sulfur and nitrogen are intriguing, as exemplified by the hypervalency in sulfuranes[10,11] or the superconducting behavior in $(SN)_x$. Both =N-S-N= and -N=S=N- linkages are fractions of $(SN)_x$, and the latter contains tetravalent sulfur. Due to this type of resonance, 1,2,5-thiadiazole, the five-membered heterocyclic ring containing the =N-S-N= linkage, exhibits aromatic character with six π–electrons. The aromaticity of naphtho[1,8-cd4,5-c'd']bis[1,2,6]thiadiazine containing =N-S-N= moieties in six-membered rings has been well examined by Haddon *et al*..[12] Another interesting feature of the =N-S-N= linkage is the close intermolecular S···N contacts in their crystal

structures, which have been observed for a wide variety of compounds. The substitution of Se for S strengthens these intermolecular contacts.[13] In this connection, fused thiadiazole and selenadiazole rings are of interest, because stronger intermolecular interactions are expected by larger polarization of =N-S-N= and =N-Se-N= linkages,[14] due to the delocalization of negative charge to the substituent groups and electrostatic interaction between the substituent groups and a chalcogen atom.[15] These contacts may be due to intermolecular electrostatic interaction between -N--S^{+}=N- dipoles.[16]

1.2 Benzochalcogenadiazole and its derivatives in metal coordination chemistry

With our interest in making metal organic frameworks with our ligands, we will need to examine the uses, synthesis and relevance of chalcogen heterocyclic compounds in coordination chemistry. Then we need to examine the coordinating behavior of metals with our substituent groups and that of our ligands, which we will tend to extend into making metal organic frameworks (MOF)s.[17a,17b,17c,] Benzothiadiazoles are known to participate in coordination chemistry with the nitrogen atom as the electron donating species in the ring. A simple search in the literature of crystal engineering reveals that 2,1,3-benzochalcogenadiazoles are promising but underutilized ligands in coordination chemistry, carrying two heterocyclic nitrogen atoms, separated by the chalcogen heteroatom. Munakata *et al.* reported in 1994 that thiadiazoles are readily available ligands with a potential of complex formation. By using them as structural interconnecting N-coordination ligands, they can be used for developing unusual metal complex architectures that can bring together Cu and Ag atoms to form two dimensional frameworks.[18] Zhou *et al.* went further in 2005 by exploring the complex formation of selenadiazoles with Ag cations.[19] The N atoms are potentially capable of bridging metal

ions and the presence of the chalcogen atom between the nitrogens offers the benzochalcogenadiazole ligand the possibility to assemble through exotic N·····chalcogen interactions. The benzofused thiadiazole molecule, which contains an aromatic ring, also offers the possibility of forming π·····π stacking interactions,[20] therefore chalcogenadiazoles are good candidates in coordination chemistry. Most recently, Mukherjee *et al.* have reported a series of metal complexes, including Ag(I), of which the ligands coordinate through both a thiadiazole ring N atom and the N atom from the fused pyridine as shown in Figure 1.3, with relatively short Ag•••Ag contacts of 2.931(1) Å.[21]

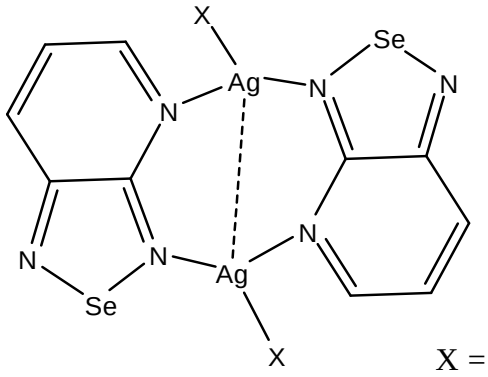

X = CF_3COO^-, NO_3^-

Figure 1.3 Ag(1) complex of chalcogenadiazole [21]

1.2.1 4,7-dinitrile-2,1,3-benzothiadiazole (DCBTD) and metal coordination

The dinitrile substituent (C≡N) in coordination chemistry had been studied extensively. Leznoff *et al.* demonstrated that cyanide anions play a prominent role in the design of supramolecular coordination polymers,[22] since they readily form strong bonds with transition metal cations. When two cyanides are bound in a linear metal complex such as with Au(I), the complex can act as if it were an organic nitrile by further bonding through nitrogen lone pairs. Venkataraman and co-workers reported the hydrated structure of 1,4-

dicyanobenzene with Ag^+ in complex formation, where two semi-linear complexes are linked together through two water molecules in the crystal lattice.[23]

It is interesting to know that DCBTD (Fig. 1.4a) complexes have not been reported in the literature. For benzonitriles, X-ray structures of only six di- and about two hundred mononitrile substituted derivatives with Ag^+ complexes are known.[24,25] This thesis reports five new DCBTD silver complexes. The two nitrile groups on the benzothiadiazole ring contribute to the coordinating properties by serving as pendent electron donors in the ligand, creating more points of coordination, with stronger and more versatile coordination to the metal.

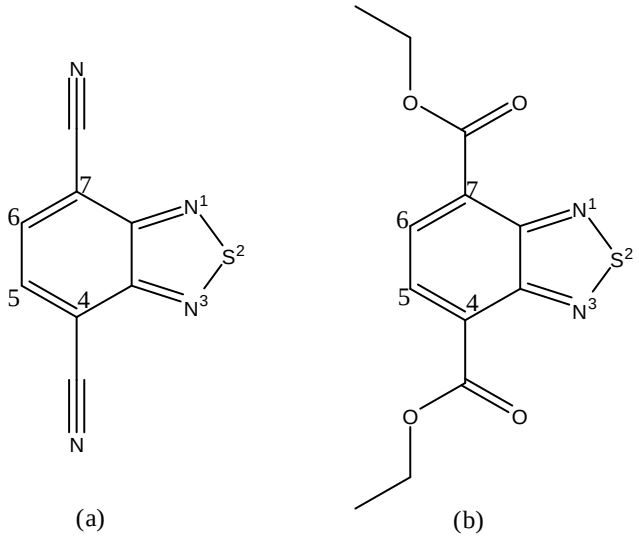

(a) (b)

Figure 1.4 Structure of (a) DCBTD and (b) DEBTD

1.2.2 Diethyl-2,1,3-benzothiadiazole-4,7-dicarboxylate (DEBTD) and 2,1,3-benzothiadiazole-4,7-dicarboxylic acid in metal coordination chemistry

It is well known that carboxylates rapidly coordinate to metal ions, especially to silver ions to form polymeric structures.[26] Several groups have used different synthetic methods to arrive at their desired complexes. Mak and co-workers have generated polymeric

structures in silver(I) carboxylate complexes by various Zwitterionic betaine-type ligands.[27,28] Michaelides and co-workers have reported a novel succinate disilver(I) complex synthesized by gel permeation.[29] Smith and co-workers have obtained a series of silver polycarboxylate complexes by using ammonia to enhance the solubility of the carboxylate.[30] There are many other metal complexes that have been reported in the literature but nowhere in the literature has a complex of DEBTD (Fig. 1.4b) been reported, or that of its di-acid analog. Christian and co-workers reported copper(II) complexes with different aromatic polycarboxylato spacers such as 1,3,5-benzenetricarboxylic acid, 2,5-dihydroxy-terephthalic acid and 5-hydroxy-isophthalic acid.[31] We observed that in complex formation of benzoic acid, the two oxygen atoms are the electron donating species in the ligand, but our di-acid ligand has the extra nitrogen atoms of the thiadiazole ring as electron donating groups for coordination. For benzene carboxylic acid esters, only very few complexes are reported; in those instances it is only the carbonyl oxygens that are used for coordination to the metals and not the oxygen attached to the alkyl group. Whitcomb et al., obtained a structure with a short Ag•••Ag distance of 2.7529(16) Å.[32,33] We now report five DEBTD silver complexes, with the carboxylate enhancing chelate complex formation with one of the nitrogen atoms in the thiadiazole ring.

1.3 Background on Synthetic Methods

4,7-Dibromo-2,1,3-benzothiadiazole is the most commonly used intermediate for the synthesis of most benzothiadiazole derivatives that possess donor character. Since one of the main objectives is to identify a versatile heteroaromatic unit which is electron-accepting, it can be modified with any substituent or copolymerized with any other group

to obtain the appropriate choice of derivative.[34,35,36] The BTD was treated with molecular bromine (Br_2) in hydrobromic acid by drop-wise addition, followed by reflux, which gave the exact result according to the regioselectivity and mechanism as proposed and explained by K. Pilgram, M. Zupan and R. Skiles in 1970.[37] The synthesis of BTD and 4,7-dibromo BTD are both obtained in appreciable yields of 82 and 96 %, respectively.

1.4 Structural and electrical properties of chalcogenadiazoles

The secondary bonding interaction (SBI) exhibited by these compounds have attracted much attention.[22,38,39,40] The behavior of weak interactions among molecules due to well-known hydrogen bonding, van der Waals forces and π-π interactions form the basis of highly specific recognition in the reaction and transport processes in chalcogenadiazoles. A number of techniques have been employed to study the electronic properties of benzochalcogenadiazoles, such as density functional theory (DFT), Hartee-Fock (HF) etc. to analyze SBI and discuss the inter-atomic chalcogen···nitrogen bond distances and the donor acceptor character that is relevant to the Coulombic contribution. The increase in binding energy down the series of chalcogen–nitrogen can be rationalized as a consequence of both the concept in the energies of the chalcogen(E)–nitrogen(N) orbitals as the intramolecular bond weakens and the increasing differences in electronegativity between E and N which attributes larger partial charges to the chalcogen and nitrogen atoms. As the chalcogen becomes heavier, π electrons become less delocalized into the ring. It is known that the E–N bond is covalent, but it is increasingly polarized from S to Te, which accompanies an increase in the C–N bond order and influences nitrogen contribution to the π interaction in the system.[41,42,] The region of space opposite E–N

bonds are depleted of electron density which confers the positive charge to the chalcogen atom.

Charlotte Mallet *et al*. studied the electronic properties of chalcogenadiazoles through D–A–D triads based on 3–alkoxy-4-cyanothiophene and benzothienothiophenes.[43] Appropriate modifications of their π conjugated systems allow for control of the HOMO and LUMO energy levels. Thamos Anu and co-workers observed that benzothiadiazole (BTD) and benzobis(thiadiazole) (BBT), which differs from BTD by an extra thiadiazole ring, exhibit good semiconducting properties, such as high electron mobility and low LUMO energy level.[44] Calculations at the B3LYP/cc-pVTZ level revealed that all the BTD molecules have lower lying LUMO energies (3.70 – 4.11 eV) compared to the BTD derivatives (2.56 – 3.41 eV) with similar substitution.[45] This led to the conclusion that the difference in behavior was due to inherited biradicaloid character from the parent molecule. Also the bond energy of BTD had been studied using different methodologies like calorimetric combustion, calorimetric sublimation and differential thermal analysis.[46] A pair of 1,2,5-chalcogenadiazole molecules is often associated with two X···N (X = S, Se, Te) contacts in the crystals. The average S···N, Se···N, and Te···N distances in the crystals (3.20, 2.95, and 2.77 Å, respectively) are shorter than the corresponding sums of the van der Waals' radii (3.26, 3.36, and 3.54 Å, respectively).[47] The average Te···N distance is especially short. The short contact suggests that a strong attraction exists between the chalcogen and nitrogen atoms.

Suzuki *et al.* reported that there exist attractive electrostatic interactions between selenium and nitrogen atoms from atomic charge distributions of a 1,2,5-selenadiazole derivative based on HF/STO-3G level ab initio calculation.[48] Cozzolino *et al.* reported

recently that the orbital mixing (charge-transfer interaction) was mainly responsible for the attraction between the chalcogen and nitrogen atoms.[49] This characteristic property of chalcogenadiazole derivatives allows them to be building blocks in supramolecular design due to their propensity to associate through SBIs as shown in Figure 1.5.

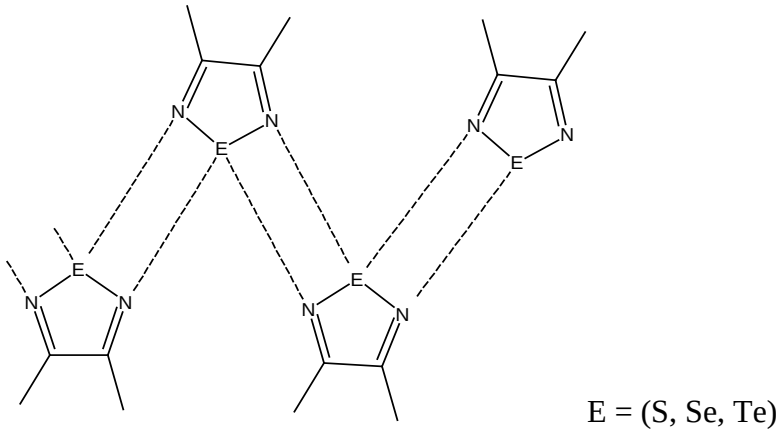

Figure 1.5 Showing SBI between the chalcogenadiazole molecules

The composition and characteristic properties of chalcogens is essentially identical, the energies and the order of the inner orbitals show small variations between functional (O, S, Se and Te),[50] which accounts for the various electronic structures of benzochalcogenadiazoles. Interaction energy curves show the attractive electrostatic intermolecular interaction energies for 1,2,5-chalcogenadiazole dimers. The HF and MP2 level interaction energy curves calculated for the 1,2,5-chalcogenadiazole dimers using the cc-pVTZ basis set shows the depth of the HF level interaction increases in the order of S < Se < Te.[51] The MP2 level interaction energy curves have deeper minima in comparison with the corresponding HF level interaction energy curves. The magnitude of electron correlation contributions increases in the order of S < Se < Te. The molecular polarizabilities calculated for the SH_2, SeH_2, and TeH_2 at the HF/aug-cc-pV5Z level are 24, 30, and 40 au respectively, which shows that tellurium has large atomic polarizability

in comparison with sulfur and selenium. The large atomic polarizability of tellurium is one of the causes of the large dispersion interaction in the 1,2,5-telluradiazole dimer.[52] This influences their reactivity,[53] solubility, melting[54] and boiling points of the chalcogen compounds.

1.5 Electrochemistry of chalcogenadiazoles and their derivatives

Most polymers containing benzochalcogenadiazole in the reported literature have an optical absorption profile consisting of both a low and high-energy optical transition. Moving from S to Se to Te leads to a red shift and decreasing intensity in the low energy transition,[55] while the high-energy band remains relatively constant. A series of optical spectroscopy experiments, solvatochromism studies, and density functional theory (DFT) calculations reveals the red shift in the low-energy absorption is due to both a decrease in ionization potential of the heavy chalcogen and a loss of acceptor aromaticity. The loss of intensity of the low energy band is likely the result of a decrease in chalcogen electronegativity and the resulting acceptor unit's ability to separate charge.[56,43]

Boeré and Roemmele have explained that S, N compounds are electron rich, but they are also good electron acceptors, the same behavior is reported for 2,1,3-thiadiazole as in the figure below.[39]

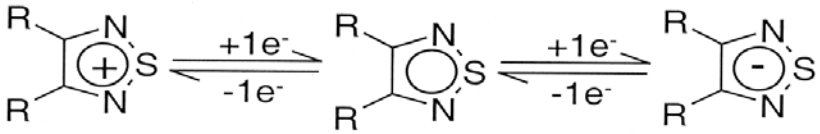

Scheme 1.1 Redox scheme for 2,1,3-thiadiazole showing one electron reduction and oxidation.[39]

1.6 Metal Organic Frameworks (MOFs)

Metal organic frameworks (MOFs) are made by linking of two component parts, the inorganic and the organic units by strong bonds, through a coordination network of repeating units, which Yaghi *et al.* referred to as reticular synthesis.[57a,57b] The high rate with which MOFs had been made in the last decade is due to its demand in material science and the flexibility to which the constituents' geometry, size and functionality can be varied. MOFs are a subset of coordination polymers, we could not classify the compounds made in this work as MOFs,[58] but they are coordination polymers.

1.6.1 Synthesis of MOFs,

This class of hybrid porous solid material was introduced by Kitagawa and co-workers,[59] and has no specific route of synthesis. According to Osama Shekhah and co-worker, 'it was possible to demonstrate that the formation of a highly ordered MOF occurs first via an assembly of the primary building blocks to defined secondary building blocks and then to the MOF crystallite'.[60] Some MOFs with stable structures have been synthesized by hydro or solvothermal crystallization at very high temperatures using conventional electrical heating.[61] With the view of obtaining desired MOFs with lower temperature and a shorter time, several effective alternative methods have been sought for the synthesis of MOFs and a few new techniques have been explored. For instance, ultrasound has been used to synthesize copper complexes of 1,3,5-benzenetricarboxylate and 1,4-benzenedicarboxylates.[62,63,64] Microwaves have been used, preferred to ultrasound for the synthesis of MOFs, because the product obtained have the advantages of fast crystallization, phase selectivity and diverse morphology or size.[65,66] Electrochemical routes have also been applied to synthesize MOFs.[67] Ionothermal synthesis was applied successfully by Parnham and Morris, through which they

discovered several new phases through this approach.[68] The use of immiscible solvents for biphasic synthesis was introduced by Cheetham and co-worker, which lead to the production of single crystals of the desired phase.[69] To evaluate rapidly the effect of reaction conditions and to search for optimal conditions for a phase that is hard to synthesize, Stock and co-workers used what is called the high-throughput synthesis in the crystallization of MOFs.[70] As synthetic chemists are still sorting which method works best, which should be based on the reaction conditions of the desired MOFs, Enamul Haque and co-workers used a combination of ultrasound and microwave to obtain iron an terephthalate, known as MIL-53(Fe), an MOF material synthesized at relatively low temperature.[61]

1.6.2 Characteristics and Applications of MOFs

MOFs are crystalline materials with exceptional porosity,[18c] high thermal and chemically stability, that often accommodate solvents as guest molecule during their synthesis. These guest molecules can be eliminated so the internal volume can be used for (gas) storage. While more research work is geared towards the synthesis of viable products in material sciences, the synthesis and introduction of benzo-2,1,3-chalcogenadiazole derivatives into MOFs, using different precursors, will enhance the already known applications, such as drug delivery, biological processes, potential bio-imaging, therapeutic agents and sensing devices. Recent findings show that MOFs are chemically stable to some degree and this finding has boosted their applications further. Furthermore, the physical characteristic properties of MOFs, which includes optical, electronic and magnetic properties, have also attracted industrial interest. Over the years, the effect of carbon dioxide accumulation in the atmosphere has becomes a global problem, and storage is an

issue. But with the development of MOFs which are efficient for carbon dioxide capture, and with specific ability for gas separation applications, there is hope for solving the problem.[71] Some MOFs show high CO_2 storage capacity at room temperature in comparison to other methods. After a series of studies, the temperature and pressure at which hydrogen gas can conveniently be stored was found, but with a note that higher surface area MOFs generally tend toward higher hydrogen storage capacity, however it cannot be assumed that a high surface always implies higher capacity.[72] The storage of methane is very important, hence the European government is investing 2.9 billion Euros on organic waste recycling for the generation of methane gas as alternative energy. The same methane gas is being flared in some petroleum producing countries, simply because they lack storage facilities. MOFs are also used for sensing devices,[73] with the properties based on the readiness of its analyte binding exhibiting a noticeable signal via changes in color, redox potential and other properties. Generally the sensing property can be described as a framework of luminescence[74] with signal transduction consisting of luminescence quenching.[76] Summarizing, the use of MOFs for drug administration and sensing devices will help to improve the health of human society. Its use for storage of CO_2, methane and hydrogen will reduce the emission of CO_2 that is responsible for global warming and also solve the problem of alternative fuel (H_2 and CH_4) storage, leading to reduction in environmental pollution.

At this juncture, it will be necessary to make a clear distinction of the porous material that makes up MOFs. Barbour J. Leonard stated that the conventional porosity functions at the molecular scale and thus requires the presence of infinite channels with a minimum diameter of about 3 Å (typically 3 to 10 Å) in a skeletal host framework. These materials

should possess the rigidity necessary to survive the evacuation of guest molecules (solvates) to yield robust porous structures.[58]

1.7 Thesis Goals

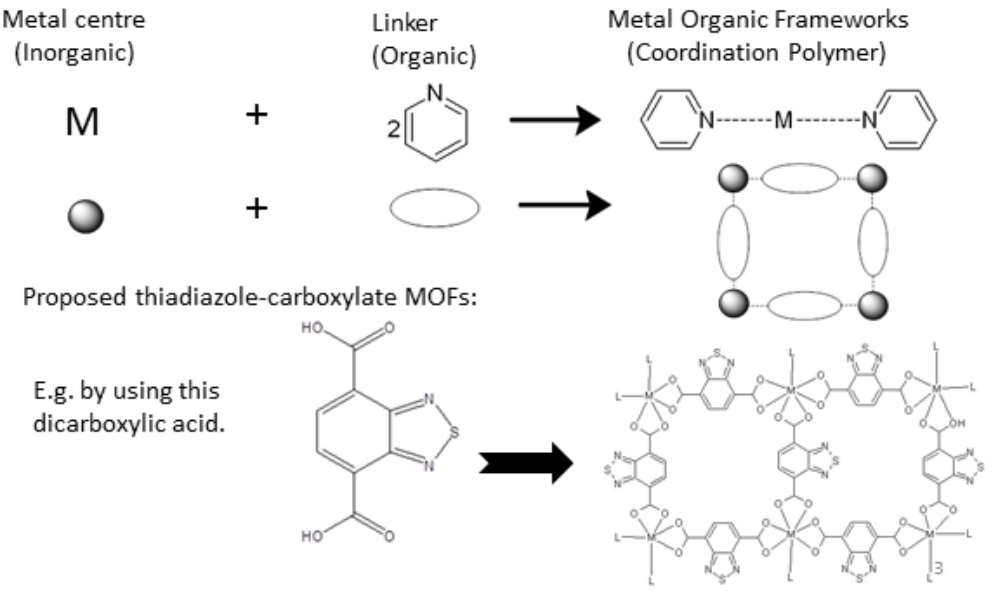

Figure 1.6 Route to proposed MOF (here "L" refers to additional carboxylate donors).

The initial goal of this thesis is converting 4,7-dicarboxylic acid-2,1,3-benzothiadiazole into metal organic frameworks (MOFs) which have become the most exciting development in nanotechnology due to its vast areas of applications and the several synthetic routes through which desired MOF compounds can be synthesized. Through the route to making the required organic framework, two other potential ligands, DCBTD and DEBTD, will be prepared as intermediates. Because of the difficulties encountered in making the acid, although it was eventually successful, we reconsidered my thesis proposal to be the coordination chemistry of DCBTD and DEBTD. The redox characteristics of DCBTD and DEBTD will be investigated in comparison with similar compounds in literature, and those of their possible complexes.

1.8 References

1. Chivers, T., *A Guide to Chalcogen-Nitrogen Chemistry*. World Scientific Publishing Co. Pte. Ltd.: 2005; p 339.
2. Fischer, W., *J. Chem. Educ.* **2001**, *78*, 1333.
3. Bryant, J. J.; Lindner, B. D.; Bunz, U. H. F., *J. Org. Chem.* **2012**, *78*, 1038-1044.
4. Gutsev, G. L.; Klyagina, A. P., *Chin. J. Chem. Phys.* **1983**, *75*, 243-252.
5. Neto, B. A. D.; Lapis, A. A. M.; Da Silva. E. N. Jr.; Dupont, J., *Eur. J. Org. Chem.* **2013**, *2013*, 228-255.
6. El-Taib, H. F.; Fouda, A. S.; Radwan, M. S. *Int. J. Electrochem. Sci.*, **2011**, 3140-3163.
7. Lonchakov, A. V.; Rakitin, O. A.; Gritsan, N. P.; Zibarev, A. V. *Molecules* **2013**, 9850-9900.
8. Oliveira, F. F.; Santos, D. C.; Lapis, A. A.; Corrêa, J. R.; Gomes, A. F.; Gozzo, F. C.; Moreira, P. F.; de Oliveira, V. C.; Quina, F. H.; Neto, B. A., *Bioorg. Med. Chem. Lett.* **2010**, *20*, 6001-6007.
9. Padhy, H.; Huang, J.-H.; Sahu, D.; Patra, D.; Kekuda, D.; Chu, C. W.; Lin, H. C., *J. Polym. Sci., Part A: Polym. Chem.* **2010**, *48*, 4823-4834.
10. Tsuzuki, S.; Sato, N., *J. Phys. Chem. B* **2013**, *117*, 6849-6855.
11. Bryant, J. J.; Lindner, B. D.; Bunz, U. H. F., *J. Org. Chem.* **2012**, *78*, 1038-1044.
12. Gieren, A.; Lamm, V.; Haddon, R. C.; Kaplan, M. L., *J. Am. Chem. Soc.* **1980**, *102*, 5070-5073.
13. Tsuzuki S., Sato, N. *J. Phys. Chem. B.* **2013**, 6849-6855.
14. Xiao, J.; Xiao, X.; Zhao, Y.; Wu, B.; Liu, Z.; Zhang, X.; Wang, S.; Zhao, X.; Liu, L.; Jiang, L., *Nanoscale* **2013**, *5*, 5420-5425.
15. Gibson, G. L.; McCormick, T. M.; Seferos, D. S., *J. Am. Chem. Soc.* **2011**, *134*, 539-547.
16. Lommerse, J. P. M.; Stone, A. J.; Taylor, R.; Allen, F. H., *J. Am. Chem. Soc.* **1996**, *118*, 3108-3116.
17. (a) Chen, Y.-H.; Lin, S.-L.; Chang, Y.-C.; Chen, Y.-C.; Lin, J. T.; Lee, R. H.; Kuo, W. J.; Jeng, R. J., *Org. Electron.* **2012**, *13*, 43-52; (b) Chen, W. N.; Chu, D. P.; Li, S. P., *Org. Electron.* **2012**, *13*, 98-103; (c) Furukawa, H.; Ko, N.; Go, Y. B.; Aratani, N.; Choi, S. B.; Choi, E.; Yazaydin, A. Ö.; Snurr, R. Q.; O'Keeffe, M.; Kim, J.; Yaghi, O. M., *Science* **2010**, *329*, 424-428.
18. Munakata, M.; Kuroda-Sowa, T.; Maekawa, M.; Nakamura, M.; Akiyama, S.; Kitagawa, S., *Inorg. Chem.* **1994**, *33*, 1284-1291.
19. Zhou, A. J.; Zheng, S. L.; Fang, Y.; Tong, M. L., *Inorg. Chem.* **2005**, *44*, 4457-4459.
20. Milios, C. J.; Ioannou, P. V.; Raptopoulou, C. P.; Papaefstathiou, G. S., *Polyhedron* **2009**, *28*, 3199-3202.
21. Mukherjee, G.; Singh, P.; Ganguri, C.; Sharma, S.; Singh, H. B.; Goel, N.; Singh, U. P.; Butcher, R. J., *Inorg. Chem.* **2012**, *51*, 8128-8140.
22. Leznoff, D. B.; Xue, B. Y.; Batchelor, R. J.; Einstein, F. W. B.; Patrick, B. O., *Inorg. Chem.* **2001**, *40*, 6026-6034.
23. Venkataraman, D.; Gardner, G. B.; Covey, A. C.; Lee, S.; Moore, J. S.; *Acta. Cryst.* **1996**, *C52*, 2416-2419.

24. Lamann-Glees, A., U. R., *Cryst. Growth Des.* **2012**, *12*, 854.
25. Elisabeth, E. Barbour, L. J.; Orr, G.W.; Holman, K. T.; J.L.Atwood, *Supramol.Chem.* **2000**, *12*, 317.
26. Wu, D. D.; Mak, T. C. W. *J. Chem. Soc., Dalton Trans.* **1995**, 2671-2678.
27. Zhang, X.; Guo, G. C.; Zheng, F. K.; Zhou, G. W.; Mao, J. G.; Dong, Z.-C.; Huang, J. S.; Mak, T. C. W. *J. Chem. Soc., Dalton Trans.* **2002**, 1344-1349.
28. Zhao, X. L.; Wang, Q. M.; Mak, T. C. W. *Chem. Eur. J.* **2005**, *11*, 2094-2102.
29. Michaelides, A.; Kiritis, V.; Skoulika, S.; Aubry, A. *Angew. Chem. Int. Ed. Engl.* **1993**, *32*, 1495–1499.
30. Smith, G.; Reddy, A. N.; Byriel, K. A.; Kennard, C. H. L., *J. Chem. Soc., Dalton Trans.* **1995**, 3565-3570.
31. Ene, C. D.; Tuna, F.; Fabelo, O.; Ruiz-Pérez, C.; Madalan, A. M.; Roesky, H. W.; Andruh, M. *Polyhedron* **2008**, *27*, 574-582.
32. Whitcomb, D. R.; Rajeswaran, M. *Polyhedron* **2006**, *25*, 1747-1752.
33. Ríos-Moreno, G.; Aguirre, G.; Parra-Hake, M.; Walsh, P. J., *Polyhedron* **2003**, *22*, 563-568.
34. Wang, M.; Hu, X.; Liu, P.; Li, W.; Gong, X.; Huang, F.; Cao, Y., *J. Am. Chem. Soc.* **2011**, *133*, 9638-9641.
35. Saeki, A.; Yoshikawa, S.; Tsuji, M.; Koizumi, Y.; Ide, M.; Vijayakumar, C.; Seki, S., *J. Am. Chem. Soc.* **2012**, *134*, 19035-19042.
36. Patel, D. G.; Feng, F.; Ohnishi, Y.-y.; Abboud, K. A.; Hirata, S.; Schanze, K. S.; Reynolds, J. R. *J. Am. Chem. Soc.* **2012**, *134*, 2599-2612.
37. Pilgram, K.; Zupan, M.; Skiles, R. *J. Heterocycl. Chem.* **1970**, *7*, 629-633.
38. Catriona, A. C. Fiona., H.; Fry, A. L.; Holme, A. Y.; Abdullah, A.; Charareh, P.; Claus J., *Org. Biomol. Chem.* **2005**, *3*, 1541-1546.
39. Boeré, R. T.; Roemmele, T. L., *Coord. Chem. Rev.* **2000**, *210*, 369-445.
40. Cozzolino, A. F.; Britten, J. F.; Vargas-Baca, I., *Cryst. Growth Des.* **2005**, *6*, 181-186.
41. Cozzolino, A. F.; Dimopoulos-Italiano, G.; Lee, L. M.; Vargas-Baca, I. *Eur. J. Org. Chem.* **2013**, *2013*, 2751-2756.
42. Gibson, G. L.; McCormick, T. M.; Seferos, D. S., *J. Am. Chem. Soc.* **2012**, *134*, 539-547.
43. Mallet, C.; Savitha, G.; Allain, M.; Kozmík, V.; Svoboda, J.; Frère, P.; Roncali, J., *J. Org. Chem.* **2012**, *77*, 2041-2046.
44. Thomas, A.; Bhanuprakash, K., *ChemPhysChem* **2012**, *13*, 597-605.
45. Alghamdi, A. A. B.; Watters, D. C.; Yi H.; Al-Faifi, S.; Almeatag, M. S.; Coles, D.; kingsley, J.; Lidzey, D. G.; Iraqi, A. *J. Mater. Chem. A* **2013**, 5165-5171.
46. Watanabe, M.; Goto, K.; Fujitsuka, M.; Tojo, S.; Majima, T.; Shinmyozu, T. *Bull. Chem. Soc. Jpn.*, **2010**, *83*, 1155-1161.
47. Rethore, C.; Madalan, A.; Fourmigue, M.; Canadell, E.; Elsa, L. B.; Almeida, M.; Clerac, R.; Avarvari, N. *New J. Chem.* **2007**, 1468-1483.
48. Suzuki, T.; Fujii, H.; Yamashita, Y.; Kabuto, C.; Tanaka, S.; Harasawa, M.; Mukai, T.; Miyashi, T., *J. Am. Chem. Soc.* **1992**, *114*, 3034-3043.
49. Cozzolino, A. F.; Vargas-Baca, I.; Mansour, S.; Mahmoudkhani, A. H., *J. Am. Chem. Soc.* **2005**, *127*, 3184-3190.
50. Ku, J.; Lansac, Y.; Jang, Y. H. *J. Phys. Chem. C*, **2011**, 21508–21516.

51. Suturina, E. A.; Semenov, N. A.; Lonchakov, A. V.; Bagryanskaya, I. Y.; Gatilov, Y. V.; Irtegova, I. G.; Vasilieva, N. V.; Lork, E.; Mews, R. d.; Gritsan, N. P.; Zibarev, A. V., *J. Phys. Chem. A* **2011**, *115*, 4851-4860.
52. Boros, E.; Earle, M. J.; Gilea, M. A.; Metlen, A.; Mudring, A.-V.; Rieger, F.; Robertson, A. J.; Seddon, K. R.; Tomaszowska, A. A.; Trusov, L.; Vyle, J. S., *Chem. Commun.* **2010**, *46*, 716-718.
53. Berg, D. J.; Burns, C. J.; Andersen, R. A.; Zalkin, A., *Organometallics* **1989**, *8*, 1865-1870.
54. Rhee, J. H.; Chung. C. C.; Diau, E. W. G. *NPG Asia Materials* **2013**, *5*, e68.
56. Furukawa, H.; Cordova, K. E.; O'Keeffe, M.; Yaghi, O. M., *Science* **2013**, *341*.
57. Barbour, L. J., *Chem. Commun.* **2006**, 1163-1168.
58. Kitagawa,S., Kiyaura, R., Noro, S. *Angew. Chem., Int. Ed.* **2004**, *43*, 2334-2375.
59. Shekhah, O.; Wang, H.; Kowarik, S.; Schreiber, F.; Paulus, M.; Tolan, M.; Sternemann, C.; Evers, F.; Zacher, D.; Fischer, R. A.; Wöll, C., *J. Am. Chem. Soc.* **2007**, *129*, 15118-15119.
60. Haque, E.; Khan, N. A.; Park, J. H.; Jhung, S. H. *Chem.-Eur. J.* **2010**, *16*, 1046-1052.
61. Li, Z.-Q.; Qiu, L. G.; Xu, T.; Wu, Y.; Wang, W.; Wu, Z.-Y.; Jiang, X., *Mater. Lett.* **2009**, *63*, 78-80.
62. Li, Z.-Q.; Qiu, L. G.; Wang, W.; Xu, T.; Wu, Y.; Jiang, X., *Inorg. Chem. Commun.* **2008**, *11*, 1375-1377.
63. Qiu, L.; Li, Z. Q.; Wu, Y.; Wang, W.; Xu, T.; Jiang, X. *Chem. Commun.* **2008**, 3642-3644.
64. Tompsett, G.; Conner, W. C.; Yngvesson, K. S. *ChemPhysChem* **2006**, *7*, 296.
65. Jhung, S. H.; Chang, J. S.; Hwang, J. S.; Park, S. E. *Micropor. Mesopor. Mater.* **2003**, *64*, 33.
66. Mueller, U.; Schubert, M.; Teich, F.; Puetter, H.; Schierle-Arndt, K.; Pastre, J., *J. Mater. Chem.* **2006**, *16*, 626-636.
67. Parnham, E. R.; Morris, R. E. *Acc. Chem. Res.* **2007**, *40*, 1005-1013.
68. Forster, P. M., Thomas, P. M., Cheetham, A. K., *Chem. Mater.* **2002**, *14*, 17.
69. Sonnauer, A.; Hoffmann, F.; Fröba, M.; Kienle, L.; Duppel, V.; Thommes, M.; Serre, C.; Férey, G.; Stock, N., *Angew. Chem., Int. Ed.* **2009**, *48*, 3791-3794.
70. Li, H.; Eddaoudi, M.; Groy, T. L.; Yaghi, O. M. *J. Am. Chem. Soc.* **1998**, *120*, 8571-8572.
71. Zhou, W.; Wu, H.; Yildirim, T. *J. Am. Chem. Soc.* **2008**, *130*, 15268-15269.
72. Verduzco, R.; Botiz, I.; Pickel, D. L.; Kilbey, S. M.; Hong, K.; Dimasi, E.; Darling, S. B., *Macromolecules* **2011**, *44*, 530-539.
73. Bloking, J. T.; Han, X.; Higgs, A. T.; Kastrop, J. P.; Pandey, L.; Norton, J. E.; Risko, C.; Chen, C. E.; Brédas, J.-L.; McGehee, M. D.; Sellinger, A., *Chem. Mater.* **2011**, 23, 5484-5490.
74. Anant, P.; Lucas, N. T.; Jacob, J., *Org. Lett.* **2008**, *10*, 5533-5536.

CHAPTER 2: 4,7-DINITRILE-2,1,3-BENZOTHIADIAZOLE AND ITS COMPLEXES

2.1 Introduction

In this chapter, the chemistry of benzothiadiazoles is extended by studying DCBTD and its coordination chemistry. Pilgram and co-workers reported the synthesis of DCBTD many years ago for use as an herbicide, but little else has been done with this interesting compound.[1] Here, the synthesis of DCBTD has been repeated and optimized, its structure and electronic properties determined and the redox behavior investigated. This DCBTD is step one in a longer plan to use it in making a 4,7-dicarboxylic acid or more precisely the doubly ionized dicarboxylate. The overall goal is to make redox-active coordination polymers and MOFs, therefore increasing the number of possible applications. Organonitrile ligands are well known in coordination chemistry even though they are not considered the best class of donors. Thus the utility of the dinitrile itself as a bridging ligand for coordination polymers has been investigated by studying its interaction with Ag^{+}.

2.2 Synthesis of 2,1,3-benzothiadiazole and entry into 4,7-substituted derivatives

2,1,3-benzothiadiazole is often prepared (Scheme 2.1) by the action of thionyl chloride on o-phenylenediamine using toluene as a solvent through a method of ring-closure.[2,3,4,5] Nunn and Ralph found that boiling the reactants under reflux for 3 hours and distillation of the product gave a high yield of 85% of the heterocycle.[6] See Figure 2.1 for the atom-numbering scheme for this "parent" heterocyclic compound. Throughout this thesis, reference will be made to compounds using this numbering system.

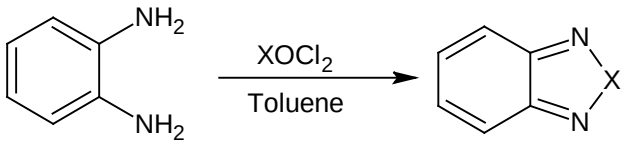

Scheme 2.1 Synthesis and Molecular Structure of 2,1,3-benzothiadiazole

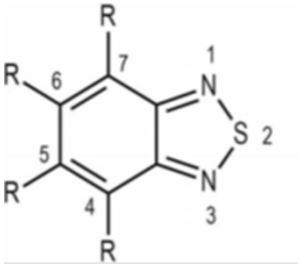

Figure 2.1 Atom numbering for substituted 2,1,3-benzothiadiazoles

4,7-dibromo-2,1,3-benzothiadiazole is the most commonly used intermediate for the synthesis of 2,1,3-benzothiadiazole derivatives containing π-extended compounds. 4,7-dibromo-2,1,3-benzothiadiazole can easily be prepared from 2,1,3-benzothiadiazole in high yield. The reaction of 2,1,3-benzothiadiazole with molecular bromine by slow addition in hydrobromic acid (HBr), gives exclusively the 4,7-disubstituted regioisomer (Scheme 2.2).[7,8,9] After electrophilic addition at the position 4 and 7 of the 2,1,3-benzothiadiazole, further substitution can occur at the 5 and 6 positions.[10]

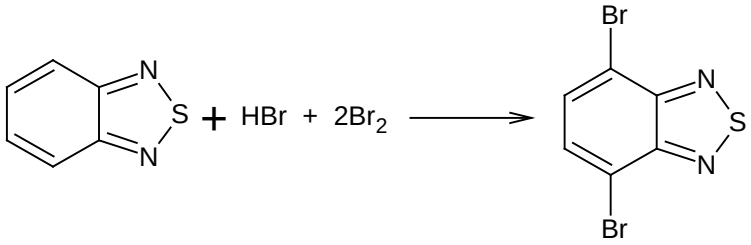

Scheme 2.2 Synthesis of 4,7-dibromo-2,1,3-benzothiadiazole

The fast addition of molecular bromine (Br_2) leads to tetrabrominated thiadiazole,[11,12] which is avoided through slow addition using strictly stoichiometric quantities of reagents. The product is purified by the addition of saturated sodium bisulphite to remove

any excess bromine, washed with water, dried and recrystallized in ethanol. Ji Hye Son *et al.*[13] carried out this reaction, using the same reagent, but refluxed for 4 hours and had a yield of 72.6%. Rokib Hassan's thesis reports using sulfuric acid and Ag_2SO_4 in a different procedure which obtained 98 % yield.[14] Here we decided not to use the same method of Hassan due to the cost of Ag_2SO_4, but used Br_2 in the presence of HBr with refluxing for 6 hours, to obtain the product in 94.3% yield. It was confirmed by comparing the melting point, IR and ^{1}H NMR spectra with the literature data.[14,13]

2.3 Synthesis of 4,7-dinitrile-2,1,3-benzothiadiazole.

The main work on this thesis started with the synthesis of DCBTD (derived from the alternate name: 4,7-dicyanbenzo-2,1,3-benzothiadiazole), from which other compounds and complexes in this work were made. DCBTD had been proposed as a herbicide; other studies showed that it can be used as a photosensitizer and electron-transfer agent.[15,16] DCBTD has been prepared by different methods,[17,18,19] the most common method is the reaction of dibromo-2,1,3-benzothiadiazole with copper cyanide and refluxing in DMF.[20a, 20b,21] The by-product of this reaction is copper bromide, which is water soluble and extraction with benzene is tedious, because the reaction mixture easily forms emulsions and forms a stable complex with the product. This is overcome by reacting it with conc. HCl and H_2O_2 which destroys the copper (I) complex.

The optimized synthetic procedure involves refluxing 4,7-dibromo-2,1,3-benzothiadiazole and copper cyanide in DMF for 12 hours, cooling to RT, concentrating to ¼ the original volume (removing the solvent completely results in the formation of tar on the addition of concentrated HCl and then H_2O_2). Then concentrated hydrochloric acid is added, followed by dropwise addition of 30% hydrogen peroxide while keeping the

temperature below 40 ^{o}C.[20a,22] Workup afforded 7.20 g of crude product which was recrystallized from 95% ethanol to give plate like yellow crystals, 5.8 g (62 %). Gallardo *et al.*[23] made this same compound using a different technique and obtained product in 65% yield.

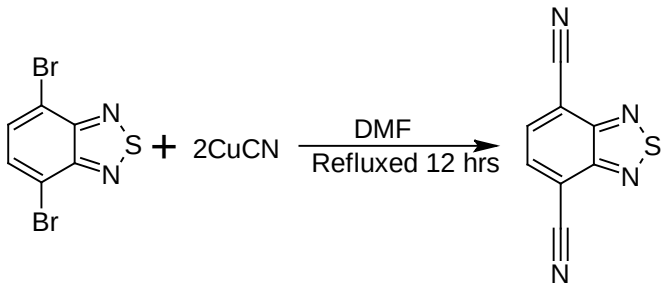

Scheme 2.3 Synthesis of (DCBTD)

Using a different method but with a lower yield, we tried K. Pilgram's method by refluxing at room temperature for 10 hours and obtain 77.4 % crude yield, recrystallization from 95 % ethanol gave us better X-ray quality crystal with preference to benzene used in the literature with repeated recrystallization.[19] The problem with ethanol is hydrolysis, so that the whole bulk material could not be converted to crystals. Hence, only 47.3 % pure crystal yield was obtained from EtOH, confirmed by melting point, IR and ^{1}H NMR spectra in comparison with literature values.

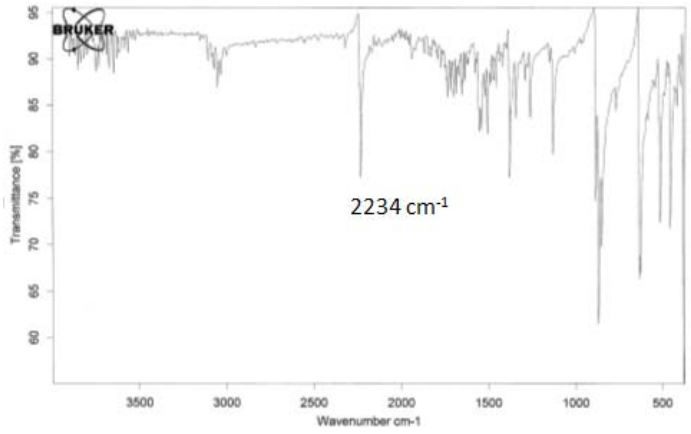

Figure 2.2 IR spectrum of DCBTD

2.3.1 IR and NMR of DCBTD

The IR spectrum of DCBDT shows weak bands for the aromatic C-H stretches. It shows a medium-intensity band for the nitrile stretch at 2234 cm^{-1}. There are also a number of bands in the fingerprint region, but overall the spectrum is quite simple.

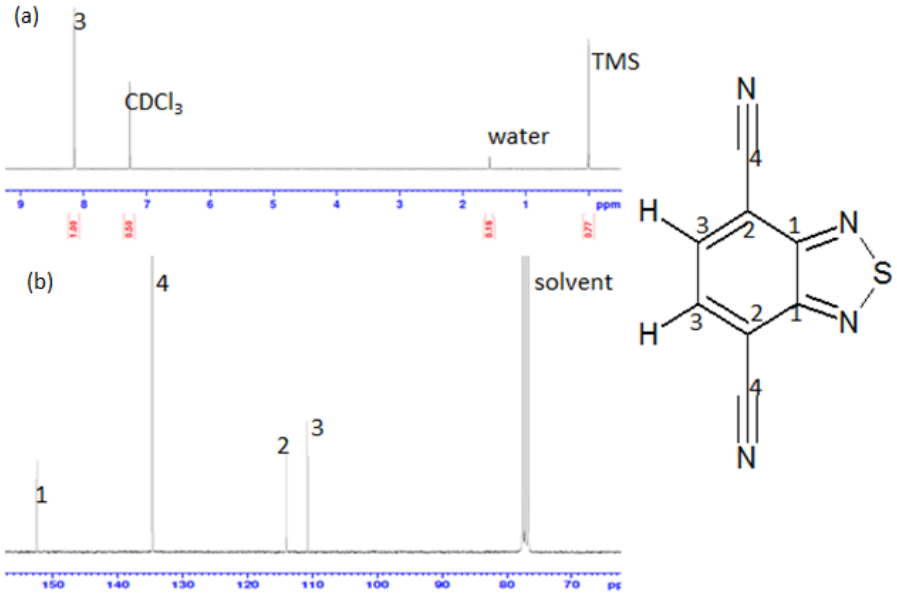

Figure 2.3 (a) ^{1}H and (b) ^{13}C NMR spectra of compound DCBTD

The ^{1}H NMR spectrum of DCBTD in Figure 2.3(a) shows a singlet at δ 8.150 ppm, which is the only proton peak for the structure in the spectrum, indicating the equivalency of the two protons attached to the benzothiadiazole rings with a perfect symmetry between them. The ^{13}C NMR spectrum has four distinct signals to the four different carbon atoms in the structure according to symmetry as shown in Figure 2.3(b) above and 2.4 below.

2.4 X-Ray Crystallography of DCBTD

The synthesis of DCBTD was first reported in a patent and later in the literature,[17, 20a] but structural characterization had not been reported. We therefore determined the structure by single-crystal X-ray crystallography.

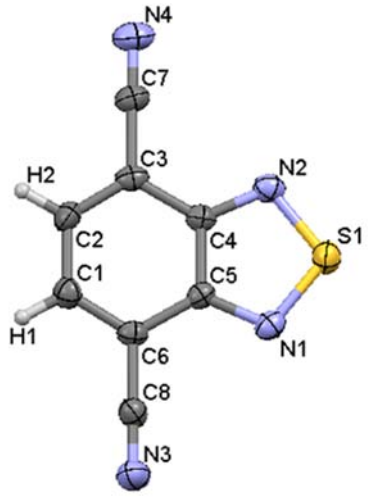

Figure 2.4 X-ray crystal structure of DCBTD

Table 2.1 Selected bond distances in (Å) and angles in (°) for DCBTD

S(1)-N(1)	1.607(19)	C(3)-C(7)	1.447(3)
S(1)-N(2)	1.615(2)	C(1)-C(2)	1.404(3)
C(6)-C(1)	1.375(3)	C(5)-N(1)	1.349(3)
C(6)-C(5)	1.417(3)	C(5)-C(4)	1.417(3)
C(6)-C(8)	1.445(3)	C(7)-N(4)	1.134(3)
C(3)-C(2)	1.360(3)	C(8)-N(3)	1.139(3)
C(3)-C(4)	1.429(3)	C(4)-N(2)	1.347(3)
N(1)-S(1)-N(2)	101.52(11)	N(2)-C(4)-C(5)	114.3(2)
N(1)-C(5)-C(6)	127.0(2)	N(2)-C(4)-C(3)	125.9(2)
N(1)-C(5)-C(4)	112.9(2)	C(5)-C(4)-C(3)	119.8(19)
C(6)-C(5)-C(4)	120.08(19)	C(5)-N(1)-S(1)	106.1(16)
N(4)-C(7)-C(3)	178.8(3)	C(4)-N(2)-S(1)	105.2(16)

In comparison to related compounds, the bond distances did not significantly differ from those reported in literature. The bond length of C≡N, for example, in *p*-dicyanobenzene is 1.145(2) Å,[24] for DCBTD is C≡N (1.143(3) Å). The bond lengths within the benzothiadiazole rings remained significantly the same, while the bonds between the

benzene ring and the substituent C atoms (C6-C8) 1.445 (3) Å, as to (C3-C7) 1.447(3) Å attached at the 4,7 positions, *para* to each other, are not statistically different.

Table 2.2 Crystal data and structure refinement for DCBTD

Empirical Formula	$C_8 H_2 N_4 S$	
Temperature	296(2) K	
Crystal system	Orthorhombic	
Space group	$P2_12_12_1$	
Unit cell dimensions	a = 5.8823(16) Å	α = 90°
	b = 7.0552(19) Å	β = 90°
	c = 19.654(5) Å	γ = 90°
Z	4	
Goodness-of-fit on F^2	0.931	
Final R indices [I>2sigma(I)]	R1 = 0.0421, wR2 = 0.0814	
R indices (all data)	R1 = 0.0612, wR2 = 0.0865	

The single crystal of DCBTD suitable for X-ray diffraction was obtained by recrystallization from 95 % ethanol through slow evaporation of the solvent, the structure was flat, the plane angles are not quite different from literature reported analogs,[24] the C3-C7-N4 and C6-C8-N3 angles is almost linear, at 178.8(3)°, those reported had other substituents attached, which are not planar about the benzene ring and this steric effect could have accounted for some geometrical differences, like the small difference in the bond lengths and angles in the benzothiadiazole rings. Among the literature analogues, those with pyridine are more closely related, particularly 4-pyridine, 2-pyridine had larger dihedral angles[25,5,26] which make the substituents twisted out of plane.

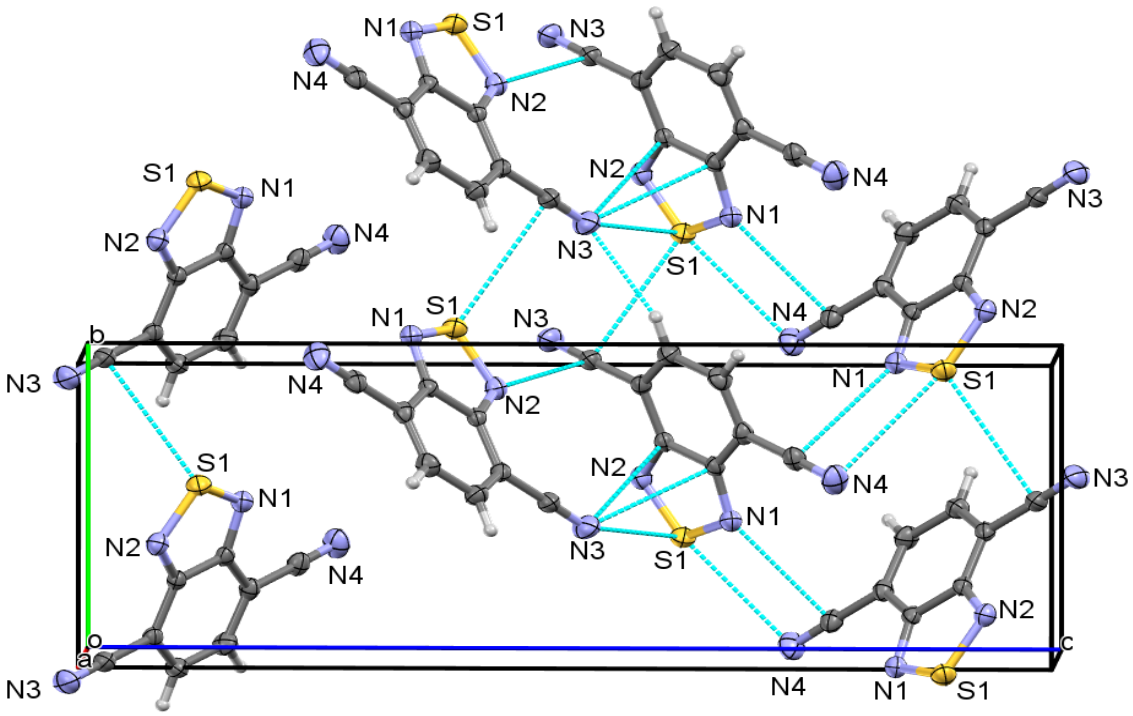

Figure 2.5 Packing diagram of DCBTD showing the most important intermolecular contacts.

From the packing diagram as shown in Figure 2.5, the most remarkable feature of the crystal structure is the existence of short S···N inter heteroatom contacts (3.346(2) Å) between 2,1,3-thiadiazole rings, other short contacts are that of the C(C=N) ···ring N (3.121(3) Å) and C(benzene ring) ···C(C=N) (3.234(3) Å). The unique stacking structures as shown in Figure 2.5, the molecule are in slanting position to each other and not completely head to head arrangement, but the thiadiazole ring of one molecule and the dinitrile end of the other are more tilted to the same direction which account for the intermolecular bonds between the thiadiazole rings and the dinitrile. Intermolecular weak contacts are between NS and SN in the parent compound, with a distances of 3.346(3) Å, between the DCBTD molecules the crystal packing is dominated by C≡N and SN through S···N and C···N contacts, with E---N(average) = 3.443(2) Å where E = S.[14]

2.5 Electrochemistry

2.5.1 Voltammetry of DCBTD

The voltammetry measurements of the degassed 2.5×10^{-5} M solutions of the compound in MeCN and CH_2Cl_2 were performed at RT in an argon atmosphere. The measurements were carried out using cyclic voltammetry (CV) and square wave voltammetry (SWV) was used to determine the solvent limits. CV was undertaken at a glassy carbon working electrode, with 0.1 M $[^nBu_4N][PF_6]$ as supporting electrolyte, over a scan rate of 0.05 – 1.00 Vs^{-1}. Potential data are reported according to IUPAC recommended scale versus the ferrocene/ferrocenium redox couple as an internal standard at 0.00 V. The compound gave rise to two reduction processes in both MeCN and CH_2Cl_2 which appear to involve one electron transferred at each process (Figure 2.6). Both processes are close to reversible, that is $I_p^{ox} = I_p^{red}$ or $I^{ox}{}_p/I_p^{red} = \sim 1$ and the anodic (E_p^a) and cathodic (E_p^c) peak-to-peak separation is also close to electrochemically reversible behavior, at 79 mV. The two reduction processes occurred as follows, -1/0 wave with E_{m1}= -1.06 V, -2/-1 wave with E_{m2} = -1.90 V and ΔE = 0.84 V, in both solvents.

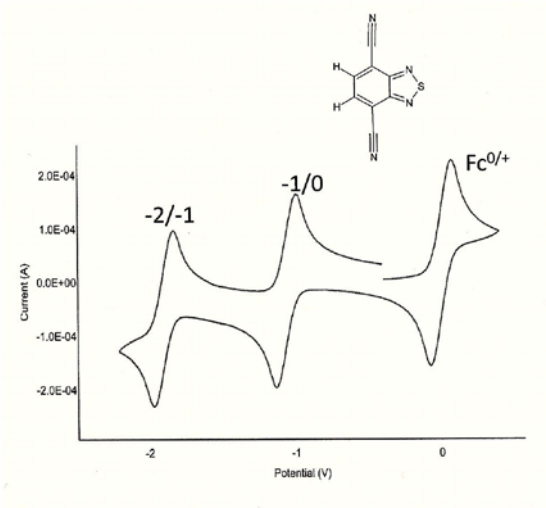

Figure 2.6 Cyclic voltammogram for DCBTD recorded in MeCN

2.6 Electron Paramagnetic Resonance Spectroscopy of DCBTD

The electron paramagnetic resonance (EPR) spectrum of DCBTD had been previously measured by Camilleri and co-workers[27] after one electron reduction of the neutral compound, and they obtained the radical anion $[DCBTD]^{-\bullet}$. The large potential window of $\Delta E = 0.84$ V is a measure of the stability of this radical and the possibility of its further reduction of the radical to di-anion. The redox properties of DCBTD in organic solvents such as MeCN and CH_2Cl_2 look so interesting, incorporation of an electron into the neutral molecule generates a radical anion. The hyperfine couplings of two equivalent N (I = 1, quintet) of the thiadiazole ring, to two equivalent protons (I = ½ triplet) on the benzene ring, and then very small coupling to the nitrile (N) of the C≡N groups are observed, which are the magnetically active nuclei in the molecule. The hyperfine couplings of (a^{N1}) × 2, 0.2860 mT, (a^{H}) × 2, 0.2326 mT, (a^{N2}) × 2, 0.0754 mT obtained in this experiment is slightly lower than literature report of (a^{N1} 0.3, a^{N2} 0.08 and a^{H} 0.24 mT).[27] We think the differences arise from differences between water and CH_2Cl_2, such as differences in solvent viscosity.

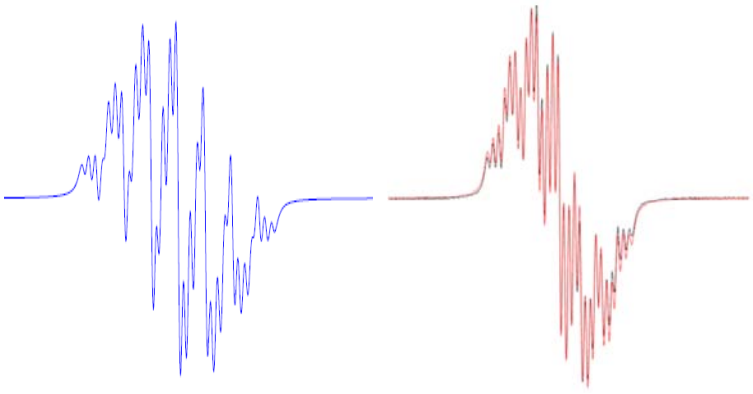

(a) (b)

Figure 2.7 (a) experimental derivative EPR spectra of DCBTD in CH_2Cl_2 (0.1 M[$^{n}Bu_4N$][PF_6], (b) Simulated overlapped with experimental.

2.7 Synthesis and characterization of DCBTD complexes of Ag^+

Different silver salts were reacted with the ligand through liquid–liquid layering processes,[28] from all the trials setup, we could only harvest X-ray quality crystals from the ligand and $AgBF_4$ and $AgPF_6$. In this process, the ligand was dissolved in CH_2Cl_2, the silver salt in benzene, the first solution was transferred into the crystallization tube and with the aid of a pipette the second solution was gently placed on top of the first without turbulence. We then chose direct reaction of the ligand with the silver salts in benzene by heating and stirring for 30 minute, cool to RT and filter, the precipitate obtained was recrystallized in methanol, from which we were able to obtained crystals for the $AgClO_4$ and $AgSbF_6$.[29] The different structures obtained were dependent on the anion used, hence it was the anion which determined the morphology of the complex. Most of the complexes crystallized in the same crystal system (monoclinic) and in the same space group C2/c, except PF_6^-, which crystallized in an as yet undetermined space group. The ratio of the ligand to the silver salt varies as shown in Table 2.3 below. The Z value of these five crystals is 4 except the complex obtained using $AgClO_4$ for which Z is 16 and the second BF_4^- salt for which Z is 2. Some of these complexes were formed with void spaces which are occupied by the solvent. The method of preparation was not the determinant of these void spaces, since only one each of the layered and the recrystallized has this property. We cannot conclude that Ag^+ needed more coordinating molecules in the reaction mixture that was while it took up benzene, since in the $AgBF_4$ and $AgClO_4$ it did not take up benzene. The anions in these complexes exhibit different behaviors with the Ag^+. Those of BF_4^- and PF_6^- are not coordinated to the silver ion, therefore exhibits the outer-sphere complex coordination. Two of every ClO_4^- anion and all of SbF_6^- anions

coordinated to the silver ion (inner sphere complex coordination).[30] We conclude that the complexes are all ionic, but this coordinating behavior influences the properties of the different silver complex with respect to solubility in different solvents. For instance, the $[Ag(DCBTD)](PF_6).C_6H_6$ is not soluble in water and $[Ag_2(DCBTD)][(SbF_6)_2].2C_6H_6$ salt is not soluble in $CHCl_3$ at RT.

Beside X-ray crystallography, infrared spectroscopy was used to initially determine the formation of the complexes based on the shift of the dinitrile (C=N) band between the ligand and the complex. This was a shift to higher frequency for all the complexes. This difference in vibrational frequency is smallest in the ClO_4^- complex, and highest in the SbF_6^- complex. Table 2.3 shown below reports the nitrile stretching frequencies.

Table 2.3 Dinitrile stretching frequencies (C=N) of the free ligand DCBTD and its complexes

Ligand/Complex	IR band cm^{-1}	$\Delta(\nu CN)$ cm^{-1}
DCBTD ($C_8H_2N_4S$)	2234	N/A
1 $[Ag_4(DCBTD)_5](BF_4)_4$	2254	20
2 $[Ag(DCBTD)_2]BF_4$	2254	20
3 $[Ag_4(DCBTD)_5[(ClO_4)_4$	2247	13
4 $[Ag_2(DCBTD)][(SbF_6)_2.2C_6H_6$	2267	33
5 $[Ag(DCBTD)](PF_6).C_6H_6$	2260	26

2.7.1 Synthesis and Characterization of $[Ag_4(DCBTD)_5](BF_4)_4$ **1**

DCBTD was dissolved in CH_2Cl_2, layered with $AgBF_4$ dissolved in warm benzene in a crystallization tube with pure benzene placed between the layers to prevent instant mixing of the two layers, which gave plate like brown colored crystals. The complex has the expected shift towards higher energy for the C≡N bond stretch (Table 2.3) but its structure could only be established by a single-crystal X-ray diffraction study, the results of which are reported here.

Table 2.4 A summary of crystal data and structure refinement of 4,7-dinitrile-2,1,3-benzothiadiazole silver complexes

Complex	**1**	**2**	**3**	**4**	**5**
Formula	$[Ag_4L_5][BF_4]_4$	$[AgL_2]BF_4$	$[Ag_4L_5][ClO_4]_4$	$[Ag_2L](SbF_6)_2.2C_6H_6$	$[AgL]PF_6.C_6H_6$
Temp, K	173(2)	173(2)	173(2)	173(2)	100(2)
Crystal system	Monoclinic	Monoclinic	Monoclinic	Monoclinic	Triclinic
Space group	*C*2/*c*	*P*n	*C*2/*c*	*C*2/*c*	*P*1
Unit cell: *a*, Å	20.0901(15)	13.0863(9)	20.3770(13)	15.4381(8)	7.928(3)
b, Å	11.6858(8)	5.1876(3)	11.6818(8)	11.5729(6)	12.612(4)
c, Å	22.7231(16)	14.3580(10)	22.7506(15)	15.3649(8)	17.207(6)
α, °	90	90	90	90	85.235(4)
β, °	94.3	100.43(10)	94.7620(10)	103.0880(10)	82.699(4)
γ, °	90	90	90	90	80.163(4)
V, Å^3	5324.8(6)	958.59(11)	5396.9(6)	1678.14	2673.8(2)
Z	4	2	16	4	4
Density, g/cm^3	2.133	1.965	2.166	2.558	2.047
GOF	1.060	1.046	1.064	1.047	1.068
R_1	0.0250	0.0213	0.0237	0.0169	0.0796
wR_2	0.0583	0.0479	0.0546	0.0407	0.1619

The crystal and refinement parameters for the structure of **1** are provided in Table 2.4, along with those of four additional crystallographically characterized silver network coordination compounds. Selected bond distances and angles are provided in Table 2.5,

and an analysis of the coordination environment for the two crystallographically independent silver cations is presented in Table 2.6.

The complex structure has three crystallographically independent DCBTD ligands, one of which (the one which contains S3) is located on a crystallographic two-fold rotation axis, so that only half of this ring contributes to the asymmetric unit. A good starting point for gaining an understanding of this complex is to consider the displacement ellipsoids plot of the asymmetric unit that is provided in Figure 2.8.

Table 2.5 Selected bond distances and angles in Å of $[Ag_4(DCBTD)_5](BF_4)_4$, **1**

N1 – Ag1	2.4805(19)	N3 – Ag2	2.259(2)
N7 – Ag1	2.332(2)	N4 – Ag2	2.222(2)
N8 – Ag1	2.1762(19)	N6 – Ag2	2.2895(18)
N10 – Ag1	2.243(2)	Ag1 – Ag2	4.1823(3)
N1 – Ag1 – N7	90.32(7)	N8 – Ag1 – N10	131.32(9)
N1 – Ag1 – N10	88.75(10)	N3 – Ag2 – N4	116.06(7)
N1 – Ag1 – N8	116.74(7)	N3 – Ag2 – N6	110.27(8)
N7 – Ag1 – N8	122.95(7)	N4 – Ag2 – N6	133.07(7)
N7 – Ag1 – N10	95.51(9)		

The coordination pattern in this structure is quite complex. It can best be described with reference to Table 2.5 in conjunction with Figure 2.9. The atom labelled as Ag1 is four coordinate in a very distorted tetrahedral arrangement with donation from three nitrile group nitrogens (N7,8,10) and one thiadiazole ring nitrogen N2. The Ag–N distances range between 2.1762(9) – 2.4805(19) Å. In addition, the N3 atom which is attached on the same side of the DCBTD ring as the coordinated N2 ring nitrogen is found to be proximate to the Ag^+ position with a distance of 3.438(2) Å. While this is much longer than the sums of the v.d. Waals' radii of Ag and N (3.27 Å), the position of this nitrile group probably blocks optimal approach to the silver ion by the ligands and thus

contributes to the distortion of the environment around this ion.

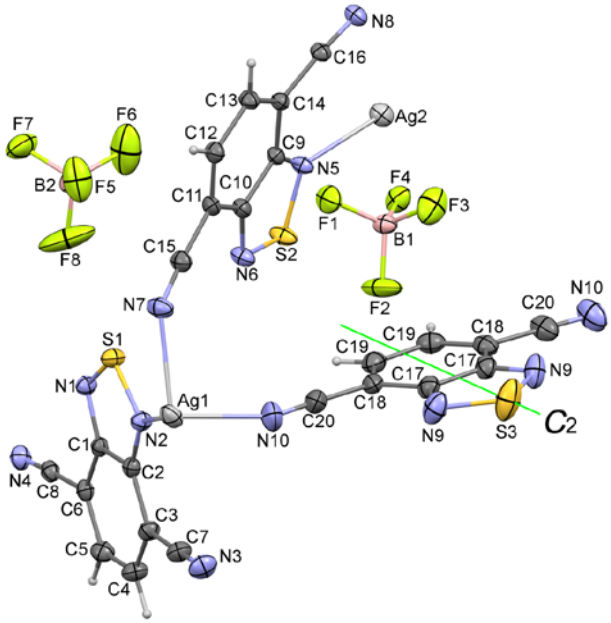

Figure 2.8 Displacement ellipsoids plot of the asymmetric unit in $[Ag_4(DCBTD)_5](BF_4)_4$ **1** showing the atom numbering scheme. Only half the formula unit belongs to the asymmetric unit and the DCBDT molecule containing S3 is symmetry-duplicated by a two-fold rotation axis indicated as C_2 on the diagram (green line).

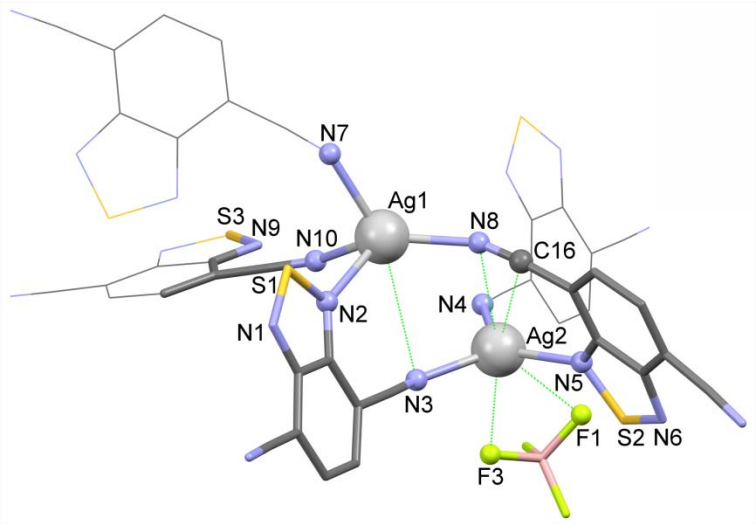

Figure 2.9 Coordination environment of the two independent silver ions in the crystal structure of $[Ag_4(DCBTD)_5](BF_4)_4$ **1**. Donor and acceptor atoms drawn as spheres.

Table 2.6 Analysis of Donor-Acceptor interactions in $[Ag_4(DCBTD)_5](BF_4)_4$, **1**

DCBTD molecule (by S atom label)	Donor Type	Ag1	Ag2
S1	Ring N	N2	—
S1	Ring N	(non-coord.)	(non-coord.)
S1	–C≡N	—	N3
S1	–C≡N	—	N4
S2	Ring N	—	N5
S2	Ring N	(non-coord.)	(non-coord.)
S2	–C≡N	N7	—
S2	–C≡N	N8	—
S3	Ring N	—	—
S3	–C≡N	N10	—
	Sum: (C.N.) =	4	3
	Geom. =	Tetrahed. (dist.)	Trigon. (dist.)
			Ag—Ag = 4.182(3) Å

The atom labelled as Ag2 is three-coordinate, through two nitrile nitrogens (N3,4) and one ring nitrogen N5 (distances range from 2.222(2) – 2.258(2) Å). The primary distorted trigonal coordination of this silver ion is filled out by two sets of contacts less than the sums of the v.d. Waals' radii. The first of these is to two fluorine atoms of the BF_4^- ion (distances Ag2–F1 = 2.887(2) and Ag2–F3 = 2.702(2) Å), and the second is a side-on donation from the nitrile group C16≡N8 (distances Ag2–C16 = 3.289(2) and Ag2–N8 = 3.221(2) Å). The asymmetry of the environments is highlighted by the differential in N3–Ag1 and N8–Ag2 distances.

The overall results is that the structure is a densely packed metal organic framework, the cavities are filled with the non-coordinating anion (BF_4^-)[31,32] which are in contact with the Ag^+ and the aromatic rings. The three-dimensional framework structure that is developed from the interactions provided in Table 2.6 can be appreciated with reference to the unit-cell packing diagram provided in Figure 2.10.

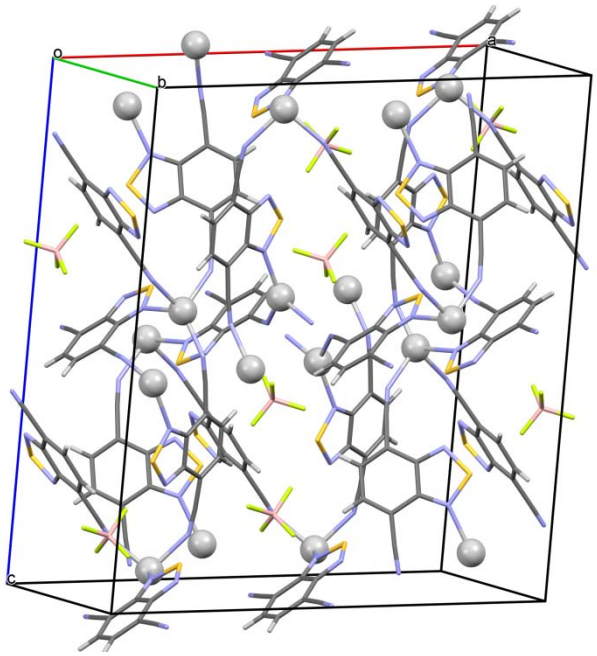

Figure 2.10 Unit cell packing diagram of $[Ag_4(DCBTD)_5](BF_4)_4$ **1** with the ligands and anions depicted by tubes and the silver atoms by spheres. The dense packing arrangement is evident.

2.7.2 Synthesis and Characterization of $[Ag(DCBTD)_2]BF_4$ **2**

In this particular synthesis, $AgBF_4$ was dissolved in sufficient benzene to dissolve at RT before layering above the DCBTD in CH_2Cl_2 solution. After storing in the fume hood for one week, thin brown plate-like crystals were obtained including some that were suitable to obtain a single-crystal X-ray structure.

Even though the constituent components of **2** are the same as found for **1**, the resulting coordination polymer structure is quite different (Figure 2.11). The stoichiometry here is 2:1 for L and Ag^+, compared to 1.25:1 in **1**. Here only nitrogen atoms from the nitrile (C≡N) groups coordinate to the silver, and the unique Ag^+ is four-coordinate with a distorted tetrahedral geometry, with the angles around the metal as N3-Ag-N7 109.9(1), N8-Ag-N3 113.2(1), N4-Ag-N8 108.9(1), N4-Ag-N7 105.3(1), N8-Ag-N7 99.2(1), N3-

Ag-N4 118.3(1)°. The bond distances between the respective N and the Ag^+ are quite variable, with N3-Ag 2.225(4), N7-Ag 2.304(4), N4-Ag 2.282(4), N8-Ag 2.296(4) Å. That only the nitrile N atoms are used for coordination is an indication that these are better electron donors than the ring N atoms are.

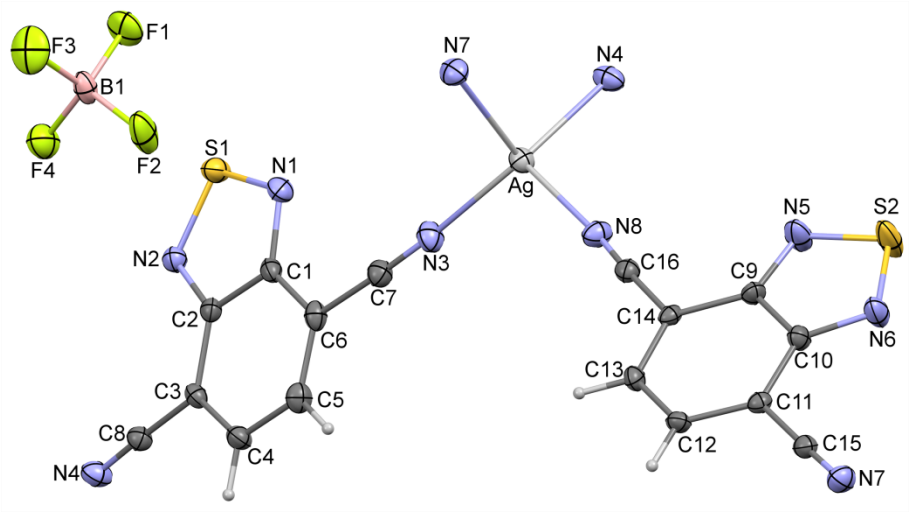

Figure 2.11 Displacement ellipsoids plot of the asymmetric unit in $[Ag(DCBTD)]BF_4$, **2** showing the atom numbering scheme. The unique Ag^+ ion is coordinated by all four nitrile N atoms and to emphasize this, N4 and N7 are repeated in the figure.

Table 2.7 Selected bond distances (Å) and angles (°) for $[Ag(DCBTD)]BF_4$, **2**

N8-Ag	2.282(4)	N3-Ag	2.225(4)
N8-Ag	2.296(4)	N7-Ag	2.304(4)
N8-Ag-N4	108.9(1)	N8-Ag-N3	113.2(1)
N8-Ag-N7	99.2(1)	N4-Ag-N7	105.3(1)
N3-Ag-N7	109.9(1)	N4-Ag-N3	118.3(1)

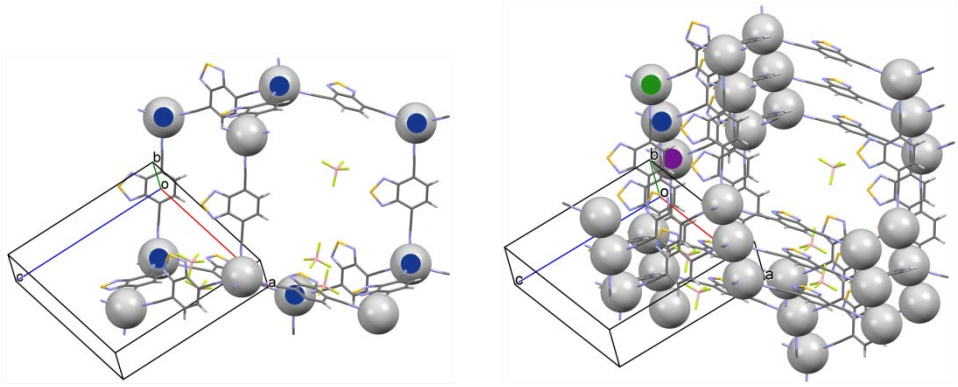

Figure 2.12 (Left) an adamantyl cage in the diamondoid coordination of DCBTD to silver with blue circles identifying one of the Ag_6 boat structures, and (right) the elaboration of layers of the left hand structure by additional layers of Ag^+ ions above and below the base structure (green and mauve circles).

The resulting crystal structure is very appealing with a network structure that is somewhat reminiscent of the structure of diamond (with the Ag^+ ions taking the place of carbon and the *para*-dinitrile groups acting as the "bonds" linking Ag^+ ions together.) The tetrahedral coordination thus defines large rings in a "boat" conformation, which are themselves built into adamantane-like cage structures (Figure 2.12). But whereas a diamond lattice is very open, this structure possesses an interlaced infilling of the lattice through a Ag·Ag spacing that occurs with each unit cell repeat along the *b* axis, resulting in the stacks of Ag^+ ions that are clearly visible in Figure 2.12 and 2.13, i.e. every 5.1876(3) Å.

When the resulting "hexagon" rings are viewed down the crystallographic *b* axis, the channels in the lattice appear to be square (Figure 2.13). These channels are occupied by the anions; an analysis of the void spaces created by removal of the anions clearly shows that the BF_4^- anions are tightly held in the lattice. Indeed, there are anion-ring short contacts clearly visible in the lower half of the cell "diamonds" in Figure 2.13, between

F2 and S1, 2.836(3) Å, F4 and S2' on the adjacent BTD unit, 3.010(4) Å, as well as between N2 and S2', 3.290(3) Å, all of which are less than the sums of the respective v.d. Waals' radii. These are likely to be an important organizing principle in the lattice in accordance with the well-known partial charges $F^{\delta-}$, $N^{\delta-}$ and $S^{\delta+}$. The crystal lattice of **2** is about 8% less dense than that of **1**, even though the proportion of $AgBF_4$ is 20% higher.

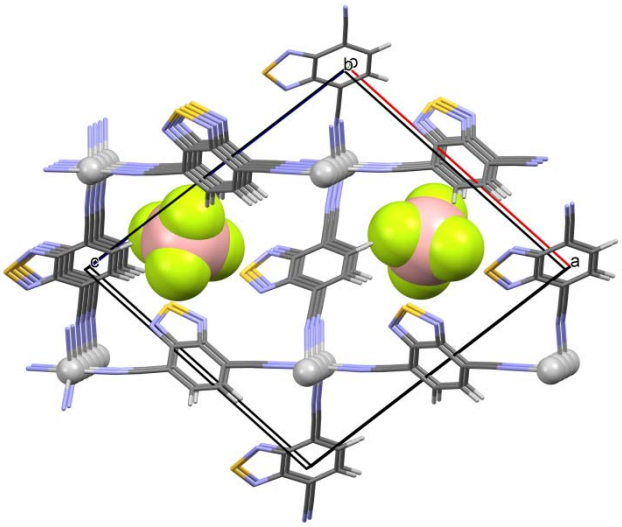

Figure 2.13 Unit cell packing diagram of [Ag(DCBTD)]BF_4 **2** with the ligands and anions depicted by tubes, the silver atoms by spheres and the anions as space-filling. The more open diamondoid lattice from coordination only through C≡N is clearly visible, but the anions are tightly bound within the framework.

2.7.3 Synthesis and Characterization of $[Ag_4(DCBTD)_5][(ClO_4)_4]$ **3**

DCBTD and $AgClO_4$ were weighed and transferred into a round bottom flask containing a magnetic stirrer; benzene was added with stirring and heating to dissolve all solids. On cooling to RT, a precipitate was generated which was collected, dried, and recrystallized from methanol to obtain both powder and crystals of the product. An X-ray quality crystal was selected from the batch and the structure was successfully determined.

The crystal structure determined for **3** is essentially isostructural to that reported above for **1** as can readily be seen by comparing Figures 2.14 with 2.8. Here too there are three crystallographically independent DCBTD ligands, with the one containing S3 located on the two-fold axis. The atom labelled as Ag1 is again four coordinate from three C≡N donors (N7,8,10) and the thiadiazole N1. The Ag–N distances range between 2.180(19) – 2.489(19) Å, very close to the values obtained for **1** despite the difference in anion. The nitrile group from the S1 DCBTD ring, N4, makes a close approach at 3.448(2) Å.

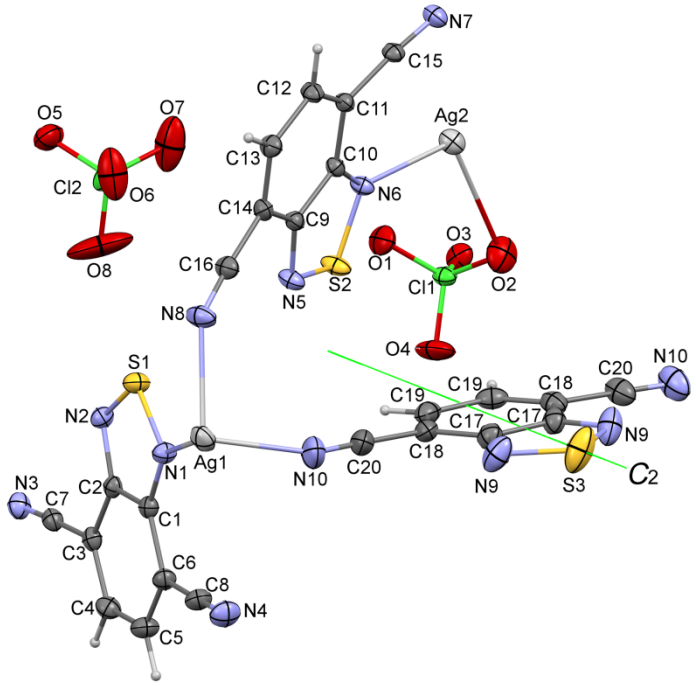

Figure 2.14 Displacement ellipsoids plot of the asymmetric unit in $[Ag_4(DCBTD)_5](ClO_4)_4$ **3** showing the atom numbering scheme. Only half the formula unit belongs to the asymmetric unit and the DCBDT molecule containing S3 is symmetry-duplicated by a two-fold rotation axis indicated as C_2 on the diagram (green line). The view emphasizes that **3** is isostructural with **1**.

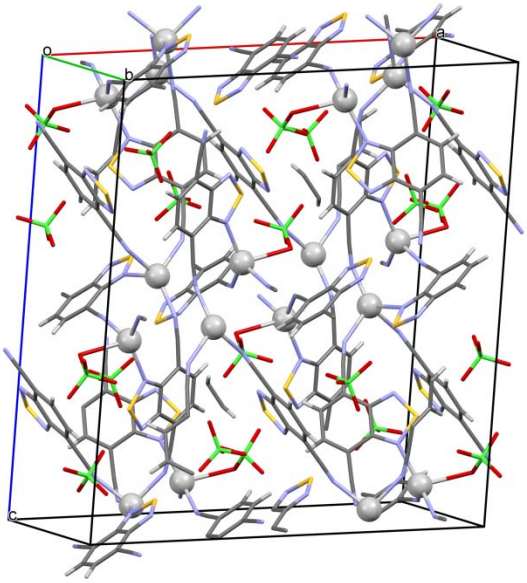

Figure 2.15 Unit cell packing diagram of $[Ag_4(DCBTD)_5][(ClO_4)_4]$ **3** with the ligands and anions depicted by tubes and the silver atoms by spheres.

Table 2.8 Selected bond distances and angles in Å of $[Ag_4(DCBTD)_5][(ClO_4)_4]$ **3**

Ag1 – N10(C≡N)	2.245 (2)	Ag2 - N4(C≡N)	2.265(2)
Ag1 – N7	2.180(19)	Ag1 – N1(ring)	2.489(19)
Ag1 – N8	2.329(2)	Ag2 – N(ring)	2.300(18)
Ag2 – N3(C≡N)	2.236(19)	Ag2 – O(ClO4)	2.703
Ag1 – Ag2	4.488(1)		
N1 – Ag1 – N1	115.15(7)	N4 – Ag2 - N6	123.12(7)
N3 – Ag2 – N4	114.73(8)	N7 – Ag1 – N10	132.10(9)
N3 – Ag2 – N6	134.14(7)	N8 – Ag1 – N1	87.52(9)
N3 – Ag2 – O2	89.40	N8 – Ag1 – N1	91.27(7)
N6 – Ag1 – O2	110.03(8)	N8 – Ag1 – N10	96.01(9)
N7 – Ag1 – N8	104.30		

The atom labelled as Ag2 is three-coordinate, through two nitrile nitrogen atoms (N3,4) and one ring nitrogen N6 (distances range from 2.236(2) – 2.300(2) Å). The distorted

trigonal coordination of this silver ion is also filled out by two sets of contacts less than the sums of the v.d. Waals' radii, to two oxygen atoms of the ClO_4^- ion (distances Ag2–O1 = 2.883(2) and Ag2–O2 = 2.703(2) Å), and the second is a side-on donation from the nitrile group C15≡N7 (distances Ag2–C15 = 3.329(2) and Ag2–N7 = 3.269(2) Å). The main difference from **1** is that Ag2–O2 is here slightly shorter than the sums of covalent radii. Selected bond lengths and angles are presented in Table 2.8. A packing diagram for **3** is provided in Figure 2.15, which also emphasizes the great similarity of the crystal lattice with that found for **1**.

2.7.4 Synthesis and Characterization of $[Ag_2(DCBTD)][(SbF_6)_2].2C_6H_6$ **4**

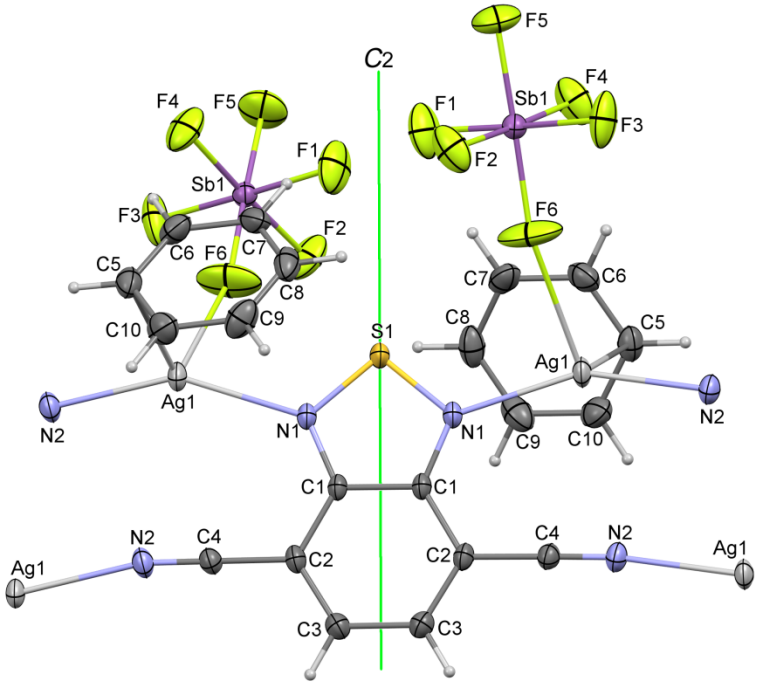

Figure 2.16 Displacement ellipsoids plot of *double* the asymmetric unit in $[Ag_2(DCBTD)][(SbF_6)_2]$.$2C_6H_6$ **4** with the atom numbering scheme. The Ag1 silver ion is shown in total four times. Only half the formula unit belongs to the asymmetric unit, symmetry-duplicated by a two-fold rotation axis indicated as C_2 on the diagram (green line). The high degree of thermal order for the benzene solvent is noteworthy.

DCBTD and $AgSbF_6$ were both dissolved in warm benzene with vigorous stirring in an RBF, cooled to RT, precipitate formed on cooling, was filtered and recrystallized in methanol, to obtained yellow plate crystals, X-ray crystals were selected from the mixture of crystals and powder. The crystal structure was determined at 100 K and 173 K.

This structure differs from all the others principally in its stoichiometry. There are two equivalents of $AgSbF_6$ per DCBTD ligand, and even with *all* the ligand N atoms involved in coordination (i.e. both ring atoms and both C≡N groups) there are only enough donors to provide a dicoordinate Ag^+ environment, which is close to linear. A depiction of the molecular structure is provided in Figure 2.16, and further details of the coordination sphere around silver are provided in Figure 2.17. As expected, the two unique Ag–N distances are quite short at 2.297(17) and 2.234(19) Å (Table 2.9), since there is little competition from other ligands. The N–Ag–N angle is 149.62(7)°, thus approaching linearity as expected for a two-coordinate metal centre. However, this represents a severely coordinatively unsaturated silver environment, and not surprisingly as is evident from the figures, three additional weak donors surround the silver ion to give a distorted trigonal bipyramidal environment. These donors are F6 from the SbF_6^- group at 2.641(2) Å, C6 from η^1–benzene π coordination at 2.589(3) Å, and the side-on nitrile group C4≡N2 which coordinates in this fashion *in addition to* the N2 σ-donor contribution.

The geometry of this interaction is 3.277(2) and 3.253(2) Å for the N and C to Ag^+ distances. Here the silver-fluoride distances, 2.641(2) Å is fully 17% less than the sums of their v.d. Waals' raddi (3.182 Å). The silver-carbon distance, 2.589(3) Å is also very short, at 24% less than the v.d (3.407Å). Waals' sum. For example, in catena-($(\mu^2$-η^2,η^2-

benzene)-perchlorato-silver), both carbon atoms are 2.563(5) Å from Ag^{+},[33] about 25% less than the sum of the v.d. Waals' radii (3.417 Å), so that the coordination in **4** is as strong as observed in a pure benzene-silver π complex.

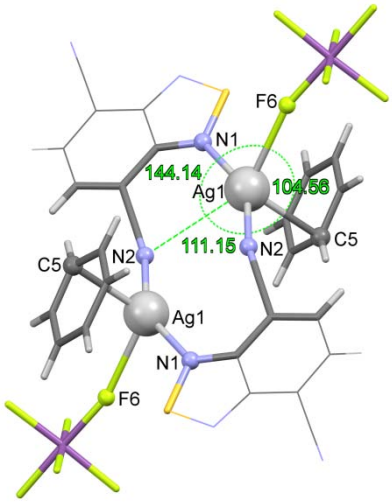

Figure 2.17 The approximately trigonal bipyramidal coordination around the Ag^{+} ion with N1,2 axial and the C≡N, F6 and η^{1}–C_6H_6 filling the equatorial plane. Donor and acceptor atoms drawn as spheres.

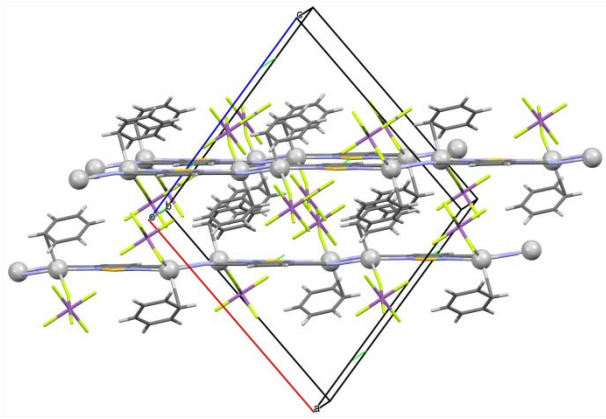

Figure 2.18 The off-set double-layer structure of the crystal lattice in **4** clearly showing the interstitial space occupied by alternating C_6H_6 and SbF_6^{-} groups.

The coordination environment produces an infinite ladder-geometry as is readily appreciated from Figure 2.18, as the structure alternates with a thiadiazole group point "up" and pointing "down" w.r.t. the page orientation; this direction is the crystallographic

b axis. These ribbons are very close to planar and adjacent ribbons are found to be co-planar also, leading to a description of the structure as layers of DCBTD-Ag^+ complexes separated by an intermediate region that "houses" the benzene and anions (Figure 2.18).

The ribbons of DCBTD-Ag^+ are offset by half the *b* distance with each layer, creating a robust interconnected lattice. The perpendicular separation between adjacent least-squares planes is 6.030 Å. The robustness of this lattice possibly explains why the thermal ellipsoids of the benzene rings as well as those of the anions are only slightly larger than those of the in-plane coordinated atoms of DCBTD-Ag^+. Despite this behavior, it can be clearly seen in Figure 2.18 that the benzene molecule lie along four well-defined channels within each unit cell, aligned with the crystallographic *b* axis.

Table 2.9 Showing some selected bond distances and angles in (Å) for $[Ag_2(DCBTD)][(SbF_6)_2]\ .2C_6H_6$ **4**

N2 – Ag	2.234(19)	F6 – Ag	2.641(2)
N1 – Ag	2.297(17)	C5 –Ag	2.589(3)
N2 – Ag – N1	149.62(7)	N1 – Ag – C5	113.13(7)
N2 – Ag – F6	110.53(8)	F6 – Ag – C5	104.56(8)
N1 – Ag – F6	87.17(7)	C5 – Ag – N2	86.91(8)

2.7.5 Synthesis and Characterization of $[Ag(DCBTD)](PF_6).C_6H_6$ **5**

DCBTD in CH_2Cl_2 was layered with $AgPF_6$ in benzene, gave small yellow platelet-like crystals after four days. The structure was determined but could only be solved in space group P1. A depiction of the unit cell is provided in Figure 2.19, which shows considerable evidence of higher symmetry in the true structure, but the intensity data does not support a higher-symmetry solution. Nevertheless, the solution in P1 is of

surprisingly good quality with an R_1 of 0.08 and it is being included in this thesis for the sake of completeness. A detailed reliance on the derived parameters is not warranted, but the main features of the coordination environment can be fully trusted.

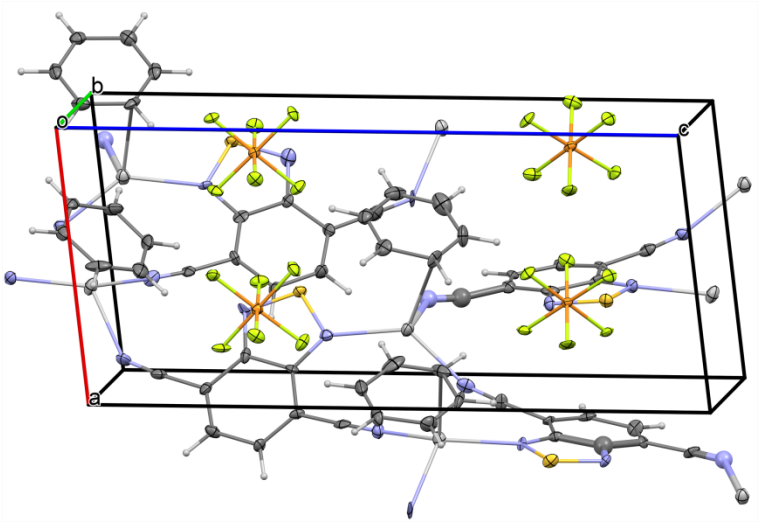

Figure 2.19 Displacement ellipsoids plot of [Ag(DCBTD)]PF_6.C_6H_6 **5** as a unit cell plot in space group *P*1. The local coordination environment is quite similar to that in **4**.

Table 2.10 Showing some selected bond lengths and angles in (Å) for [Ag(DCBTD)]PF_6.C_6H_6

N7 – Ag3	2.451(8)	N3 – Ag4	2.394(9)
N16 – Ag3	2.231(8)	N12 – Ag4	2.268(9)
N9 – Ag3	2.314(9)	N13 – Ag4	2.253(9)
C13S – Ag3	2.577(1)	Ag1 – Ag2	4.488(1)
N9 – Ag3 – N7	97.17(3)	Ag3 – Ag4	4.563(2)
N7 – Ag3 – C13S	103.92(3)	N16 – Ag3 – N7	105.18(3)
N9 – Ag3 – N16	135.87(3)	N12 – Ag4 – N3	92.92(3)
N9 – Ag3 – C13S	93.95(3)	N12 – Ag4 – N13	142.39(3)
N13 – Ag4 – N3	115.05(3)	N16 – Ag3 -C13S	116.13(3)

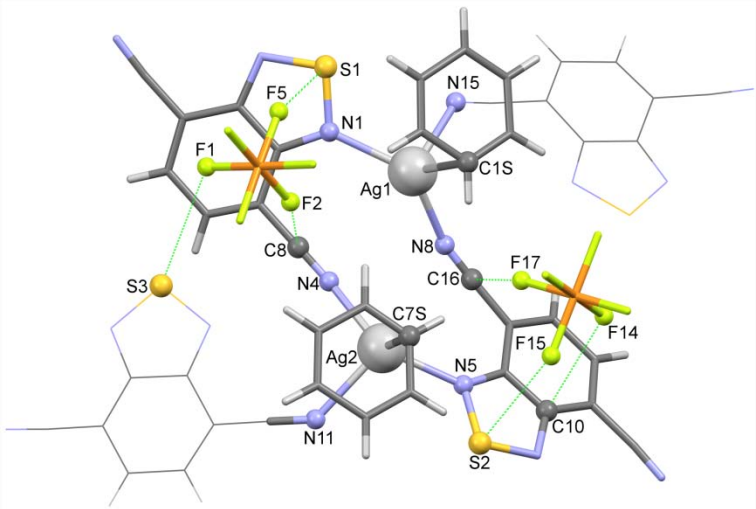

Figure 2.20 Coordination environment of two of four independent silver ions in the crystal structure of [Ag(DCBTD)](PF_6).C_6H_6 **5**. Donor and acceptor atoms drawn as spheres.

The crystal lattice of **5** has incorporated benzene as also observed for **4** and there are other similarities, despite the difference in stoichiometry. Here the DCBTD to Ag^+ ratio is 1:1 rather than 2:1 but there is also one benzene per silver ion. With more ligand to metal available, only the two C≡N and one of the ring N atoms are employed, similar to what is observed for **1** and **3**. Despite these significant changes, the coordination environment at silver is remarkably similar to what is observed for **4** as can be ascertained from comparing Figure 2.19 with Figure 2.16. The primary coordination is again close to linear, involving one C≡N and one ring N donor per silver, with relatively short Ag–N distances, ranging from 2.22(1) to 2.28(1) Å. This is complemented by three weaker donors for an overall trigonal bipyramidal coordination environment involving the adjacent C≡N side-on coordinated (contact distances at Ag·N of 3.42(1), 3.46(1) Å and Ag···C of 3.40(1), 3.40(1) Å somewhat longer than observed for **4**), and an η^1–C_6H_6 group of comparable bond strength to what is observed for **4**. The third "equatorial" site is taken up by a terminal σ-donor C≡N group *in place of* an anion F atom, for which the

N–Ag distances are 2.41(1) and 2.49(1) Å. Thus, the PF_6^- group holds a different function in the lattice and is instead found to have multiple short contacts with the DCBTD ligand, of which the most significant is F2···C8 and F17···C16 which are ~7% less than the sums of the v.d. Waals' radii of F and C.

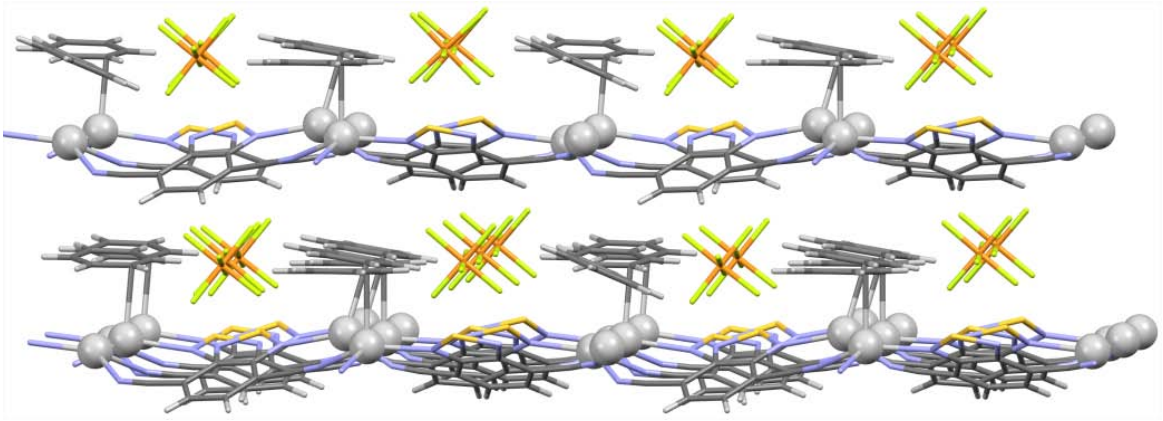

Figure 2.21 The corrugated-layer structure of the crystal lattice in **5** clearly showing the interstitial space occupied by alternating C_6H_6 and PF_6^- groups.

Unlike the regular and quite flat ribbons that associate into layers in **4**, the DCBTD-Ag^+ array in **5** is intrinsically two-dimensional, but the layers are corrugated (Figure 2.21). To these layers are attached the coordinated benzene molecules, here all to one side of the planes. The weakly bound PF_6^- anions fill channels that fit between the benzenes, and the resulting structure has the solvent and anions arranged in a staggered fashion such that there are channels for each in *both* the *b* and *c* directions of the lattice. The inter-planar spacing is approximately 7.12 Å, which is larger than in **4**, despite the fact that the "filling" between the layers is better organized and "thinner" in **5**. The origin of the greater spacing can be found in the corrugation of the DCBTD-Ag^+ layers.

2.7.6 Exploratory ESI Mass Spectroscopic Study

The observations made during the synthesis and in some cases successful recrystallization of **1** – **5** strongly suggested that these silver(I) complexes dissolve by

breaking most or all of the coordinate bonds. To test this hypothesis, $[Ag_4(DCBTD)_5][ClO_4]_4$ was subjected to an ESI mass spectrometric analysis. The solvent that worked best was acetonitrile. Spectra were collected in both positive and negative ion mode. The latter detected the presence of the perchlorate ion with both the parent ion signal and that from loss of one oxygen atom clearly distinguishable. In positive ion mode, the only major peaks could be reliably assigned to Ag^+, $Ag(CH_3CN)^+$ and $Ag(CH_3CN)_2^+$. In particular, no peaks could be attributed to silver adducts of the DCBTD ligand, which supports the notion that these complexes dissociate in CH_3CN.

2.8 Discussion

The preparation of DCBTD from 4,7-dibromo-2,1,3-benzothiadiazole and cuprous cyanide and the optimized work-up described in this thesis is adequate. Issues remain with the purification, which is not fully understood, but the procedure works well enough. The dinitrile is an important intermediate for further derivatisation as will be described in Chapters 3 and 4 of this thesis. The crystal structure of DCBTD has been described for the first time and shows a complex network of short-contacts. This richness of association through the S, ring N and C≡N atoms observed in its crystal lattice was the major inducement to examine the coordination chemistry of this compound as a ligand in its own right.

DCBTD is redox active. Its electrochemical behavior is very similar in both CH_3CN and CH_2Cl_2, with two reversible redox peaks at normal scan rates which correspond to two reduction processes: $-1/0$ at $E_{m1} = -1.06$ V; $-2/-1$ at $E_{m2} = -1.90$ V on the IUPAC-recommended $Fc^{+/0}$ scale. The radical anion stability range is given by $\Delta E = 0.84$ V. The first reduction process is in reasonable agreement with the literature report for the

reduction in aqueous buffer, with $E_{1/2}$ as −0.51 V vs. SCE (approximately −0.89 V vs Fc).[27] The identity of the radical anion as the product of the first reduction was confirmed by *in-situ* reduction in an EPR spectrometer; spectrum agrees well with the literature.[27]

As mentioned in section 1.2 of the Introduction to this thesis, there are very few examples of silver coordination complexes of chalcogenadiazoles of any kind and only a single structurally characterized example of a thiadiazole Ag^+ complex before the work reported in this thesis.[40] The concept of using a helper-donor to expand on the coordinating ability of the BTD group has also been used only once in a very recent paper by Mukherjee et al., who showed that 1,2,5-selenadiazolopyridine forms interesting bimetallic complexes with a variety of metals, including Ag^+.[41] Here it has been shown that DCBTD with two nitrile "helper-donors" is a very capable ligand towards Ag^+ and five new structurally characterized examples are reported.

It is well known that the coordination sphere of silver is very flexible and can adopt different coordination number between two and six, due to its d^{10} valence shell. It is a large and easily polarizable metal, and therefore has the capacity to accommodate a large number of ligands in its coordination sphere.[34] The complexes reported here reflect this flexibility with Ag^+ found in a variety of different geometries and with variable donor sets. A close-to-linear geometry is found in the structures of **4** and **5** from the strongest donors which are a terminal C≡N: and a ring N donor. However, further ligands are required to stabilize the large ion which appear to be selected by their geometrical availability, and can include a side-bonded nitrile, π-bonded benzene, one or more anion fluorine atoms or even a much more weakly-bound terminal nitrile. In the isostructural **1** and **3**, there are three-coordinate trigonal Ag^+ ions with one ring-N and two terminal

C≡N: donors, augmented in this case by weak axial contacts from side-bonded nitrile and anion fluorine atoms. A second kind of Ag^+ is four-coordinate in a quite distorted tetrahedral arrangement, using three terminal C≡N: and one ring N donor. A significantly less-distorted tetrahedral arrangement is found in the beautiful structure of **2** where all the nitrile groups coordinate terminally and no ring N atoms are involved.

In this study, all the silver salts contained what are considered to be "weakly coordinating" anions, namely BF_4^-, ClO_4^-, PF_6^- and SbF_6^-. There does seem to be an influence of the anion on the resultant structure. Thus the first two, which are tetrahedral, are capable of forming isostructural crystal lattices (**1** and **3**), although variability is seen with **2** which is an alternate geometry with the same anion (BF_4^-). The larger octahedral anions PF_6^- and SbF_6^- both result in structures that spontaneously incorporate solvent benzene into the lattice, with the benzene η^1-coordinated to the Ag^+ ion in each case. These results suggest that, despite terminal nitrile N donors being classified as weak compared to strong donors like pyridine, terminal C≡N: was consistently shown to be the best donor from the available options in DCBTD AgX coordination polymers. The π electron delocalization in DCBTD is weaker, hence the ability of the ring N to donate electron for coordination is low. The Ag–N bond lengths are within the well-known literature values of 2.085 to 2.979 Å.[35,.36, 37,38,] In summary the Ag–N bond lengths in each of the complex are $[Ag_2(DCBTD)](SbF_6)_2.2C_6H_6$ 2.234(19) – 2.297(17), $[Ag_4(DCBTD)_5](ClO_4)_4$ 2.180(19) – 2.489(19), $[Ag(DCBTD)](PF_6)$ 2.231(8) -2.451(8), $[Ag_4(DCBTD)_5](BF_4)_4$ 2.1762(19) – 2.480(4), $[Ag(DCBTD)_2]BF_4$ 2.225(4) – 2.304(4) Å. The Ag–N bond lengths of terminal C≡N: (an average of 2.209 Å) are found generally shorter than Ag–N from the thiadiazole ring (an average of 2.473 Å.)

2.9 References

1. Pilgram, K.; Skile, R. D. *J. Heterocycl. Chem.* **1974,** *11*, 777-780.
2. Mikroyannidis, J. A.; Tsagkournos, D. V.; Sharma, S. S.; Vijay, Y. K.; Sharma, G. D. *J. Mater. Chem.* **2011,** *21*, 4679-4688.
3. Xu, S.; Liu, Y.; Li, J.; Wang, Y.; Cao, S. *Polym. Adv. Technol.* **2010,** *21*, 663-668.
4. Beecken, H. *Chem. Ber.* **1967,** *100*, 2164-2169.
5. Akhtaruzzaman, M.; Tomura, M.; Nishida, J.-I.; Yamashita, Y. *J. Org. Chem.* **2004,** *69*, 2953-2958.
6. Nunn, A. J.; Ralph, J. T. *J. Chem. Soc.* **1965,** 6769-6777.
7. Misra, R.; Gautam, P.; Jadhav, T.; Mobin, S. M., *J. Org. Chem.* **2013,** *78*, 4940-4948.
8. Neto, B. A. D.; Correa, J. R.; Silva, R. G., *RSC Adv.* **2013,** *3*, 5291-5301.
9. Neto, B. A. D.; Lapis, A. A. M.; Da Silva, E. N., Jr.; Dupont, J. *Eur. J. Org. Chem.* **2013,** *2013*, 228-255.
10. Chivers, T.; Krouse, I.; Parvez, M.; Vargas-Baca, I.; Ziegler, T.; Zoricak, P. *Inorg. Chem.* **1996,** *35*, 5836-5842.
11. Sun, X.; Zhuang, X.; Ren, Y., *Adv. Mater. Res. (Durnten-Zurich, Switz.)* **2012,** *482-484*, 1221-1224.
12. Cozzolino, A. F.; Vargas-Baca, I.; Mansour, S.; Mahmoudkhani, A. H. *J. Am. Chem. Soc.* **2005,** *127*, 3184-3190.
13. Son, J. H.; Jang, G.; Lee, T. S. *Polym. Adv. Technol.* **2013,** *54*, 3542-3547.
14. Hassan, M. R. Self-Assembled Molecular Rods and Squares with Chalcogenadiazole Framework Ligands. University of Lethbridge, Lethbridge, 2010.
15. Grubb, C. J.; Cole-Hamilton, D. J.; Whittlesey, M. K. *J. Chem. Soc., Faraday Trans.* **1996,** *92*, 5005-5012.
16. Robinson, J. N.; Cole-Hamilton, D. J. *Chem. Soc. Rev.* **1991,** *20*, 49-94.
17. Schieferstein, R. H.; Pilgram, K. *J. Agric. Food Chem.* **1975,** *23*, 392-395.
18. Vanelle, P.; Liegeois, C. T.; Meuche, J.; Maldonado, J.; Crozet, M. P. *Heterocycles* **1997,** *45*, 955-962.
19. Pilgram, K.; Skiles, R. D. *J. Heterocycl. Chem.* **1974,** *11*, 777-780.
20. Garo, F.; Häner, R. *Eur. J. Org. Chem.* **2012,** *2012*, 2801-2808.
21. Koopman, H.; van Daalen, J. J.; Daams, J., *Weed Res.* **1967,** *7*, 200-207.
22. Baldwin, R. W. W. Defoliant 2,1,3-benzothiadiazole-4,7-dicarbonitriles. US3501285A, 1970.
23. Gallardo, H.; Conte, G.; Tuzimoto, P. A.; Behramand, B.; Molin, F.; Eccher, J.; Bechtold, I. H. *Liquid Crystals* **2012,** *39*, 1099-1111.
24. M.Colapietro, A. D.; Portalone, G.; Schultz, G.; Hargittai, I. *J.Mol.Struct.* **1984**, 141.
25. Akhtaruzzaman, M. T. M.; Yamashita, Y. *Cryst. Struct. Commun.* **2001,** *C57*, 751-753.
26. Kato, S.; Matsumoto, T.; Ishi, T.; Thiemann, T.; Shigeiwa, M.; Gorohmaru, H.; Maeda, S.; Yamashita, Y.; Mataka, S. *Chem. Commun.* **2004,** 2342-2343.

27. Camilleri, P.; Dearing, A.; Cole-Hamilton, D. J.; O'Neill, P. *J. Chem. Soc., Perkin Trans. 2* **1986,** 569-572.
28. Inagaki, S., Fukushima, Y., Kuroda, K, *J. Chem. Soc., Chem. Commun.* **1993**, 680-682.
29. Ratilainen, J.; Airola, K.; Fröhlich, R.; Nieger, M.; Rissanen, K., *Polyhedron* **1999,** *18*, 2265-2273.
30. Duward, E. S., Atkins, P. W., Langford, C. H. *Inorganic Chemistry*. Oxford University Press: New York, 1990; p 34.
31. Liddle, B. J.; Hall, D.; Lindeman, S. V.; Smith, M. D.; Gardinier, J. R. *Inorg. Chem.* **2009,** *48*, 8404-8414.
32. McKechnie, J. S.; Paul, I. C. *J. Chem. Soc.* **1968**, 1445-1452.
33. McMullan R. K., K. F., Fritchie C. J. J. *Acta Crystallogr., Sect. B: Struct. Sci.* **1997,** *53*, 645.
34. Tsutsui, Y.; Sugimoto, K.-I.; Wasada, H.; Inada, Y.; Funahashi, S. *J. Phys. Chem. A* **1997,** *101*, 2900-2905.
35. Shoeib, T.; El Aribi, H.; Siu, K. W. M.; Hopkinson, A. C. *J. Phys. Chem. A* **2001,** *105*, 710-719.
36. Shorock, C. J.; Xue, B. Y.; Kim, P. B.; Batchelor, R. J.; Brain O. P.; Leznoff, D. B. *Inorg. Chem.* **2002,** *41*, 6743-6753.
37. Bowmaker, A.; Effendy, G.; Junk, P. C.; White, A. H. *J. Chem. Soc., Dalton Trans.* **1998**, 2131-2138.
38. Bowmaker, A.; Effendy, G.; Junk. P.C.; White, A. H. *J. Chem. Soc., Dalton Trans.* **1998**, 2139-2146.

CHAPTER 3: DIETHYL-2,1,3-BENZOTHIADIAZOLE-4,7-DICARBOXYLATE

3.1 Introduction to diethyl 2,1,3-benzothiadiazole-4,7-dicarboxylate

Along the way towards harnessing 2,1,3-benzothiadiazole-4,7-dicarboxylates as bridging ligands for coordination polymers and MOFs, it was necessary to prepare the corresponding esters. The first preparation of such esters was already outlined by Pilgram and Skiles in their attempts to prepare the dicarboxylic acid.[1] Later, because of interest in redox active π-conjugated molecules that have well-defined, luminescent properties for use as photosensitizers and electron transfer agents, Grubb and co-worker repeated and extended the synthesis of esters of 2,1,3-benzothiadiazole-4,7-dicarboxylic acid.[2] Since then, little further work has been reported on this interesting class of compounds.

The preparation of esters appears to be a necessary step in the conversion of 2,1,3-benzothiadiazole-4,7-dicarbonitrile to the dicarboxylic acid. The crude hydrolysis product is first converted to an acid chloride, then to diethyl ester, and the latter can then be hydrolyzed once again to the acid. The conversion of ester to acid requires a fine balance and control of the reaction, because desulfurization of the thiadiazole with the formation of ortho-benzenediamine is a competing reaction (see Section 4.4).

In the course of our work it was realized that the diesters themselves might be good ligands for coordination polymers based in part on computed charges showing the ester carbonyl and the thiadiazole nitrogen atoms as having particularly high concentrations of negative charge density. Here the synthesis and characterization of the ethyl ester, diethyl 2,1,3-benzothiadiazole-4,7-dicarboxylate (DEBTD), is described and its use in the formation of coordination polymers.

3.2 Synthesis of DEBTD

Synthesis of the ester is achieved in a two-part reaction. In the first step (Scheme 3.1), DCBTD is hydrolyzed by refluxing with an excess of 25% aqueous sodium hydroxide until evolution of ammonia ceases as monitored with moist litmus. The crude acid was recovered by evaporation along with the NaCl by-product, and the mixture was then thoroughly dried using a vacuum desiccator. Subsequently this mixture was suspended in thionyl chloride and heated to reflux, cooled and filtered. The evaporated filtrate contains 2,1,3-benzothiadiazole-4,7-dicarbonyl dichloride (Scheme 3.1) along with an unknown impurity.

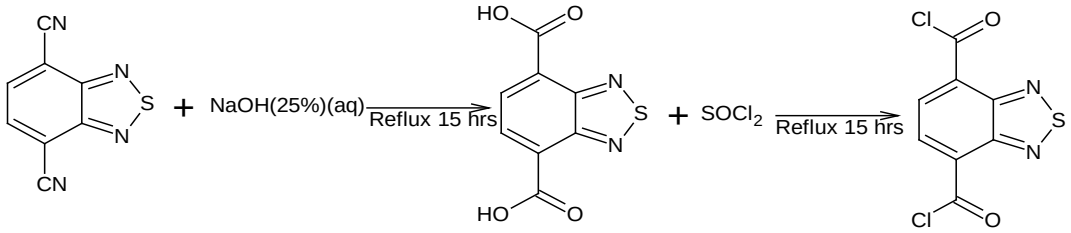

Scheme 3.1 Synthesis of 2,1,3-benzothiadiazole-4,7-dicarbonyl dichloride

In a second step, this diacid dichloride is converted to the ethyl ester (Scheme 3.2) by refluxing with ethanol in pyridine. Upon quenching with water, the crude product is decolorized with activated charcoal and recrystallized from *n*-hexane to afford the product as pale yellow needles in 51% overall yield. Formation of the compound was confirmed by comparing the melting point, IR and NMR spectra with literature values.[3]

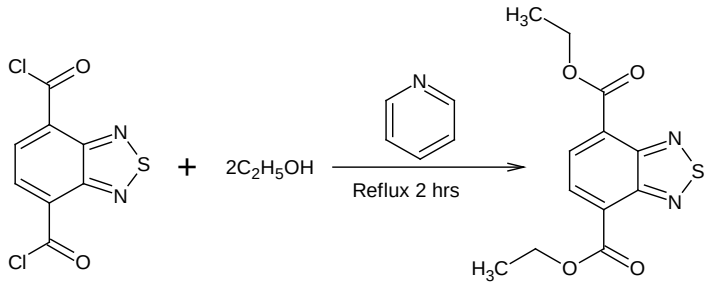

Scheme 3.2 Synthesis of DEBTD

3.2.1 IR and NMR of DEBTD

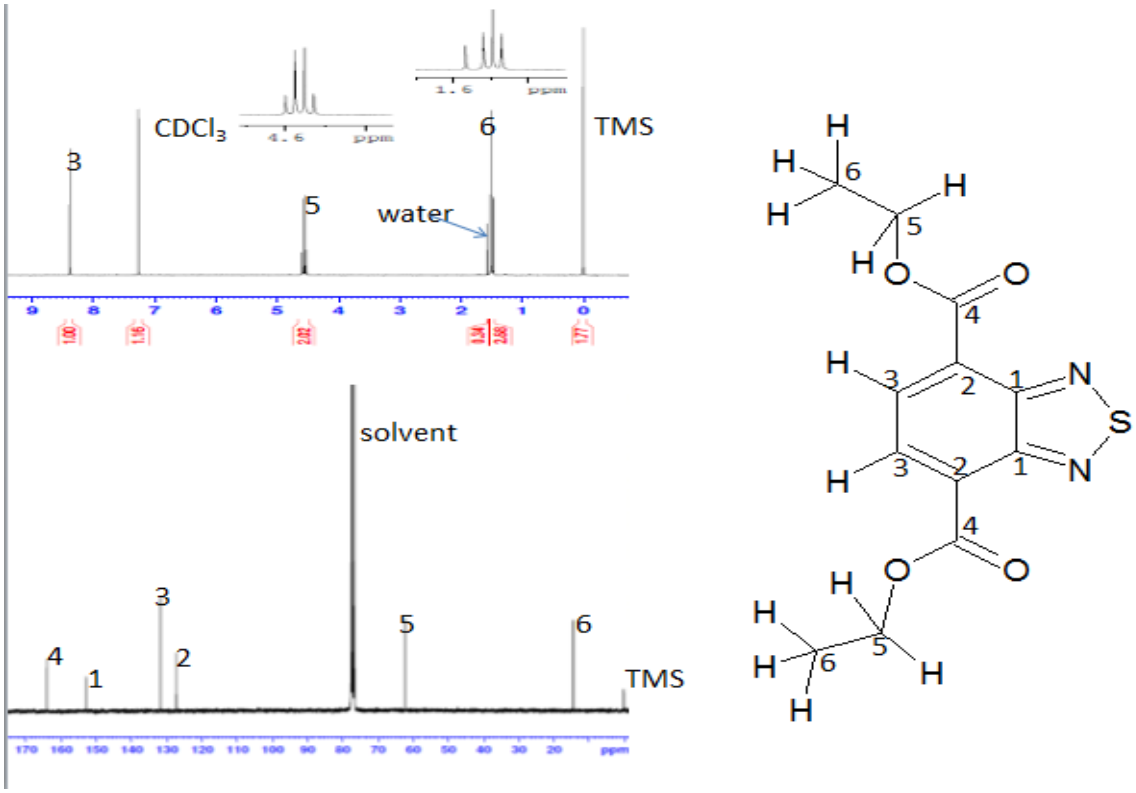

Figure 3.1 ^{1}H (top) and ^{13}C (bottom) NMR spectra of DEBTD with peaks labeled according to the structure diagram.

The ^{1}H NMR spectrum contains the expected signals for the three kinds of protons in the structure. The two protons on the benzene ring are equivalent and integrate to 2 at 8.39 ppm, the CH_2 display the expected quartet at 4.56 ppm and integrate to 4. The methyl protons form a triplet at 1.50 ppm with integration of six. The ^{13}C NMR displays six distinct peaks labeled 1 – 6 as shown in Figure 3.1 above, the quaternary carbon atom labeled 1 at 152.95 ppm has a small intensity due to slow relaxation and lack of nuclear Overhauser enhancement. The carbon labeled 2 at 127.36 ppm is the atom through which the ester substituent groups are attached to the ring. Atom 3 at 131.91 ppm is the carbon atom carrying the ring hydrogens and has the expected high intensity. Carbon 4 at 164.10

ppm is the carbonyl C, while the methylene C is at 62.33 ppm and the methyl C is found at 14.52 ppm.

3.3 X-Ray Crystallography of DEBTD

The structure of this compound was further confirmed by X-ray crystallography. The X-ray characterization reports two conformers in the same structure, with the carbonyl oxygen and the ethyl groups in different orientations. The crystal packing (Figure 3.2) clearly shows the mixture of *endo/exo* and *endo/endo* conformers, which curiously are linked *each to its own kind*. Thus the former connects through a short carbonyl oxygen to thiadiazole sulfur link S1···O3 = 3.144(4) Å; these connect into chains aligned with the *b* axis of the cell. The latter forms a NBI side-by-side dimer typical of thiadiazoles via a centrosymmetric S··N contact of 3.145(4) Å. These pairs of identical molecules stack along the *a* axis of the cell. Both conformers possess short "bay" region ΘN contacts ranging from 2.769(5) to 2.915(5) Å in length.

The most interesting bands in the IR spectrum are the carbonyl bands, ν(C=O), which appear as near equal intensity bands at 1702 and 1735 cm^{-1}. The frequency difference is 33 cm^{-1}. It seems possible that this outcome reflects the presence of the two conformers in the solid state. In support of this notion, B3LYP/6-31+G(2d,p) hybrid DFT calculated vibrational spectra predict a single band at 1751 cm^{-1} for the *endo/endo* conformer, but two bands at 1749 and 1781 cm^{-1} for the *exo*/*endo* conformer, and indicate that when a carbonyl group is aligned with the S–N bond this becomes a higher energy vibration. For comparison, diethylterephthalate displays a single band at 1727 cm^{-1}.[4]

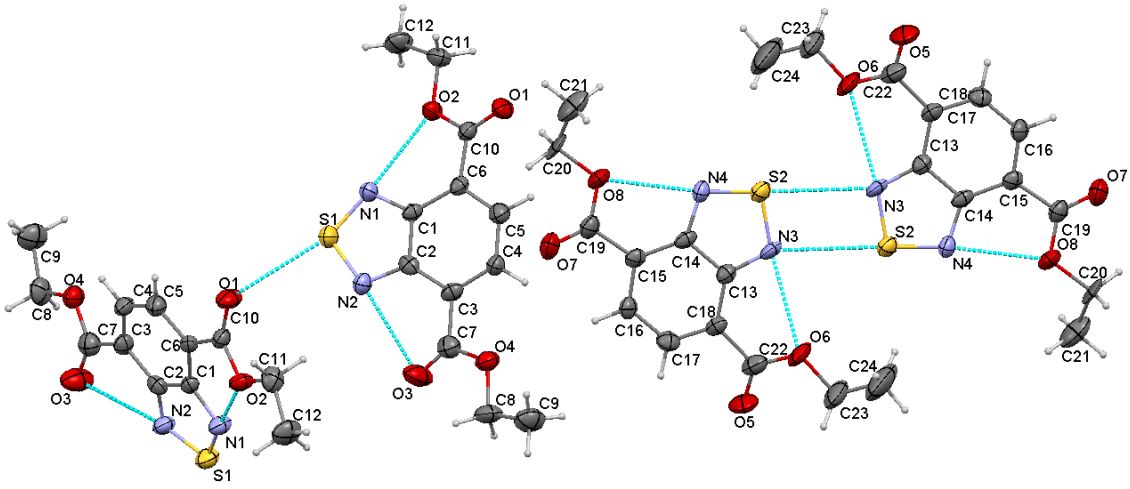

Figure 3.2 Thermal ellipsoids plot of the two independent molecules (*endo/exo* and *endo/endo* conformers) in the crystal structure of DEBTD with the atom numbering scheme. The most important short contacts link molecules of the same type as shown.

Table 3.1 Crystal data and structure refinement for DEBTD

Empirical formula	$C_{12}\ H_{12}\ N_2\ O_4\ S$	
Formula weight	280.30	
Temperature	173(2) K	
Crystal system	Monoclinic	
Space group	P2(1)/n	
Unit cell dimensions	*a* = 4.0605(18) Å	α = 90°
	b = 15.698(7) Å	β = 90.393(6)°
	c = 39.737(17) Å	γ = 90°
Z	8	
Goodness-of-fit on F^2	0.836	
Final R indices [I>2sigma(I)]	R1 = 0.0617, wR2 = 0.1160	
R indices (all data)	R1 = 0.2252, wR2 = 0.1541	

Table 3.2 Selected bond distances (Å), angles in (°) and short contacts in the mixture of endo/exo and endo/endo isomers of DEBTD.

Distance	Å	Distance	Å	Distance	Å
S(1)-N(1)	1.611(4)	S(2)-N(3)	1.610(4)	S(2)-N(4)	1.604(4
S(1)-N(2)	1.630(4)	N(3)-C(13)	1.354(6)	C(8)-C(9)	1.493(6
N(1)-C(1)	1.351(5)	N(4)-C(14)	1.356(6)	C(23)-C(24)	1.378(8)
N(2)-C(2)	1.352(5)	O(5)-C(22)	1.202(6)	C(6)-C(10)	1.498(6),
O(1)-C(10)	1.207(5)	O(6)-C(22)	1.309(6)	C(20)-C(21)	1.481(7),
O(2)-C(10),	1.344(5)	O(6)-C(23)	1.473(6)	C(5)-C(6)	1.377(6)
O(2)-C(11)	1.475(5)	O(7)-C(19)	1.194(6)	C(18)-C(22)	1.490(7)
O(3)-C(7)	1.193(6)	O(8)-C(19)	1.315(6)	C(4)-C(5)	1.422(6)
O(4)-C(7)	1.361(6)	O(8)-C(20)	1.456(5)	C(17)-C(18)	1.349(6)
O(4)-C(8)	1.476(5)	C(13)-C(18)	1.433(6)	C(3)-C(7)	1.508(7)
C(1)-C(2)	1.442(6)	C(13)-C(14)	1.441(6)	C(16)-C(17)	1.409(6)
Angle	°	Angle	°	Angle	°
N(1)-S(1)-N(2)	102.3(2)	C(7)-O(4)-C(8)	116.2(4)	C(10)-O(2)-C(11)	115.5(4)
C(1)-N(1)-S(1)	105.4(3)	C(3)-C(2)-C(1)	120.5(4)	C(24)-C(23)-O(6)	109.2(5).
C(2)-N(2)-S(1)	105.0(3)	C(4)-C(3)-C(2)	116.6(5)	O(5)-C(22)-C(18)	121.2(6)
C(4)-C(3)-C(7)	122.5(5)	C(22)-O(6)-C(23)	112.9(4)	O(6)-C(22)-C(18)	114.8(5)
C(2)-C(3)-C(7)	120.9(5)	C(19)-O(8)-C(20)	115.9(4)	O(8)-C(20)-C(21)	107.7(5)
C(3)-C(4)-C(5)	123.3(5)	N(3)-C(13)-C(18)	127.7(5)	O(5)-C(22)-O(6)	124.0(5)
C(6)-C(5)-C(4)	122.2(5)	N(3)-C(13)-C(14)	112.3(4)	O(7)-C(19)-C(15)	121.2(5)
C(5)-C(6)-C(1)	116.5(4)	C(18)-C(13)-C(14)	119.9(5)	O(8)-C(19)-C(15)	113.4(5)
C(5)-C(6)-C(10)	117.2(5)	N(4)-C(14)-C(15)	127.5(4)	C(14)-N(4)-S(2)	106.9(3)
C(1)-C(6)-C(10)	126.3(4)	N(4)-C(14)-C(13)	112.8(5)	O(7)-C(19)-O(8)	125.3(5)
O(3)-C(7)-O(4)	123.0(5)	C(15)-C(14)-C(13	119.7(5)	C(13)-N(3)-S(2)	107.1(3)
O(3)-C(7)-C(3)	126.5(5)	C(16)-C(15)-C(14)	117.7(5)	C(13)-C(18)-C(22)	125.4(5)
O(4)-C(7)-C(3)	110.5(5)	C(16)-C(15)-C(19)	116.8(5)	O(2)-C(11)-C(12)	107.2(4)
O(4)-C(8)-C(9)	107.4(4)	C(14)-C(15)-C(19)	125.5(5)	C(17)-C(18)-C(22)	116.9(5)
O(1)-C(10)-O(2)	124.4(5)	C(15)-C(16)-C(17)	122.6(5)	O(2)-C(10)-C(6)	112.7(4)
O(1)-C(10)-C(6)	122.9(4)	C(18)-C(17)-C(16)	122.4(5)	C(17)-C(18)-C(13)	117.8(5)

3.4 Voltammetry of DEBTD

The electrochemical measurements were carried out with the same measurement conditions as for the dinitrile, starting with degassed 2.5×10^{-5} M solutions of the compound in MeCN and CH_2Cl_2 with 0.1 M $[^nBu_4N][PF_6]$ as supporting electrolyte. The measurements were carried out in cyclic voltammetry (CV) and square wave voltammetry (SWV) modes, in a conical electrochemical cell, three electrode configuration with a glassy carbon working electrode. CVs were obtained over a scan rate of 0.05 – 1.00 Vs^{-1}. Potential data are reported according to IUPAC recommended scale

versus the ferrocene/ferrocenium redox couple as an internal standard at 0.00 V. The compound in both MeCN and CH_2Cl_2 with $[^nBu_4N][PF_6]$ as supporting electrolyte gave rise to two reduction processes which appear to involve one electron transferred at each process, both processes are close to reversible and the $I_p^{ox} = I_p^{ox}$ or $I_p^{ox}/I_p^{ox} = \sim 1$. The peak-to-peak separation of anodic (E_p^a) and cathodic (E_p^c) processes of 51 mV is close to electrochemically reversible behavior. The two processes of reduction are as follows: −1/0 wave with $E_{m1} = -1.36$ V, −2/−1 wave with $E_{m2} = -1.96$ V and $|\Delta E| = 0.60$ V. The analyte behaved the same way in both solvents and a representative CV trace is shown in Figure 3.3. For purposes of comparison, the parent BTD has been reported to show a single reversible redox process with the half-wave reduction potential $^{red}E_{1/2}(I) = -1.98$ V vs. Fc/Fc^+ in CH_2Cl_2.[5] Thus the ester substituents impart a significant lowering of the LUMO energy compared to BTD. However, by comparison with DCBTD (Section 2.5.1) the ester substituents exercise a significantly lesser electron withdrawing effect on the LUMO than do nitrile substituents. It may also be significant that the values of the *second* reduction are very similar in the two compounds. As a result, DEBTD has a reduced "stability window" for the radical anion that is ~30% smaller than DCBTD.

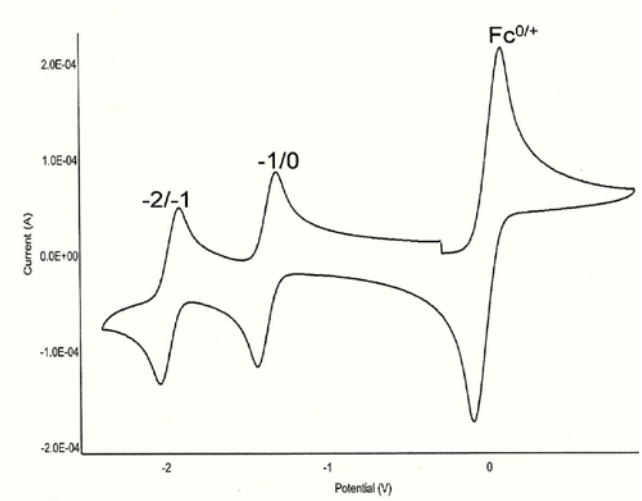

Figure 3.3 CV curve of DEBTD

3.5 EPR Spectroscopy of DEBTD

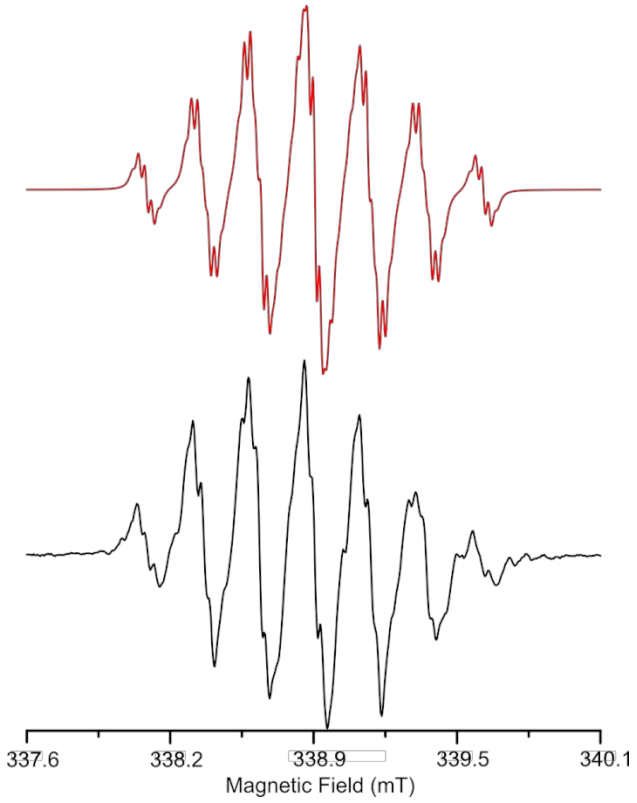

Figure 3.4 Top: experimental first derivative EPR spectrum obtained during the reductive electrolysis of DEBTD at RT in CH_2Cl_2 (0.1 M [$^nBu_4N$][PF_6]). Bottom: simulation with LW of 0.019 mT

The electrochemical EPR reduction experiment was conducted in CH_2Cl_2 noting that the CV in both MeCN and CH_2Cl_2 gave the same result, that is, the solvent had no interference in the reductive behavior of the compound under analysis. The reductive electrolysis gave a very strong EPR signal (Figure 3.4) with one electron reduction for the generation of the radical anion of diethyl-2,1,3-benzothiadiazole-4,7-dicarboxylate ($DEBTD^{-\bullet}$). The splitting pattern obtained was a result of the hyperfine coupling of both nitrogen and hydrogen nuclei in the system. Two nitrogen atoms in the thiadiazole ring, $2NI + 1$ rule, and N spin 1 gave 5 lines. Additional coupling with the two protons split

the 5 lines further into three each and due to overlap resulted in seven lines. The seven lines are split further into smaller multiplets by the methylene protons. The parameters employed in the simulation are: $2 \times a(^{14}N) = 0.231$ mT, $2 \times a(^{1}H) = 0.274$ mT, $4 \times a(^{1}H) = 0.027$ mT. Uncertainty in the hyperfine coupling for this compound is a result of the broad lines, which may reflect some slowed re-orientational motion of the ethyl groups if in fact there are preferred orientations of the ester functional group in solution.

3.6 Synthesis and characterization of DEBTD complexes of Ag^+

Like the dinitrile, the preparation of these complexes was first carried out by reacting the ligand in CH_2Cl_2 (lower layer) and the different silver salts in benzene (upper layer) through liquid-liquid layering. This procedure resulted in the formation of X-ray quality crystals of the complexes of three Ag^+ salts (ClO_4^-, PF_6^- and SbF_6^-). In all three cases, the small golden blocks of crystals were accompanied by a considerable amount of powder. In other cases, such as BF_4^- and ClO_4^-, the reactions only gave powdered solids. In these two cases, both the ligand and silver salt were placed in benzene, warmed and stirred for 30 minutes to dissolve, and on cooling precipitates were generated, which were filtered and dried. Upon recrystallization from methanol, crystalline samples of complexes of Ag^+ salts with BF_4^- and ClO_4^- counterions were obtained. The perchlorate complex from this method yielded a different structure from that prepared by solvent layering.

In both the layering and the recrystallization processes, the X-ray quality crystals used for the crystallography were sorted from the bulk product under a microscope. Unlike the diversity observed for the dinitrile coordination polymers, all five crystallized in $P2_1/c$. The products fall into three groups, a silver perchlorate that is unsolvated, **6**, a perchlorate

7, hexafluoroantimonate **8** and hexafluorophosphate **10** that are benzene solvates and a tetrafluoroborate **9** that is a hydrate.

Table 3.3 A summary of crystal data and structure refinement of DEBTD silver complexes

Complex	**6**	**7**	**8**	**9**	**10**
Formula	$[AgL]ClO_4$	$[AgL]ClO_4 \cdot C_6H_6$	$[AgL]SbF_6 \cdot C_6H_6$	$[AgL]BF_4 \cdot H_2O$	$[AgL]PF_6 \cdot C_6H_6$
Temp, K	100(2)	173(2)	173(2)	173(2)	173(2)
Crystal system	Monoclinic	Monoclinic	Monoclinic	Monoclinic	Monoclinic
Space group	$P2_1/c$	$P2_1/c$	$P2_1/c$	$P2_1/c$	$P2_1/c$
Unit cell: *a*, Å	12.665(4)	13.6993(10)	12.348(2)	8.4724(5)	14.019(4)
b, Å	10.002(3)	13.1459(10)	13.159(3)	13.3979(7)	13.195(3)
c, Å	13.728(4)	13.7246(10)	14.255(3)	14.8753(8)	14.079(3)
β, °	133.868(4)	118.157(1)	90.089(2)	99.107(1)	119.521(2)
V, $Å^3$	1590.3(8)	2179.2(3)	2316.2(8)	1667.25(16)	2266.1(9)
Z	4	4	4	4	4
Density, g/cm^3	2.037	1.724	2.013	1.964	1.792
GOF	0.992	1.009	1.073	1.028	1.023
R_1	0.0386	0.0453	0.0326	0.0246	0.0550
wR_2	0.0942	0.1284	0.0781	0.0585	0.1544

3.6.1 Synthesis and Characterization of $[Ag(DEBTD)]ClO_4$, **6**

This complex was synthesized by layering a solution of $AgClO_4$ in benzene over a solution of DEBTD in CH_2Cl_2 in a crystallization tube, which gave X-ray quality crystals after a few days' evaporation. IR spectroscopy was used to ascertain that a complex had formed (see section 6.4.2), and a crystal was selected and a successful structure

determination was accomplished (crystal parameters are in Table 3.3; selected interatomic distances and angles in Table 3.4).

In the structure (Figure 3.2), the DEBTD ligand is close to flat and is in the *exo/exo* conformation (unlike the free ligand, see Figure 3.5) so that it chelates the Ag^+ using the carbonyl oxygen O3 and the thiadiazole nitrogen N1. The structure is extremely simple and the unique silver Ag1 is also coordinated by O1 and N2 (from a different DEBDT molecule). The metal coordination environment is completed by two bridging perchlorate oxygen atoms, forming a centrosymmetric AgO_2Ag bridge to the next DEBDT chelate. Whilst the Ag^+ ion is thereby six-coordinated, the geometry is quite distorted, with the bond angles around the metal between 71.3(1) – 107.1(1)°. Bond distances between Ag^+ and N ranged between 2.371(4) – 2.466(3) Å, which is within known Ag–N bond lengths,[6] while that of the Ag^+–O (carbonyl) is 2.609(3) – 2.611(3) and Ag^+–O (ClO_4^-) is 2.419(4) – 2.685(3) Å.

There are some significant differences between the bond angles of the thiadiazole ring of the ligand from that of the complex which are as much as 1.89 °, due to the strain induced on the ring by the bond formation for the formation of the complex One could have expect this strain to reduce S1-N1-C1 and S1-N2-C2 bond angles and increase those of N1-S1-N2, N2-C2-C1 and N1-C1-C2, but what is observed is the reverse. If a plane is defined by ligand C_6N_2S atoms (rms deviation 0.02 Å), then the Ag1 atom is only 0.165(5) Å out of the plane at N1, O3, but 1.002(5) o.o.p. at N2, O1. Conversely, the corresponding carbonyl oxygen donors are o.o.p. by 0.398(5) Å (O1) and 0.239(5) Å (O3). The considerable strain involved in fitting the second chelate ring around the Ag^+ ion may factor in the formation of fairly robust solvate structures (see below.) The pairs

of Ag^+ ions bridged by perchlorate concentrate within a well-defined plane, parallel to the *bc* face and half-way along the *a* axis (Figure 3.6). The DEBTD ligands are oriented so that the ethyl groups point above and below these planes, resulting in a regular layered structure with metal ions at the middle of the *a* axis and ethyl groups (hydrocarbons) along the unit cell *bc* faces.

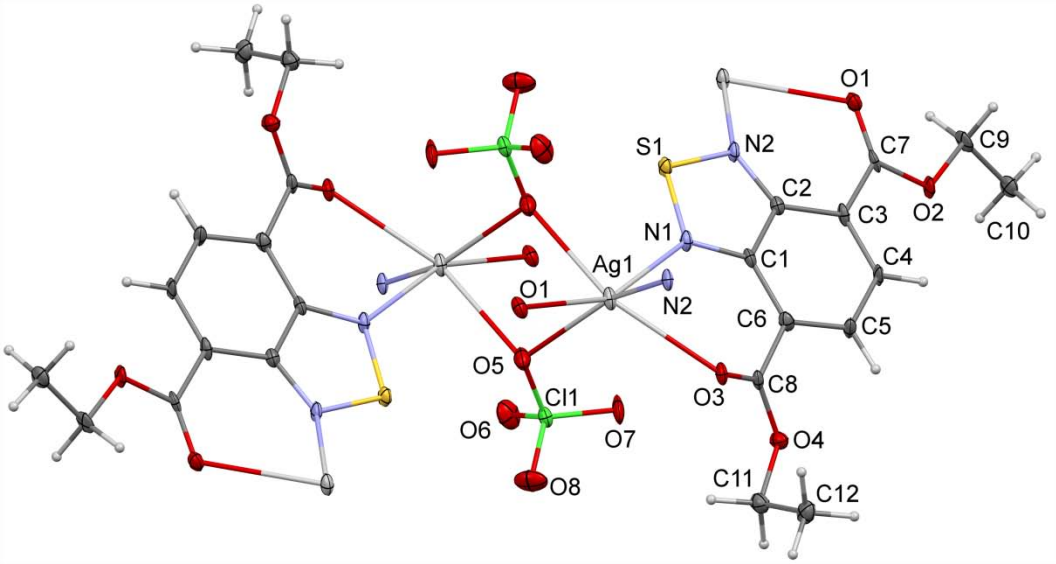

Figure 3.5 Thermal ellipsoids plot (40% probability) of a centrosymmetric chelate complex in the crystal lattice of [Ag(DEBTD)]ClO_4. The atom numbering scheme is shown for the asymmetric unit (but note that O1 and N2 are repeated at Ag1).

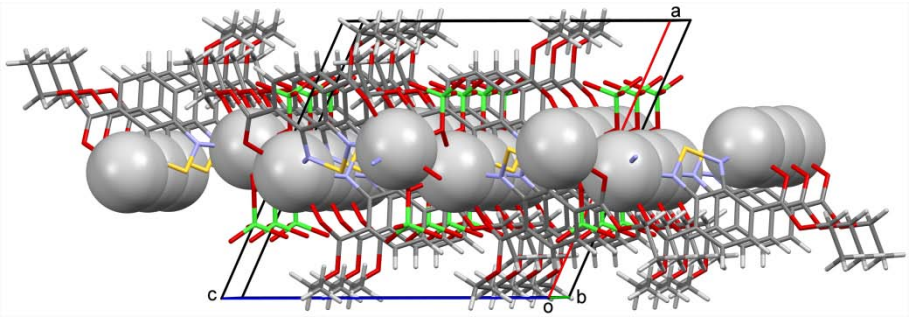

Figure 3.6 A packing diagram of the crystal lattice of [Ag(DEBTD)]ClO_4, **6**. The view is approximately down the *b* axis, with the ligand and anions represented by tubes, and the Ag^+ ions as spheres of v.d. Waals' radii. The layer structure is clearly visible.

Table 3.4 Selected bond distances (Å) and angles in (°) for $[AgL]ClO_4$, **6**

Parameter	Å or °	Parameter	Å or °
Ag1-O5	2.685(3)	N2-S1	1.629(3)
O5-Ag1	2.419(4)	C2-N2	1.353(5)
O5-Cl	1.468(4)	C1-N1	1.360(4)
Ag1-N1	2.466(3)	Ag1-O1	2.611(3)
Ag1-N2	2.372(4)	C7-O1	1.212(6)
Ag1-O3	2.609(2)	C7-O2	1.334(4)
N1-S1	1.614(4)	O5-Ag1-O5	71.30(1)
Ag1-O5-Ag1	108.70(1)	S1-N1-C1	108.00(3)
Ag1-N1-C1	131.50(3)	Ag1-O5-Cl1	116.80(2)
C2-N2-Ag1	127.80(3)	O1-C7-O2	124.60(4)
S1-N2-C2	107.40(3)	Ag1-O1-C7	119.90(3)
Ag1-N2-C2	127.80(3)	O3-C8-O4	125.10(4)

3.6.2 Synthesis and Characterization of $[Ag(DEBTD)]ClO_4.C_6H_6$, **7**

A solution of DEBTD in benzene and $AgClO_4$ in benzene was heated to dissolve the perchlorate salt. After cooling, the precipitate was recrystallized from methanol to obtain crystals which were determined by X-ray crystallography to be $[Ag(DEBTD)]ClO_4.C_6H_6$ (Figure 3.7a). Unlike the denser ClO_4^- crystal obtained by solvent layering, this crystal has large void spaces between the layers that are filled by the solvent (benzene). It is *quite remarkable* that benzene is selectively taken up during recrystallization from methanol.

The silver ion has a coordination number of 5 and is approximately square pyramidal, but as can be seen in the figure, there are also short contacts with benzene in an η^2 fashion to C4A, 2.99(2) Å, 13% less than the sums of the v.d.Waals' radii, and C3S, 3.35(3) Å, 2%

less than v.d. Waals'.[7] It should be noted that these must be regarded as very weak η^2 benzene linkages; for example, in catena-((μ^2-η^2,η^2-benzene)-perchlorato-silver), both carbon atoms are 2.563(5) Å from Ag^+,[8] about 25% less than the sum of the v.d. Waals' radii. This Ag-C distances is very typical and a quick survey of about 30 different benzene-silver complexes where the silver is also coordinated by O or N ligands, yielded only one example where much longer contacts exists for a solvate benzene in the proximity of Ag^+.[9]

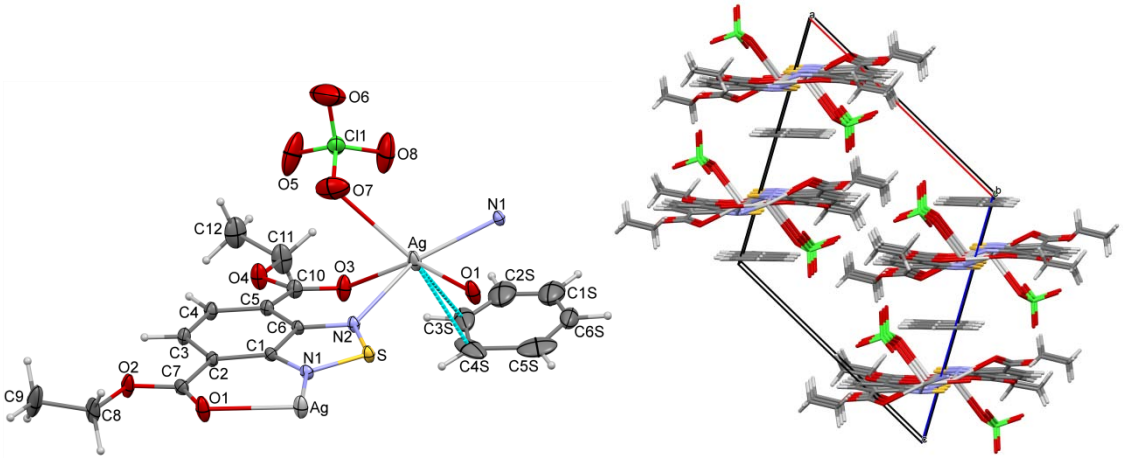

(a) (b)

Figure 3.7 (a) Thermal ellipsoids plot (20% probability) of the asymmetric unit in the crystal lattice of $[Ag(DEBTD)]ClO_4 \cdot C_6H_6$. The atom numbering scheme is shown for the asymmetric unit (but note that Ag, O1 and N2 are repeated). (b) A packing diagram with the atoms drawn as tubes, viewed down the unit cell *b* axis. The solvate benzene molecules fill long columns along the *b* axis direction.

Just as in the solvent free complex, each Ag^+ is chelated twice by the DEBTD ligand *via* both carbonyl oxygen (C=O) and ring N atoms of the ligand. The bond lengths of Ag^+–N ranges from 2.288(3) – 2.371(3) Å and Ag^+–O of the ligand between 2.464(3) - 2.551(3) Å. The single Ag^+–O distance to the ClO_4^- anion is 2.689(9) Å and thus equal to the *longer* of the two such distances in the unsolvated complex **6**. If a plane is defined by the

DEBTD C_6N_2S ring atoms (rms deviation 0.03 Å), then the Ag1 atom is 0.233(4) Å out of the plane at N1, O1, but 0.778(4) o.o.p. at N2, O3. The corresponding carbonyl oxygen donors are o.o.p. by 0.087(6) Å (O1) and 0.439(6) Å (O3). This very unsymmetrical environment of the two chelating rings is very similar to that observed for **6**, despite a different coordination number and disposition of the ligands about the metal ion.

Table 3.5 Selected bond distances (Å) and angles in (°) for $[Ag(DEBTD)]ClO_4.C_6H_6$, **7**.

N1-Ag	2.288(3)	C6-N2	1.356(4)
N2-Ag	2.371(3)	S-N1	1.619(3)
Ag-O3	2.464(3)	C1-N1	1.346(4)
Ag-O1	2.551(3)	N1-Ag	2.288(3)
Ag-O7	2.689(9)	C7-O1	1.204(5)
N2-S	1.602(3)	O7-Ag-N1	112.10(2)
N1-Ag-O1	73.10(1)	O3-Ag-O1	145.60(1)
O1-Ag-N2	78.50(1)	O3-C10-O4	123.20(5)
N2-Ag-O3	72.60(1)	O1-C7-O2	123.20(5)
O3-Ag-O7	78.40(2)	N2-S-N1	99.70(2)
S-N1-Ag	115.30(2)		

It should also be noted that this structure shows a much higher degree of thermal motion, especially for the anion and solvate, than was observed for **6**. This raises the question of whether the structure actually has full occupancy of the benzene (or even the $AgClO_4$); therefore the occupancy of each was separately tested by an independent parameter refinement for each in separate steps and combined. No significant deviation from full

occupancy was detected by this analysis. Thus, the benzene molecules seem to be well trapped in the lattice even though they are located along continuous channels (Figure 3.7b) and despite the high degree of thermal motion. The crystal structure was determined soon after the crystals were harvested. However, over time the crystals do seem to lose solvent. The question we have not answered yet is whether the crystal structure will remain or collapse in the absence of the solvent.

3.6.3 Synthesis and Characterization of ([Ag(DEBTD)]SbF_6.C_6H_6, **8**

The complex was synthesized by layering a solution of $AgSbF_6$ in benzene over a solution of DEBTD in CH_2Cl_2. The solution was kept in the fume hood and through slow evaporation and gradual mixing of these two solutions, crystals were gradually formed at the interface, then gradually dropped to the bottom of the crystallization tube and harvested after a few days. The IR spectrum was used to determine that a complex had formed, with a new single carbonyl band at 1687 cm^{-1}.

The Ag^+ in this compound, as for **7**, is chelated twice by the ester C=O and a ring N. It has coordination number 4 and the AgN_2O_2 coordination sphere is very close to planar (deviations range 0.03 – 0.13 Å), but with the DEBTD ligands tilted out of this plane by 17.0 and 20.5°.[10] The four angles around the Ag^+ are N1-Ag-O3 75.18(8), N2-Ag-O3 80.39(8), N2-Ag-O1 73.58(8), N1-Ag-O1 131.32(8)°. The Ag^+ is coordinated to two carbonyl oxygens (C=O) with bond distances of 2.536(2), 2.416(2) and to the ring N atoms of the thiadiazole with bond distances of 2.350(2), 2.269(2). Just as for **7**, there are also short contacts with benzene in an η^2 fashion to C1S, 2.890(5) Å, 15% less, and C2S, 3.099(5) Å, 9% less than the sums of the v.d.Waals' radii, so that the benzene is somewhat more strongly attached to the silver ion though these are still weak for such

linkages. A possible origin for the stronger silver-carbon contacts may be found in the weaker "coordination" of the anion. The Ag–F contact distances are 2.861(7) Å to F3 and 3.128(8) Å to F5. This may be compared to an average Ag–F distance of 2.6(1) Å from nine crystal structures in the Cambridge Structural Database. Only one previously reported structure contains such a weakly-attached SbF_6^- anion at silver, in which the short contact is 3.002(4) Å to a single F atom.[9] Note that in the structure of **8**, the SbF_6^- anion is positionally disordered with the indicated major component (54% occupancy). The minor component (46% occupancy) is twisted such that only F3A is oriented towards silver, with an Ag-F3A distance of 2.80(1) Å.

Table 3.6 Selected bond distances (Å) and angles in (°) for $[AgL]SbF_6.C_6H_6$

N2-Ag	2.352(4)	S-N2	1.610(4)
O3-Ag	2.535(4)	C2-N2	1.338(6)
O1-Ag	2.418(4)	C1-N1	1.349(7)
Ag-N1	2.260(4)	N2-Ag	2.352(4)
N1-S	1.1616(4)	O3-C10	1.207(6)
O1-Ag-N2	73.60(1)	O3-C10-O4	124.90(5)
N2-Ag-O3	79.70(1)	O1-C7-O2	123.50(5)
O3-Ag-N1	75.10(1)	Ag-O3-C10	126.90(3)
N1-Ag-O1	131.90(1)	Ag-O1-C7	127.90(3)
Ag-N10-S	117.00(2)	N1-C1-C6	127.10(4)
N2-S-N1	99.60(2)	N2-C2-C3	127.40(4)

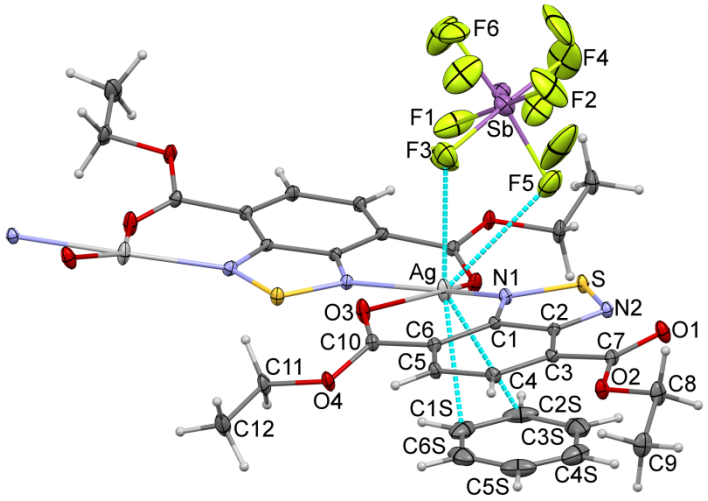

Figure 3.8 Thermal ellipsoids plot (20% probability) of the chelated Ag^{+} complex in the crystal lattice of $[Ag(DEBTD)]SbF_6 \cdot C_6H_6$. The atom numbering scheme is shown for the asymmetric unit. Short intermolecular contacts from Ag to η^2-C_6H_6 and to the major component of the disordered SbF_6^- anion are shown as dashed tubes.

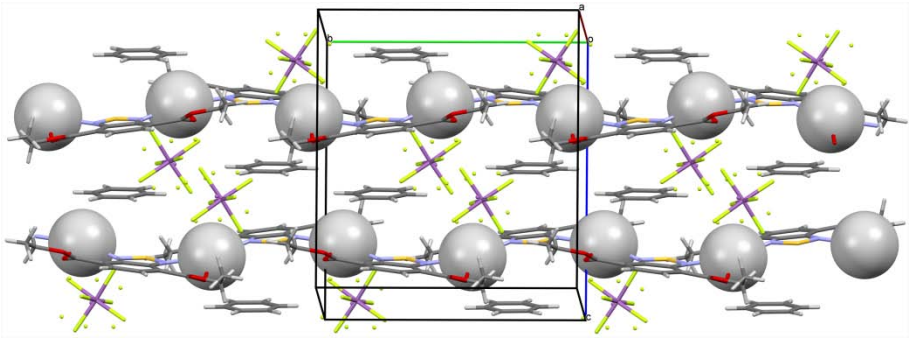

Figure 3.9 A packing diagram of $[Ag(DEBTD)]SbF_6 \cdot C_6H_6$ with the atoms drawn as tubes except silver, which are spheres with the v.d. Waals' radius. The *b* axis is horizontal and the view is approximately down the *a* axis. The layer structure of the coordination polymer is shown with benzene and SbF_6^- arranged between the layers.

The arrangement of the crystal lattice is shown in Figure 3.9 which shows that the DEBTD-silver complex forms ribbons in the *b* direction, which further aggregate into weakly-corrugated layers parallel to the *ab* planes. Between these layers are the anions

(SbF_6^-) and the benzene rings which occupy the void spaces in the lattice (along with a few of the ethyl groups from the diester), with benzene positions alternating with SbF_6^-. The distance between the complex layers is on the average of 6.188 Å.

3.6.4 Synthesis and Characterization of $[Ag(DEBTD)]BF_4.H_2O$, **9**

This complex was obtained by heating together a solution of DEBTD in benzene and $AgBF_4$ in benzene with stirring for about 30 minutes. The precipitate generated on cooling was recrystallized from methanol which gave the crystals. IR spectroscopy was used to ascertain that a complex had formed and X-ray quality crystals were sorted with the use of a microscope. A structure determined on a single crystal is shown in Figure 3.11.

Unlike what is observed for **7** and **8**, the silver atom in **9** is distinctly square pyramidal with the Ag 0.730 Å above the plane defined by C=O and N from the ligands. This plane also contains the whole of both DEBTD rings. The fifth site on Ag^+ is occupied by a strongly-bound water ligand through O5. Bond distances to the ligand are: Ag^+-O2 2.417(2), Ag^+-O3 2.507(2), Ag^+-N2 2.292(2), Ag^+-N1 2.470(2) and Ag^+-O5 2.374(2) Å. The Ag^+ sphere coordination angles are O3-Ag-N2 74.95(6), N2-Ag-O1 112.39(6), O3-Ag-N1 78.25(5), N1-Ag-O1 72.12(6), N2-Ag-O5 127.49(6)°. The bonding to water in this complex appears to be quite strong. A survey of sixteen crystal structures in the CSD which have a terminal H_2O ligand attached to Ag^+ along with two other N and O donors indicated a mean Ag-O distance of 2.5(1) Å, with a range of 2.150(2) - 2.638(4) Å and a median value of 2.477 Å. The reported structure with a distance closest to that in **9** is a mixed pyridyl/carboxylate coordination polymer with Ag-O = 2.291(6) Å.[10]

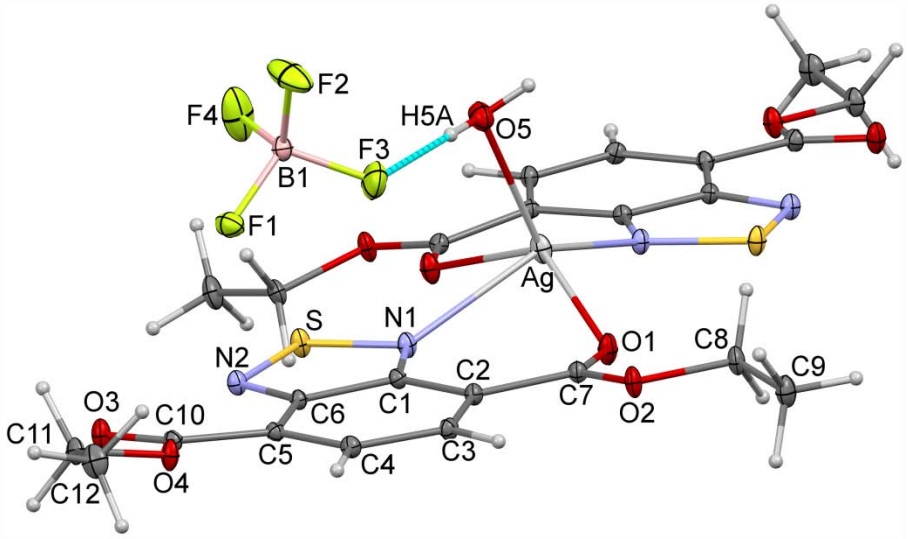

Figure 3.10 Thermal ellipsoids plot (20% probability) of the chelated Ag^{+} complex in the crystal lattice of $[Ag(DEBTD)]BF_4 \cdot H_2O$. The atom numbering scheme is shown for the asymmetric unit. The hydrogen bond between F3 and the water molecule O5 is indicated by a dashed tube.

Table 3.7 Selected bond distances (Å) and angles in (°) for $[Ag(DEBTD)]BF_4 \cdot H_2O$

Ag-O5	2.374(2)	O1-C7	1.208(3)
Ag-O3	2.507(2)	O3-C10	1.205(3)
Ag-O1	2.417(2)	N1-S	1.609(2)
Ag-N2	2.292(2)	S-N2	1.616(2)
Ag-N1	2.470(2)	O3-Ag-N2	74.95(6)
N2-Ag-O1	112.39(6)	O5-Ag-N2	127.49(6)
Ag-O1-C7	132.50(1)	Ag-N1-C1	128.60(1)
O1-Ag-N1	72.12(6)	Ag-N2-S	119.45(9)
Ag-N1-S	120.78(9)	Ag-N2-C6	131.10(1)
O5-Ag-O3	107.08(6)	Ag-O3-C10	131.20(1)
O5-Ag-N1	86.31(6)		

The BF_4^- anions are arranged with bridging H bonding from F3 to H5A and F1 to H5B, forming a chain along the *b* axis. These anions do not interact further with the silver ions

or any other constituents of the unit cell. The packing of the regular layers in the structure is shown in Figure 3.12 by a view down the crystallographic *b* axis. Strictly speaking, the DEBTD ligands form a double-layer slightly offset above and below each other. Each such double-layer is bridged by silver ions above and below, with the water molecules approximately vertical. The BF_4^- ions intercalate amongst these waters. Subsequent double-layers of DEBTD are stepped to accommodate the water-anion H-bonding (which runs vertically in the view shown in Figure 3.12). Separation between the double layers is regular at 3.256 Å.

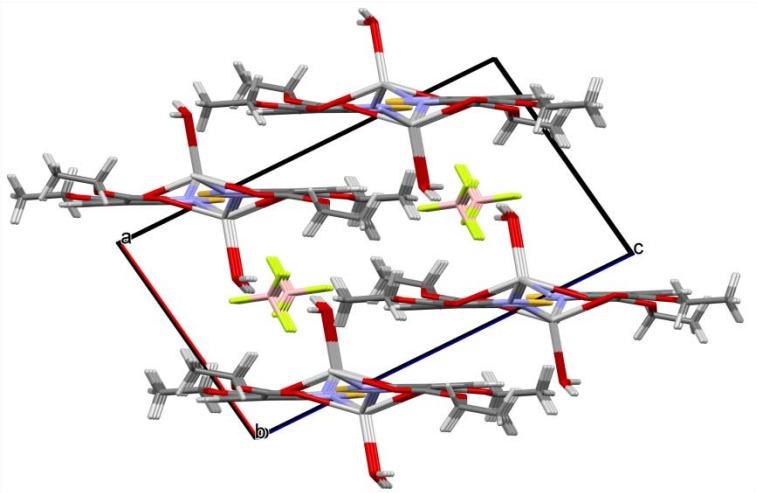

Figure 4.11 A packing diagram of [Ag(DEBTD)]BF_4·H_2O viewed down the *b* axis.

3.6.5 Cyclic Voltammetry of [Ag(DEBTD)]BF_4·H_2O, **9**.

A mass spectroscopic analysis of this complex was carried out in solution by electrospray techniques, resulting in a spectrum that is very similar to that of the other complexes see (section 3.7.2) The natural question to consider is what other evidence there is for DEBTD coordinated to silver in solution. To that end, a cyclic voltammetry study was undertaken in the same solvent, CH_3CN, as used for the ESI-MS.

The cyclic voltammogram for this complex was measured in CH_3CN under argon at RT. A representative trace without internal reference is shown in Figure 3.13 below. There are two waves at negative potentials ($E_{1/2}$ of these reversible waves occurs at -1.16 V and -1.74 V) which appear to be identical to that of DEBTD with very small shifts in potential to higher voltage. The third, highly distorted wave attributed to the reduction and re-oxidation of Ag^+, has a sharp cathodic peak potential at +0.028 V and a strongly offset re-oxidation wave, typical for surface-deposited metal.

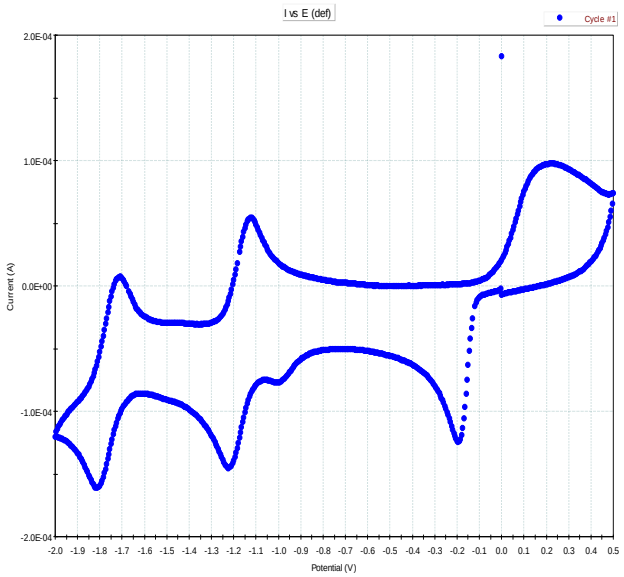

Figure 3.12 Cyclic voltammograms of $[Ag(DEBTD)]BF_4 \cdot H_2O$ in CH_3CN (0.1 M $[^nBu_4N][PF_6]$ at RT.

With ferrocene added as internal standard, we found that the ferrocene 0/+ wave overlapped completely with that of silver 0/+, making it non ideal for calibration (Fig. 3.14).

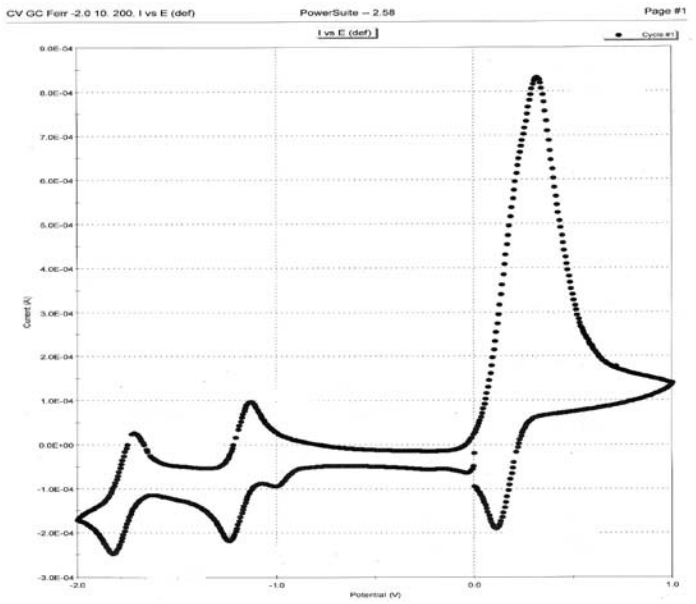

Figure 3.13 Cyclic voltammetry of $[Ag(DEBTD)]BF_4 \cdot H_2O$ in CH_3CN (0.1 M $[^nBu_4N][PF_6]$ at RT, with Fc as reference

Cobaltocenium ion was therefore used as the internal reference to establish the potentials that have been quoted above. Even though one of its two potentials overlaps with one of the two potentials of the analyte, the $Cc^{+/0}$ couple could be used to establish the voltage scale correctly as shown in Figure 3.15 below. Notice also the improved resolution for the silver bands in the positive region of the voltammogram.

The conclusion reached from the voltammetry is that there seems to be no effect from silver coordination on the redox properties of DEBTD in solution; if complexed ligand does participate in the redox process, either the potentials are not affected or the concentration of such complex ions are too low compared to those of disassociated ligand and metal ion.

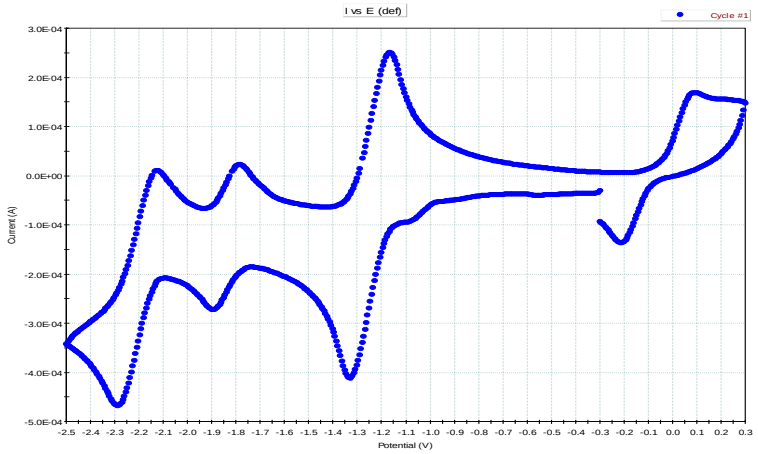

Figure 3.14 Cyclic voltammetry [Ag(DEBTD)]$BF_4 \cdot H_2O$ in CH_3CN (0.1 M [^{n}Bu_4N][PF_6] at RT, with cobaltocenium hexafluorophosphate as reference.

3.6.6 Synthesis and Characterization of [Ag(DEBTD)]$PF_6 \bullet C_6H_6$), **10**.

A solution of DEBTD in CH_2Cl_2 was layered with a solution of $AgPF_6$ in benzene, and evaporated slowly in the fume hood, yielding colorless needle crystals. IR spectroscopy was used to confirm the new product with a shift in the C=O band from 1702 and 1735 cm^{-1} of the diester to 1690 cm^{-1}, a downward shift like all other ester complexs we reported above. We attribute the downward shift to a chelating effect on the C=O band due to complex formation. X-ray quality crystals were selected using a microscope, and the structure determined by X-ray diffraction. The structure was solved in the monoclinic crystal system in space group $P2_1/n$, a non-standard setting for the space group $P2_1/c$.

The local structure (Figure 3.15) is very similar to that of SbF_6^- salt **8** (compare Figure 3.8) The coordination sphere around Ag^+ is also slightly distorted square planar,[11,12] with a bond distance of Ag^+-O1 2.411(5), Ag^+-O3 2.545(6), Ag^+-N1 2.265(4), Ag^+-N2 2.372(3) and the bond angle as O1-Ag-N1 133.13(1), O3-Ag-N1 73.89(2), N2-Ag-O3

80.63(1), O1-Ag-N2 73.41(1). There are again short contacts with benzene in an η^2 fashion to C1S, 2.897(8) Å, 15% less, and C2S, 3.122(75) Å, 9% less than the sums of the v.d.Waals' radii. The Ag–F contact distances are 2.808(8) to F2 and 2.897(8) Å to F2. Of all these dimensions, only the Ag-N2 distance is significantly different from the corresponding values in **8** at the 99% confidence level.

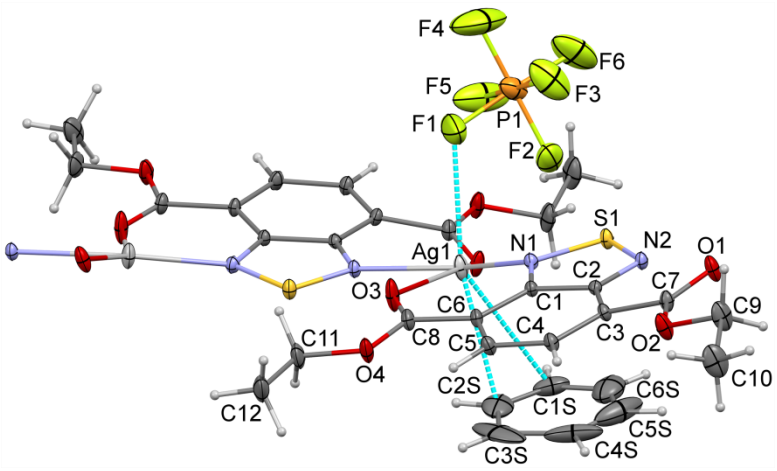

Figure 3.15 Thermal ellipsoids plot (20% probability) of the chelated Ag^+ complex in the crystal lattice of $[Ag(DEBTD)]PF_6 \cdot C_6H_6$. The atom numbering scheme is shown for the asymmetric unit. Short intermolecular contacts from Ag to η^2-C_6H_6 and to F1 of the PF_6^- anion are shown as dashed tubes.

Thus, the crystal structures of **8** and **10** can be considered *isostructural*. The only significant difference occurs in the anions, which are ordered for **10** and disordered in **8**. This similarity in structure is highlighted in the overlay diagram (Figure 3.17) which shows that the two lattices have slightly differently disposed atom positions, the major shifts being in the anion positions (although only the major component of the SbF_6^- is shown).

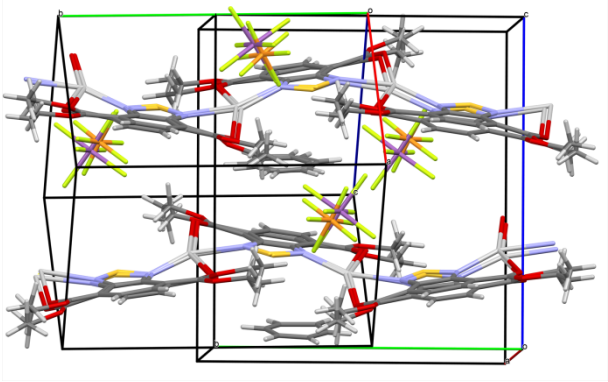

Figure 3.16 Extended packing-type diagrams of [Ag(DEBTD)]PF_6·C_6H_6 and [Ag(DEBTD)]SbF_6·C_6H_6 overlaid to emphasize their isostructural character. Note the different cell outlines resulting from $P2_1/c$ versus $P2_1/n$.

Table 3.8 Selected bond distances (Å) and angles in (°) for [Ag(DEBTD)]PF_6·C_6H_6

N2-Ag	2.372(2)	N1-S	1.625(4)
O1-Ag	2.411(5)	S-N2	1.608(4)
O3-Ag	2.545(6)	O1-C7	1.210(7)
Ag-N1	2.265(4)	O3-C8	1.209(9)
O1-Ag-N2	73.40(1)	O1-Ag-N1	133.10(1)
Ag-O1-C7	128.40(3)	N2-S1-N1	99.80(2)
Ag-N2-C3	128.00(3)	Ag-N1-C1	133.60(3)
Ag-N2-S1	122.10(2)	Ag-O3-C8	130.90(4)
S-N1-Ag	117.10(2)	O1-C7-O2	123.70(5)
N2-Ag-O3	80.60(1)	O3-C8-O4	123.70(5)

3.7 Discussion

3.7.1 Infra-red spectroscopy in the coordination polymers of DEBTD with Ag^+

Infrared spectroscopy was the first method we used to determine the formation of these complexes, looking at the "coordination shift" of the carbonyl band from that of the free ligand (ν(C=O) 1702 and 1735 cm^{-1}) in the metal complexes. In each case, a significant shift occurred, as shown in Table 4.9 below. The observed changes in the IR spectra of the ligand and that of the complexes were shifts of absorptions to a lower wavenumber. The literature indicates that in ester complexes, ν(C=O) shifts to lower and ν(C–O) to higher frequency by complex formation.[13] The X-ray structures have shown that **6 – 10** are all chelates with the ester in *exo/exo* conformer. Taking the 1735 cm^{-1} for the *exo* conformer, the coordination shifts range from 37 to 48 cm^{-1}, with a slight trend of a larger $\Delta(\nu_{CO})$ for a lower coordination number at silver.

Table 3.9 showing the difference between the carbonyl band of the ligand (C=O) from that of their complexes

	Ligand/Complex	IR band, cm^{-1}	$\Delta(\nu_{CO})$,[a] cm^{-1}	CN	Geometry
	Ester = DEBTD	1702 and 1735	n/a	n/a	n/a
1	$[Ag(DEBTD)]ClO_4$	1698	37	6	dist. octahedral
2	$[Ag(DEBTD)]ClO_4 \bullet C_6H_6$	1695	38	5+	sq. pyramidal
3	$([Ag(DEBTD)]BF_4 \bullet H_2O$	1697	40	5	sq. pyramidal
4	$[Ag(DEBTD)]PF_6 \bullet C_6H_6$	1690	45	4+	sq. planar
5	$[Ag(DEBTD)]SbF_6 \bullet C_6H_6$	1687	48	4+	sq. planar

[a] This is calculated from the 1735 cm^{-1} band which is taken to be that of the *exo* conformer.

3.7.2 Solution-phase mass spectrometry by ESI of **6-10**

Solution phase mass spectrometry was conducted on all the Ag^+ coordination polymers of DEBTD and the results are summarized in Table 3.10. A representative spectrum with labels of the purported species is provided in Figure 3.18 below. For each entry in the table below, the relative abundance of the peak is shown, as well as the disagreement parameter for the mass from that of the ideal mass calculated for the formula. Only in a few cases are peaks observed that are attributable to the (protonated) ligand itself, but a peak that fits well for the ligand less one EtO^- group is present in all the spectra. The agreement between theory and measurement for each species is excellent.

The most abundant peaks are always from Ag^+ and its solvates with acetonitrile, which is consistent with large-scale dissociation of the coordination polymer in solution. However, unlike the case for the nitrile complexes of DCBTD, there are peaks present in the ESI spectra for ligand coordinated to silver and even two ligands coordinated to a single silver ion. This suggests that the affinity for complexation is higher, which may be attributed to the chelating ability of DEBTD which is missing in DCBTD. Despite this mass spectrometric evidence, the solution voltammetry study of **9** does not show any apparent influence from silver coordination on the redox properties of DEBTD. The best solvent for all the esters was CH_3CN, the average spray voltage was 3.0 KV, and cap temperature 275 °C. The identities of as many fragments as possible were determined using a high-resolution mass calculator,

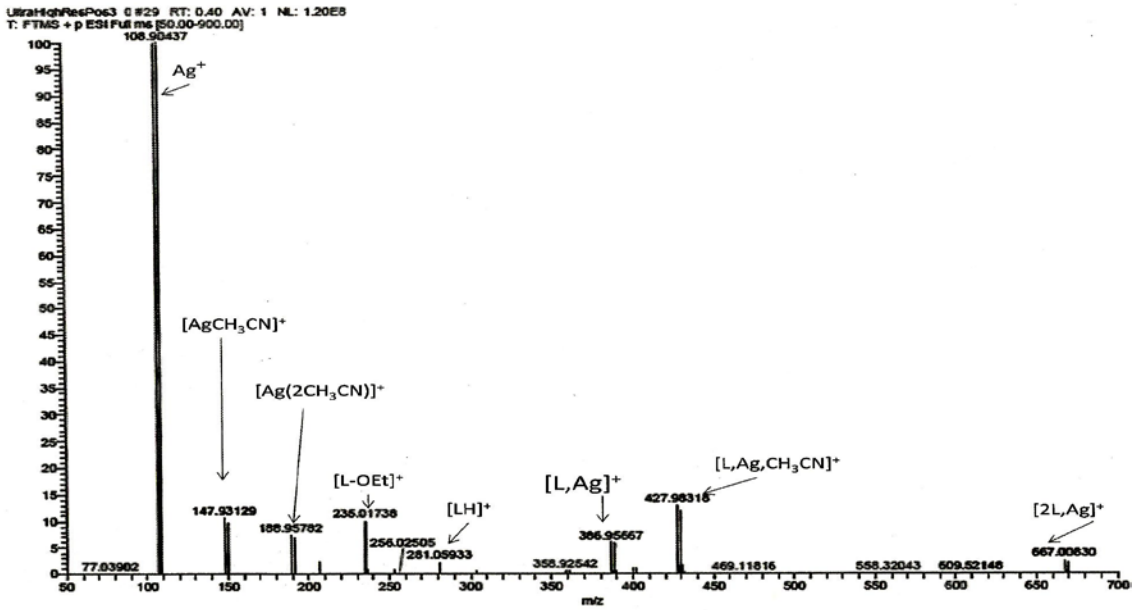

Figure 3.17 ESI-Mass spectrum of $[Ag(DEBTD)]SbF_6 \cdot C_6H_6$ complex dissolved in CH_3CN with labeling of the most abundant peaks

Table 3.10 A summary of mass spectrometric report of DEBTD silver complexes

Species	Calc. mass amu	PF_6 %	PF_6 ppm	ClO_4-L %	ClO_4-L ppm	ClO_4-R %	ClO_4-R ppm	BF_4 %	BF_4 ppm	SbF_6 %	SbF_6 ppm
Ag^+	106.90510	100	2.0	100	5.0	100	5.1	100	4.7	99.6	2.2
$[Ag(CH_3CN]^+$	147.93165	7.9	2.0	6.1	4.9	8.1	5.2	9.7	4.7	10.7	2.4
$[Ag(CH_3CN)_2]^+$	188.95820	2.5	1.5	11.5	4.7	11.5	5.0	4.0	4.4	7.5	2.0
$[L\text{-}OEt]^+$	235.01775	3.0	1.1	2.4	4.3	2.4	4.7	2.0	4.0	10.0	4.7
$[LH]^+$	281.05963	0.0	n/a	0.0	n/a	0.0	n/a	0.0	n/a	2.2	1.1
$[L, Ag]^+$	386.95690	7.1	0.2	11.6	3.6	11.6	3.9	8.1	3.3	5.8	0.6
$[L,Ag,CH3CN]^+$	427.98345	7.1	0.4	7.7	3.4	1.3	3.8	10.4	3.0	11.9	0.6
$[2L,Ag]^+$	667.00870	1.0	0.4	3.0	3.2	3.0	3.5	2.1	2.8	2.5	0.6

3 – 3.5 kV spray voltage

3.7.3 Summary of the properties of DEBTD

These compounds were prepared to explore both the structure and the electronic behavior of the thiadiazole derivatives. The *endo/exo* and *endo/endo* isomeric properties of the

compounds is a result of the free rotation of the ethyl carboxylate group to the benzene ring. In the complexes we observed chelate coordination to the Ag^+ ion through one ring N of the thiadiazole and one carbonyl oxygen from one of the ligand molecules, thus making the ligand molecule an *exo/exo* isomer - different from the parent crystal structure reported in Figure 3.2. The cyclic voltammetry of two return waves was also very interesting with E_{m1} = -1.36 V and E_{m2} = -1.96 V, giving $|\Delta E|$ = 0.60 V which differ from the parent compound and the dinitrile analogue in Chapter 2. The crystal packing was dominated by dispersion forces, with short contacts of N-S 3.152 (8) and S-O 3.149 (8) Å. There are also short contacts between the methylene hydrogen and nitrogen, and the methyl hydrogen and sulfur.

3.7.4 Summary of the silver coordination complexes of DEBTD

The silver coordination varied between four and six, and the ligand coordination remained four with two ring N atoms of the thiadiazole and two carbonyl oxygen atoms, one from each ligand coordinating to the Ag^+. The PF_6^-, SbF_6^-, solvated ClO_4^-, and BF_4^- complexes give double layered structures with inter-planar spacings of 6.17, 6.70, 6.66 and 6.76 Å, respectively. The channels are filled with benzene, except for the BF_4^- structure which is hydrated. These benzene rings have some degree of thermal motion.

The coordination environment of the silver (1) ion in the di-ester complexes, are quite different due to differences in coordination numbers. The bond lengths between Ag^+-O of the carbonyl in the carboxylate and Ag^+-N bonds of the ring thiadiazole are not significantly different, except the bond angles which are determined by the coordination numbers and the arrangement of the ligands and the coordinating atoms around the Ag^+

sphere. The bond lengths are within the normal ranges[14,15] of literature values, but there are slight differences between these in the different Ag-ester complexes. The carbonyl (C=O) bond distances of the carboxylate are within a close average of 1.205 Å, but show a decrease in all the complexes, just as reported by Reedijk and co-workers,[16] which is not also significantly different from the ester ligand. The Ag^{+}-N bond length is longest in the $AgBF_4$ complex (2.470(2) Å and differ significantly from the rest which are on the average of 2.372(3) Å, The Ag^{+}-N2 is significantly longer than Ag^{+}-N1, for instance in SbF_6^{-} the Ag^{+}-N1 is 2.269(2) and in Ag^{+}-N2 it is 2.350(2) Å. This same difference applied to all ester complex between N1 and N2 bond to Ag^{+}. The same difference applied to the Ag^{+}-O bond within the same complex as Ag^{+}-O1 is significantly shorter than Ag^{+}-O3, for example in BF_4^{-} complex it is 2.417(2) and 2.507(2) Å respectively. We also think that these bond length differences between the Ag^{+} and the coordinating atoms contributed to the significant bond angle difference as observed between C10-O3-Ag 126.5(2), and C1-N1-Ag 132.6(2), then C2-N2-Ag 129.8(2) and C7-O1-Ag 128.8(2) °. The internal bond angles of the thiadiazole ring in the ester differ significantly from those of the ester ligand, as stated above. The ring N are involved in the coordination and the angles at their position widened resulting in reduction of the N-S-N angle. There is a difference in their internal angles as it is on the ligand, and the increase in their internal angle is proportional to each other, except in the ClO_4^{-} with benzene in their lattice and BF_4^{-}, where these internal angles of N1 and N2 are almost equal. Considering the inter-planar arrangement in the crystals, the SbF_6^{-} structure is closely related to that of the PF_6^{-} compound with a spacing of 6.70 and 6.17 Å respectively. The interspacing of these layers, however is greater in SbF_6^{-}, the arrangement tend to be better fit and thermally

less mobile, as observed from their anions and the benzene rings present in their lattices. In conclusion we can say confidently that we succeeded in making and characterizing five different silver (1) complexes of di-ester, with their crystallographic and experimental data of the complexes as shown above.

3.7.5 Summary of the solvation of DCBTD and DEBTD Ag^+ complexes

Amongst the structures of metal coordination polymers determined in this thesis, some of them contain only the ligand, silver cations and the appropriate low-coordinate anions (BF_4^-, ClO_4^-, PF_6^-, or SbF_6^-). Others contain, in addition to these three types of components, a solvate. Due to the synthesis route employed, that solvate is in all cases except one, benzene. One sample, $[Ag(DEBTD)]BF_4 \cdot H_2O$, was recrystallized from moist methanol, and this incorporated water as a solvate rather than benzene.

There is considerable variation amongst these otherwise similar coordination polymers with regards to how the benzene is accommodated, leading to a considerable variation in the density of the resulting crystals. An analysis of this variation has been undertaken by using the "visualize voids" calculation incorporated into the CCDC software program "Mercury", release 3.1.1.[17] The analysis was performed using a probe diameter of 1.21 Å, and a grid of 0.21Å, which is equivalent to the default settings in the well -known "calc-void" routine of the PLATON suite of crystallography programs.[18] First of all, the visualize voids calculation was performed on non-solvated polymers L1 and L2. In all cases, the unsolvated crystals do not have any solvent-accessible voids; they are "close packed". For the solvates, the positional parameters of the solvent molecules were removed from the final Crystallographic Information Files (CIF), and the resulting voids

were analyzed in Mercury as described above with an example shown in Figure 3.18. It is important to recognize that this is an *artificial* procedure and does not in any way imply that the crystals should be describe as *being porous*. In a recent review article, Barbour has explained the characteristics of truly porous crystals such as zeolites, which must retain their crystallinity when solvent-free and must be able to have solvents actively diffusing in and out.[19] Such is not the case for the products here. Instead, the analysis of these virtual pores is undertaken to learn more about how solvents are incorporated into the lattice (during crystallization) and the structural consequences thereof.

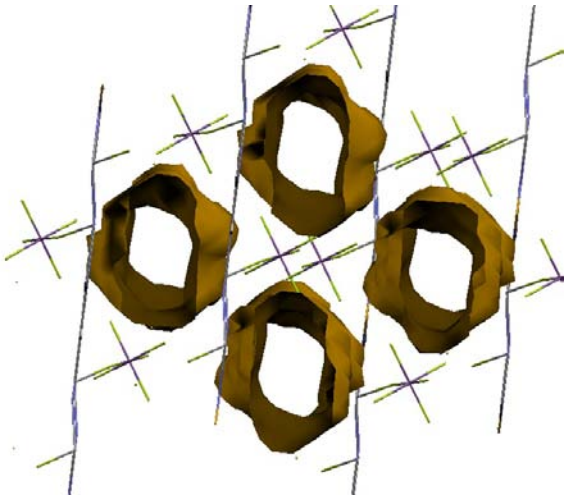

Figure 3.18 Wire frame structure of [Ag(DCBTD)]$SbF_6 \cdot C_6H_6$ with voids shown as tubes after removal of the contribution of the benzene solvate from the lattice.

The results of the analysis are reported in Table 3.11. As a benchmark for this analysis, we start with a low-temperature crystal structure of benzene itself (CSD refcode: BENZEH18). Thus in benzene at 150 K, the cell volume is 494.Å ^{3} and the Z value is 4.[20] Thus, the volume occupied by benzene in its molecular crystal is 123.6Å ^{3}. As can be seen from the results compiled in Table 3.11, the crystal density of the two dinitrile structures are the two highest of all. In the first entry, the average volume occupied by the

benzene in the crystalline lattice is less than the volume of the isolated solvent molecule. This anomaly can probably be explained by the relatively strong coordination of the benzene as a π complex to Ag^+. Consistent with this description, the benzene molecule in this structure is fully ordered and the thermal displacement ellipsoids are small, similar to those of the dinitrile ligands.

Table 3.11 Summary of the analysis of volumes occupied by solvent in Ag^+ complexes

Complex	% vol. occ. solv.	Crystal dens., g cm^{-1}	Vol. occ. by solv., $Å^3$	Comment
$[Ag_2(DCBTD)]SbF_6.(C_6H_6)_2$	33.3	2.558	111.2	Benz. coord. to Ag+
$[Ag(DCBTD)]PF_6.C_6H_6$	30.1	2.047	126.4	Benz. coord. to Ag+
$[Ag(DEBTD)]SbF_6.C_6H_6$ [a]	22.4	2.040	127	Loosely coord. solv.
$[Ag(DCBTD)]PF_6.C_6H_6$	38.5	2.063	136.1	Loosely coord. solv.
$[Ag(DEBTD)]SbF_6.C_6H_6$ [b]	23.1	2.013	137	Loosely coord. solv.
$[Ag(DEBTD)]ClO_4.C_6H_6$	28.7	1.724	156	Loose solvent.
$[Ag(DEBTD)]PF_6.C_6H_6$	28.0	1.792	158	Loose solvent.
$[Ag(DEBTD)]BF_4.H_20$ [c]	2.1	1.964	8.8	Tightly coord. to Ag^+

[a] Determined at 100 k. [b] Determined at 173 K. [c] This has water coordinated to Ag^+.

In the second entry, the crystals are less dense by a factor of almost 20%, and the occupied volume of the coordinated benzene molecule is almost identical to that of the pure benzene as found in BENZEN18. This behavior is also seen in the third entry, AgL_2SbF_6, when determined at the unusually low temperature of 100 K, although the length of the Ag-C bonds (2.884(7) Å) are longer in this latter example. There is a significant jump in the average volume occupied per benzene ring when the same complex is determined at 173 K. But the highest occupied volumes are determined for

[Ag(DEBTD)]ClO_4•C_6H_6 and [Ag(DEBTD)]PF_6•C_6H_6 at 156 and 158 $Å^3$, almost 30% higher than the volume occupied in a pure benzene lattice at 150 K. A consideration of the anisotropic displacement ellipsoids for these structures confirms that the benzene molecule in these last two examples display a large amount of thermal vibration. They are "too loose" for the cavities they occupy, and hence they appear to be able to move and/or coordinate in more than one location. The displacement ellipsoids of the benzene carbon atoms in these two structures are indeed found to be much larger than those of the coordinated ester and the silver ions. In some cases, the solvent cavities consist of infinite tubes that may be wide enough to allow for solvent diffusion, but no evidence for such diffusion has been experimentally confirmed.

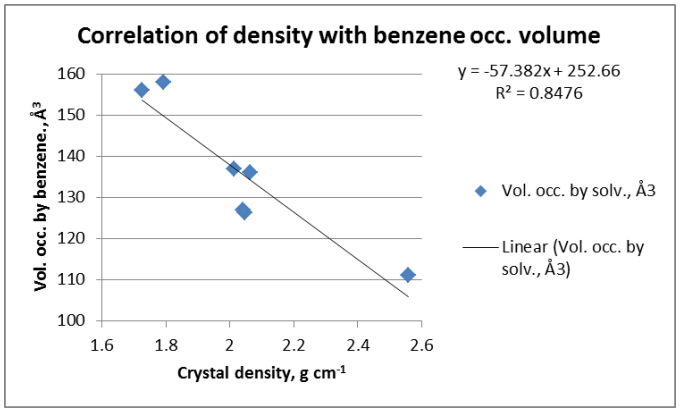

Figure 3.19 Correlation between the crystal density determined from X-ray crystallography and the "void volumes" associated with the benzene solvate.

There is a good correlation between the total crystal density and the volume occupied by the benzene molecules (Figure 3.19). At the same time, there is no correlation between the latter and the fraction of the unit cell volume occupied by solvent in the crystal lattice, which varies considerably from a low of 22.4 to a high of 38.5% of the unit cell volume. For the ester structures, it is found that when the solvent displacement ellipsoids are large, those of the anions are also large. In these structures, the solvent and the anions do

indeed occupy the same interstitial sites located between sheet-like structures of Ag^+ coordinated to the planar di-ester molecules.

Finally, mention must be made of the coordinated solvent water in $AgL_2BF_4 \bullet H_2O$, for which the occupied volume is very much smaller than typically expected for solvent water (~40 $Å^3$). This implies that there is a strong coordinated bond of the H_2O to Ag^+ in this structure.

3.8 References

1. Pilgram, K. *J. Heterocycl. Chem.* **1974**, *11*, 835-837.
2. Grubb, C. J.; Cole-Hamilton, D. J.; Whittlesey, M. K., *J. Chem. Soc., Faraday Trans.* **1996**, *92*, 5005-5012.
3. Pilgram, K.; Skiles, R. D. *J. Heterocycl. Chem.* **1974**, *11*, 777.
4. Watanabe, M., Goto, K., Fujitsuka, M., Tojo, S., Majima, T., Shinmyozu, T. *Bull. Chem. Soc. Jpn.,* **2010**, *83*, 1155-1161.
5. Shorock,C. J.; Xue, B. Y.; Kim, P. B.; Batchelor, R. J.; Brain O. P.; Leznoff, D. B. *Inorg. Chem.* **2002**, *41*, 6743-6753.
6. McMullan R. K., Koetzle, T. F., Fritchie, C. J. J. *Acta Crystallogr., Sect. B: Struct. Sci.* **1997,** *53*, 645.
7. Liu, S. Q.; Groeneveld, L. N.; Zhang, X. F.; Konaka H.; Munakata M. *Chin. J. Chem.,* **2006**, *24*, 1259.
8. Biju, A. R.; Rajasekharan, M. V. *Polyhedron* **2008**, *27*, 2065-2068.
9 Berttelli, M.; Carlicci, L.; Ciani, G.; Proserpio, D. M.; Sironi, A. *J. Mater. Chem.***1997**, 7, 1271-1276.
10 Li, C. P.; Chen, J.; Du, M. *CrystEngComm*. **2010**, 1212, 4392.
11. Smolenski, P.; Jaros, S. W.; Pettinari, C.; Lupidi, G.; Quassinti, L.; Bramucci, M.; Vitali, L. A.; Petrelli, D.; Kochel, A.; Kirillov, A. M. *Dalton Trans.* **2013**, *42*, 6572-6581.
12. Khlobystov, A. N.; Blake, A. J.; Champness, N. R.; Lemenovskii, D. A.; Majouga, A. G.; Zyk, N. V.; Schröder, M. *Coord. Chem. Rev.* **2001**, *222*, 155-192.
13. Driessen, W. L.; Groeneveld, W. L.; Van der Wey, F. W. *Rec. Trav. Chim* **1970**, *89*, 353.
14. Allen, F. H.; Olga, K.; Watson, D. G.; Brammer, L. A.; Orpen, G.; Taylor, R. *J. Chem. Soc. Perkin Trans. II* **1987**, *2*, S1 - S19.
15. Xu, Z.; Kiang, Y. H.; Lee, S.; Lobkovsky, E. B.; Emmott, N. *J. Am. Chem. Soc.* **2000**, *122*, 8376-8391.
16. Reedijk, J.; Zuur, A. P.; Groeneveld, W. L., *Rec. Trav. Chim. Pays-Bas* **1967**, *86*, 1127-1137.
17. Macrae, D. F.; Edgington, P. R.; McCabe, P.; Pidcock, E.; Shields, G. P.; Taylor, R.; Towler, M.; Van de Streek, J. *J. Appl. Cryst.* **2006**, *39*, 453-457.
18. Spek, A. L. *Acta Cryst.* **2009**, *D65*, 148-155.
19. Barbour, L. J. *Chem. Commun.*, **2006**, 1163-1168.
20. Nayak S. K.; Sathishkumar R.; Row, T. N. G. *CrystEngComm* **2010**, *12*, 3112.

CHAPTER 4: 2,1,3-BENZOTHIADIAZOLE-4,7-DICARBOXYLIC ACID AND RELATED CHEMISTRY

4.1 Introduction to 2,1,3-benzothiadiazole-4,7-dicarboxylic acid and others

Our original purpose was to make metal carboxylate MOFs, with different topologies and compositions, hence the drive of making a di-acid of benzothiadiazole, as a precursor to such products. Porous metal-organic frame works (MOFs) have attracted so much interest due to their numerous potential applications, their high and regular porosity plus their amphiphilic internal micro-environment have allowed these several applications.[1] We have not yet succeeded in the process of trying to make MOFs of this kind because we have not found the right conditions for getting the deprotonated carboxylic acid to coordinate to the metals. The results presented here describe by-products from initial attempts to construct discrete model complexes with Cd, which are nonetheless interesting. These attempts have made use of a neutral "end-capping" ligand, namely N,N-bis-(1-pyridin-2-yl-ethylidene)-ethane-1,2-diamine.

4.2 Synthesis of 2,1,3-benzothiadiazole-4,7-dicarboxylic acid

Pure diethyl-2,1,3-benxothiadiazole-4,7-dicarboxylate was refluxed for 12 hours with an aqueous solution of potassium hydroxide in a mixture of ethanol and water in 25:1 mole ratio. Then it was cooled to room temperature, concentrated in a rotary evaporator to solid, this solid was dissolved in water and acidified with concentrated hydrochloric acid during which precipitate was generated. The solid was filtered and air dried, and recrystallized in water to obtain pale yellow crystals. The formation of the product was confirmed through infrared spectroscopy (IR) and NMR, further, X-ray crystallography was used to fully confirm the structure. This same reaction was repeated using the same

parameters, the IR and NMR were exactly the same, except the color of the crystals were red. By crystallography the structure was also found to be identical to that of the yellow crystals.

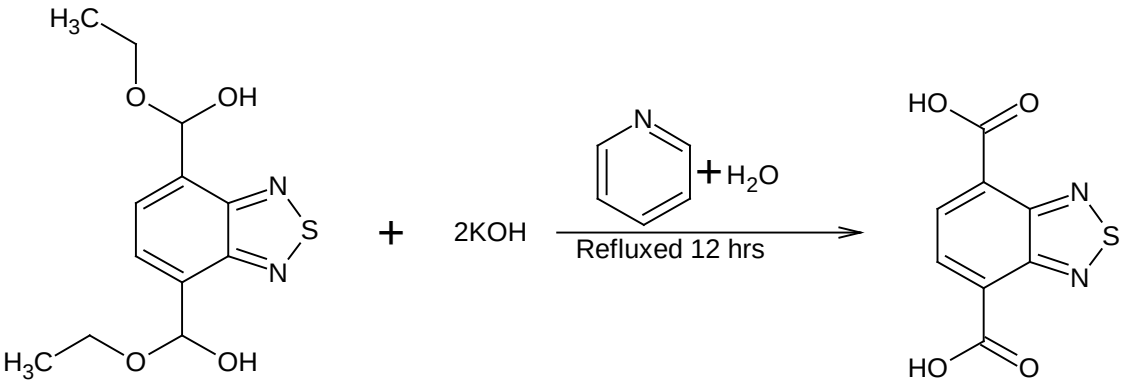

Scheme 4.1 Synthesis of 2,1,3-benzothiadiazole-4,7-dicarboxylic acid

4.2.1 IR and NMR of 2,1,3-benzothiadiazole-4,7-dicarboxylic acid.

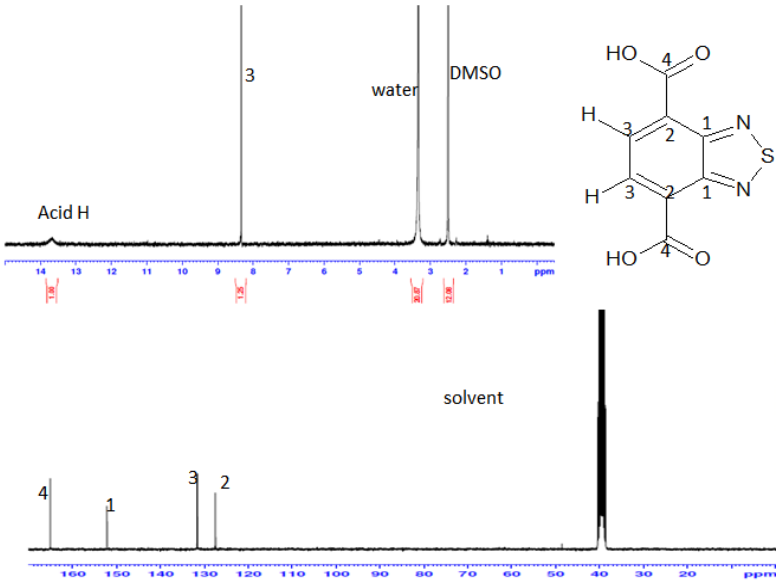

Figure 4.1 ^{1}H and ^{13}C NMR spectra of 2,1,3-benzothiadiazole-4,7-dicarboxylic acid. The signals are identified by the indicated carbon atom numbers.

The IR of the structure has two stretching bands of interest, the carbonyl bands (C=O) which appear at 1682 cm^{-1}, which can be explained with reference to the crystal structure, see Figure 4.2 below, because of different interactions of the two C=O groups. Thus, while both are involve in hydrogen bonding, the C7=O2 group is hydrogen-bonded to water (reducing the stretching frequency), whilst the C8=O4 group is involved in a short $O^{\delta-}\cdots S^{\delta+}$ intermolecular contact with a neighbouring thiadiazole moiety. The second band of interest is from ν(O–H) of the water of hydration which appears at 3424 cm^{-1} and a broad carboxylic acid OH band which absorbs at 3124 cm^{-1}.[2]

In the ^{1}H NMR spectra, there are four protons in the molecule with two symmetry-equivalent positions (in solution), so we expect two proton peaks. The two equivalent protons on the ring are at 8.33 ppm as a singlet. The acid protons appear as a broad hump at 13.63 ppm. For the ^{13}C NMR spectrum, the four peaks expected appeared in the spectra, the carbonyl C occupies the most deshielded position of 165.19 ppm. The quaternary C of C=N in the thiadiazole ring is at 152.22 ppm, and appears as the least intense peak. The carbon carrying the protons in the benzene ring is at 131.67 ppm which has the highest peak intensity and finally the carbons at position 4,7 in the ring that carry the carbonyl carbons are found at 127.54 ppm.

4.3 X-Ray Structure 2,1,3-benzothiadiazole-4,7-dicarboxylic acid.

This structure was further confirmed by X-ray crystallography, showing that the compound was a monohydrate, it was recrystallized from water, with Z = 4, each molecule is accompanied by a molecule of water in the unit cell, with short contacts between N of the ring and H of the water molecule N1-H1S 2.049(3), N1-O1S 2.849(2)

and H1S-O3 2.526(3) Å. This structure is almost completely flat, except the OH that is slightly out of plane, the bond distance difference between C7-O1 and C7-O2 is attributed to double and single bond differences, but we could observe a difference between these bonds and those of C8-O3 and C8-O4 which are longer than the previous, which might be due to the hydrogen-bond contacts between them and the water molecules. There are also intermolecular short π contacts between S and the benzene carbons holding the thiadiazole in position as S-C at 3.285(2) and 3.430(2). Within statistical error, C7-O1 and C8-O4 are identical, the difference not exceeding 2.58 × esd to be significant at the 99% confidence level. C8-O3 at 1.322+2.58 × 0.002 = 1.317 is out the range of C7-O3 at 1.301+2.58 × 0.002=1.306, a clear indication that they are not the same.

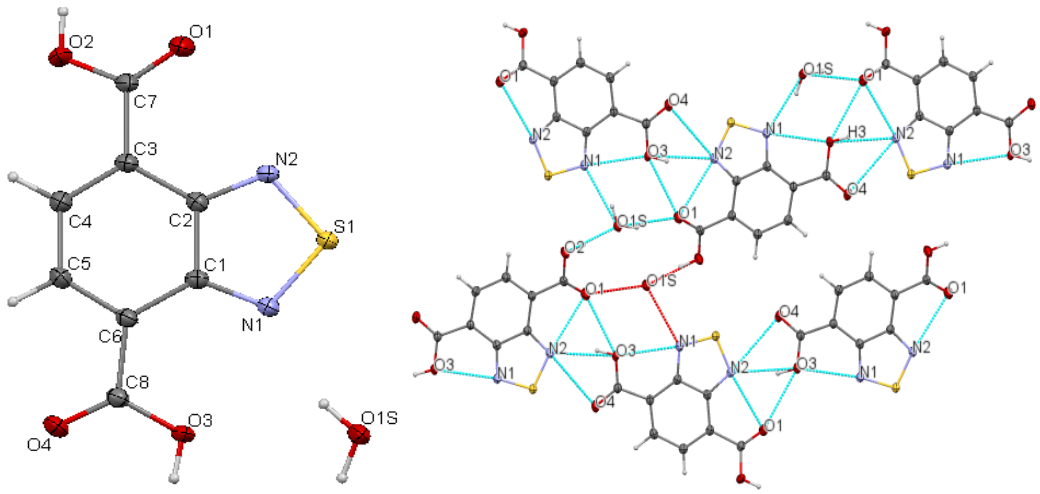

(a) (b)

Figure 4.2 (a) Thermal ellipsoids plot of the asymmetric unit. (b) Extended figure illustrating the hydrogen bond network of 2,1,3-benzothiadiazole-4,7-dicarboxylic acid.

The ring bond short intermolecular distances are shorter in the di-acid compared to the esters, only one isomer of the ester are layered, that is the *endo/endo*, the short contact is

Table 4.1 Crystal data and structure refinement parameters for 2,1,3-benzothiadiazole-4,7-dicarboxylic acid.

Empirical formula	$C_8 H_6 N_2 O_5 S$	
Formula weight	242.21	
Temperature	173(2) K	
Crystal system	Monoclinic	
Space group	$P2_1/c$	
Unit cell dimensions	a = 7.1096(5) Å	α = 90°
	b = 17.5822(12) Å	β = 90.7510(10)°
	c = 7.1361(5) Å	γ = 90°
Z	4	
Final R indices [I>2sigma(I)]	R_1 = 0.0334, wR_2 = 0.0576	
R indices (all data)	R_1 = 0.0534, wR_2 = 0.0612	

Table 4.2 Selected bond distances (Å) and angles in (°) for 2,1,3-benzothiadiazole-4,7-dicarboxylic acid.

N1-S1	1.611(1)	O1-C7	1.205(2)
N2-S1	1.616(1)	C7-O2	1.311(2)
C1-N1	1.351(2)	C7-C3	1.489(3)
C2-N2	1.341(2)	C6-C1	1.425(3)
O3-C8	1.330(2)	C2-C1	1.438(3)
C8-O4	1.211(2)	C2-C3	1.432(3)
C6-C8	1.491(3)	C6-C5	1.376(2)
N1-S1-N2	100.02(7)	O1-C7-C3	122.80(2)
C1-N2-S1	107.70(1)	C2-C3-C7	120.50(2)
C2-N2-S1	107.10(1)	O3-C8-O4	123.50(2)
O3-C8-C6	114.00(2)	O1-C7-O2	124.30(2)
C1-C6-C8	126.20(2)	N1-C1-C6	127.70(2)
N2-C2-C3	126.30(2)		

between the S2-C14 of the different molecules, which stands at 3.495(9) Å in between two layers and 3.454(1) in another two layers. That of the di-acid between C2-S1 3.430(2) and C1-S1 3.285(2), this larger distance between the layers of the ester is due to the presence of the ethyl group that is out of plane of the BTD ring.

Table 4.3 Hydrogen bonds for 2,1,3-benzothiadiazole-4,7-dicarboxylic acid in Å and °.

D-H...A	d(D-H)	d(H...A)	d(D...A)	<(DHA)
O(2)-H(2)...O(1S)#1	0.91(2)	1.63(2)	2.5155(19)	164(2)
O(3)-H(3)...N(2)#2	0.83(2)	2.10(2)	2.9130(19)	169(2)
O(3)-H(3)...O(1)#2	0.83(2)	2.42(2)	2.8528(17)	113.5(17)
O(1S)-H(1S)...N(1)	0.84(2)	2.05(2)	2.845(2)	157(2)
O(1S)-H(1S)...O(3)	0.84(2)	2.49(2)	3.0812(18)	128(2)
O(1S)-H(2S)...O(1)#2	0.91(3)	1.83(3)	2.706(2)	159(2)

Symmetry transformations used to generate equivalent atoms:

#1 -x,y+1/2,-z+1/2 #2 x+1,-y+3/2,z+1/2

4.4 Synthesis of 2,3-diaminobenzene-1,4-dicarboxylic acid

4,7-dinitrile-2,1,3-benzothiadiazole was refluxed with 25% aqueous sodium hydroxide for 15 hours, on reflux the reaction mixture become thicker and water was added to enable it to stir until the reaction mixture become stabilized, completion of the reaction is monitored as the evolution of ammonia stopped, cooled to RT and acidified with concentrated HCl, stirred for one extra hour, filtered and air dried. The solid obtained was recrystallized in water to give pale yellow colored needle shaped crystals, the formation of this product was confirmed by IR and NMR. The structure was further characterized by X-ray crystallography, elemental analysis and electrospray ionization mass spectrometry. It is noted that after acid formation, further reflux of this reaction result to

desulfurization,[3] Friedman *et al.* in 1977,[4] and Mukherjee *et al.* in 2001 reported the use of aqueous sodium hydroxide for the desulfurization/demineralization of coal,[5] from this article it is stated that even the use of hydrogen peroxide can lead to desulfurization and Wendi *et al.* in 2005 explained the effective uses of caustic soda and other sodium compounds for the desulfurization of organic compound that are chemically bonded to sulfur.[6] As observed in this reaction, desulfurization of the thiadiazole ring results in the formation of diamino-benzene dicarboxylate. When this reaction was repeated using the same parameters and a more exact stoichiometry, the product obtained became different in colour (red), with larger and better quality needle crystals.

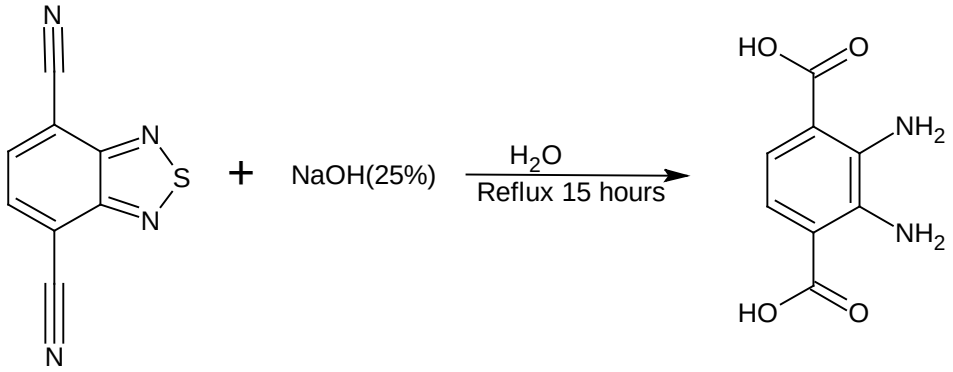

Scheme 4.2 Synthesis of 2,3-diaminobenzene-1,4-dicarboxylic acid

4.4.1 IR and NMR of 2,3-diaminobenzene-1,4-dicarboxylic acid

In the IR spectrum of the yellow crystals, the bands of interest are the C=O (carbonyl) and the NH (amine) stretches, the amine appeared in the spectra as two different bands, asymmetric at 3441 and symmetric vibration at 3346 cm^{-1} and a broad band between 3300 – 2500, centers near 3000 cm^{-1}, an indication of the carboxylic acid dimer manifestation.[2] The carbonyl v(C=O) band at 1603 cm^{-1}, with a downward shift from that of the 2,1,3-benzothiadiazole-4,7-dicarboxylic acid (section 4.2). The IR of the red product shows that it is a different compound, with some similarities in their bands, one

of the N-H stretch indicate NH_2 at 3441 cm^{-1} while the stretch that absorbed at 3347 cm^{-1} represent the NH_3^+ as we observed in the crystal structure reported in Figure 5.7. with a broad band between 2000 and 3000 cm^{-1} for OH which overlap with the band for NH_3^+, the $v(C=O)_2^-$ (asymmetric carboxylate anion) at 1557 and symmetric at 1379 cm^{-1}.[7]

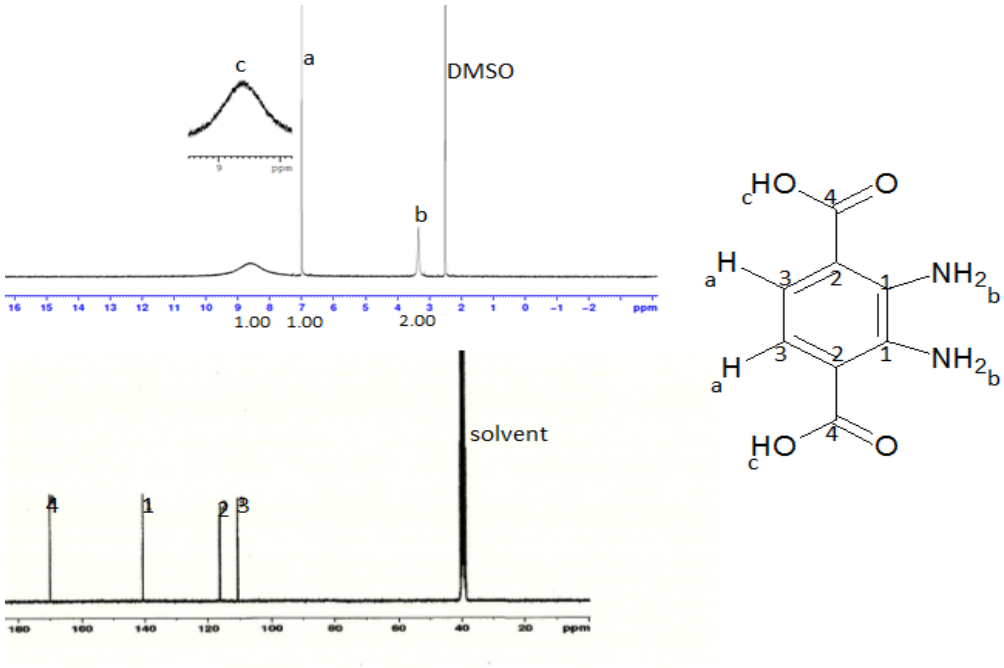

Figure 4.3 ^1H and ^{13}C NMR spectra of 2,3-diaminobenzene-1,4-dicarboxylic acid correlated to a labelled molecular structure

The ^1H NMR displayed the two NH_2 groups as equivalent and appear as a single peak "b" at 3.345 ppm, the two protons on the benzene ring are equivalent based on the symmetry through S horizontal across the ring and appear as a single peak "a" at 7.00 ppm, the two acid protons are in exchange with the four amine protons to give a broad singlet "c" at 8.615 ppm, the di-amine protons of the yellow integrated to two and that of the red integrated to 2.8 showing the presence of the extra proton in the $-NH_3^+$. The ^{13}C NMR

spectrum has four distinct peaks as expected in both cases, further characterization was carried out using X-ray crystallography with structure as shown in Figure 4.4 below.

4.4.2 X-Ray Crystal Structure structure of 2,3-diaminobenzene-1,4-dicarboxylic acid

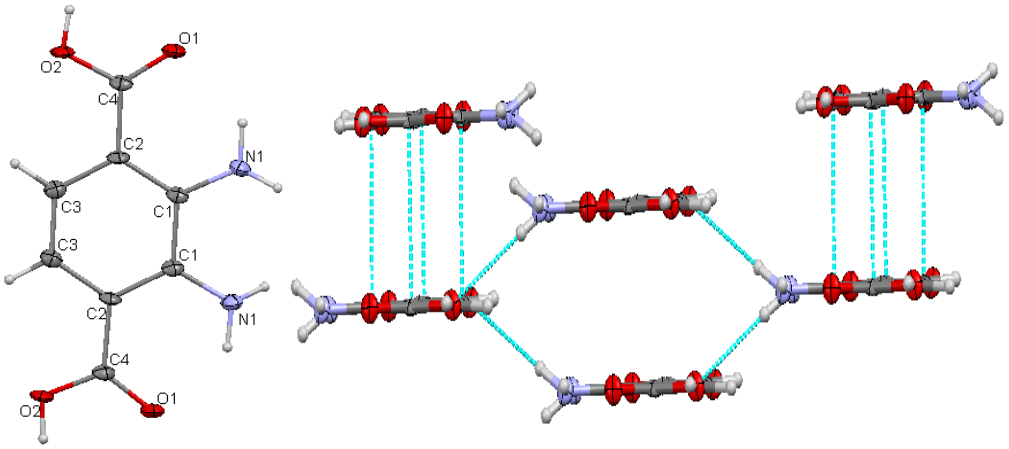

(a) (b)

Figure 4.4 (a) The molecular structure as found in the crystal with a two-fold rotation axis horizontally located with the atom numbering scheme. (b) Significant inter-molecular short contacts *other than* hydrogen bonds in the crystal structure of 2,3-diaminobenzene-1,4-dicarboxylic acid

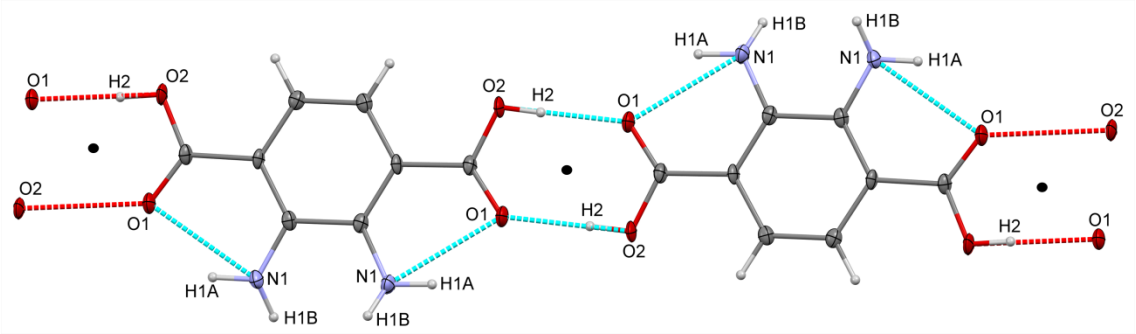

Figure 4.5 Centrosymmetric hydrogen-bond network in the crystal structure of 2,3-diaminobenzene-1,4-dicarboxylic acid. The centres of symmetry are at the midpoint of the bridges and are shown as black dots.

Table 4.4 Crystal data and structure refinement of 2,3-diaminobenzene-1,4-dicarboxylic acid

Empirical formula	$C_8 H_8 N_2 O_4$	
Formula weight	196.16	
Temperature	133(2) K	
Crystal system	Monoclinic	
Space group	C2/c	
Unit cell dimensions	a = 8.826(4) Å	α = 90°
	b = 12.539(6) Å	β = 91.141(7)°
	c = 7.193(4) Å	γ = 90°
Z	4	
Final R indices [I>2sigma(I)]	R1 = 0.0623, wR2 = 0.1356	
R indices (all data)	R1 = 0.1193, wR2 = 0.1629	

Table 4.5 Selected bond distances (Å) and angles in (°) for 2,3-diaminobenzene-1,4-dicarboxylic acid

N1-C1	1.362(3)	C1-C1	1.446(5)
C4-O1	1.231(3)	C1-C2	1.397(3)
O2-C4	1.318(3	C2-C3	1.412(3)
C2-C4	1.473(3)	C3-C3	1.363(5)
N1-C1-C1	116.50(2)	O1-C4-C2	123.20(2)
N1-C1-C2	124.60(2)	O2-C4-O1	121.30(2)
C1-C2-C4	120.20(2)	O2-C4-C2	115.50(2)
C4-C2-C3	119.20(2)		

Table 4.6 Hydrogen bonds for 2,3-diaminobenzene-1,4-dicarboxylic acid Å and °.

D-H...A	d(D-H)	d(H...A)	d(D...A)	<(DHA)
N(1)-H(1A)...O(1)	0.897(17)	1.97(2)	2.671(3)	133(2)
N(1)-H(1B)...O(2)#2	0.891(17)	2.270(19)	3.137(3)	164(2)
O(2)-H(2)...O(1)#3	0.851(18)	1.777(18)	2.625(3)	176(3)

Symmetry transformations used to generate equivalent atoms:

#1 -x,y,-z+1/2 #2 -x+1/2,y-1/2,-z+1/2 #3 -x+1,-y+2,-z

This compound was found to crystallize in two distinct forms. The first structure, for which the crystals were distinctly yellow in colour, is that of the neutral diamine-diacid. A description of this structure follows. The second set of crystals, this time a deep red-brown in colour, was found out to be a zwitterion with one deprotonated carboxylate and one protonated amine, see further in Figure 4.6 below. The two structures are in the same space group C2/c, with Z = 4. The asymmetric unit of the first structure consists of *half* a molecule, the second is a full molecular structure with one mole of water and OH. Two complete molecules are fully within the unit cell, along a two-fold rotation axis, the others are four halves. These four halves are from four molecules on the axes that run along the face of the unit cell, half of each in the unit cell and the other half outside the same unit cell in question. The second structure has four molecules at the center of the unit cell with four halves on the axis, this structure is a di hydrate, with NH_3^+ and C7=O2 hydrogen bonded to each of the water molecule and on packing these water molecules are arranged in space between the molecules. The two symmetry-equivalent NH_2 groups of the first are positioned on the benzene ring with an C2-C1-N1 angle of 124.55(2)° and an C1'-C1-N1 angle of 116.54(2)°, thus the amino groups are pinched in towards each other for reasons that are not entirely clear. The N1–C1 bond length is 1.362(3) Å which is within the known bond length distances.[8]

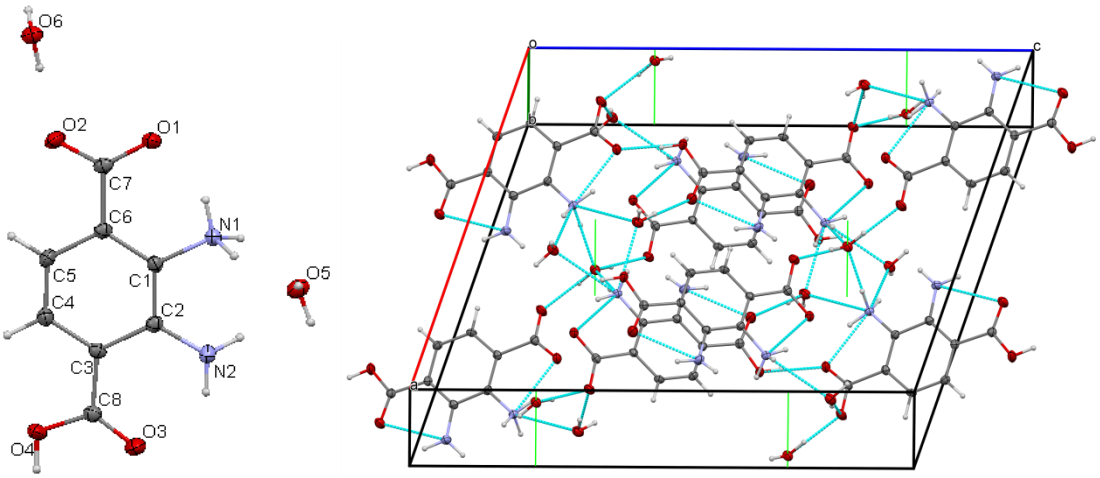

(a) (b)

Figure 4.6 (a) The asymmetric unit of the zwitterion structure of 2,3-diaminobenzene-1,4-dicarboxylic acid 1.5 hydrate with the atom numbering scheme. Oxygen 6 is located at a special position (2-fold rotation axis) and counts half to the formula. (b) A unit cell packing diagram showing the complex hydrogen bond network; six of the two-fold rotation axes in this cell are shown in green.

The crystal of the repeated product confirmed the last statement above, showing that one of the amine nitrogens is protonated to $-NH_3^+$ while one carboxylic acid is deprotonated, and the structure of the resulting zwitterion is also hydrated, as shown in Figure 5.5 above. The primary intermolecular H-bonds link O1 and O4 *via* H4A in conjunction with the intramolecular O1 to N1 link *via* H1B, creating a structure of corrugated ribbons that are aligned with the *c* axis of the cell and which aggregate into layers aligned with the *ac* planes and perpendicular to the *b* axis. The waters of hydration form hydrogen bonds linking *between* the ribbons and layers.

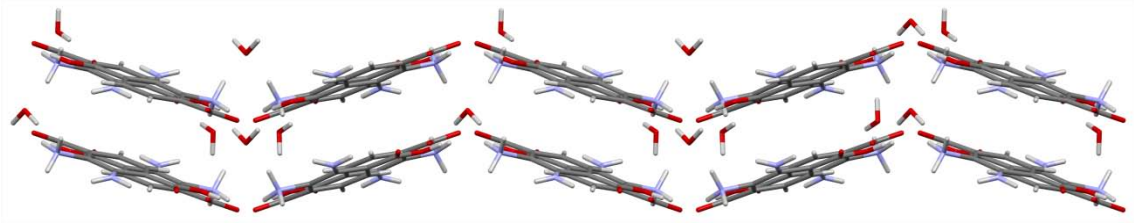

Figure 4.7 The corrugated layer structure of 2,3-diaminobenzene-1,4-dicarboxylic acid 1.5 hydrate viewed down the crystal *a* axis. Water molecules bridge between ribbons and layers.

Table 4.7 Crystal data and structure refinement of 2,3-diaminobenzene-1,4-dicarboxylic acid 1.5 hydrate

Empirical formula	$C_8 H_{11} N_2 O_{5.5}$	
Formula weight	223.17	
Temperature	173(2) K	
Crystal system	Monoclinic	
Space group	C2/c	
Unit cell dimensions	a = 14.5169(15) Å	α = 90°
	b = 7.1802(8) Å	β = 107.4750(10)°
	c = 18.7573(19) Å	γ = 90°
Z	8	
Final R indices [I>2sigma(I)]	R_1 = 0.0425, wR_2 = 0.0966	
R indices (all data)	R_1 = 0.0768, wR_2 = 0.1116	

Table 4.8 Selected bond distances (Å) and angles in (°) for 2,3-diaminobenzene-1,4-dicarboxylic acid 1.5 hydrate

C6-C7	1.516(3)	C8-O4	1.316(2)
C7-O2	1.253(2)	C2-N2	1.371(2)
C7-O1	1.262(2)	C1-N1	1.455(2)
C3-C8	1.484(3)	C1-C2	1.411(3)
C8-O3	1.219(2)	C5-C4	1.375(3)
N2-C2-C1	119.90(1)	O1-C7-O2	124.70(2)
O3-C8-C3	123.40(2)	O3-C8-O4	122.70(2)
O4-C8-C3	113.90(1)	N1-C1-C2	117.20(1)
C6-C7-O1	119.20(1)	N1-C1-C6	120.10(1)
C6-C7-O2	116.10(1)	N2-C2-C3	122.90(1)

Table 4.9. Hydrogen bonds for 2,3-diaminobenzene-1,4-dicarboxylic acid 1.5 hydrate Å and °.

D-H...A	d(D-H)	d(H...A)	d(D...A)	<(DHA)
N(1)-H(1B)...O(1)	0.904(15)	1.818(16)	2.6299(19)	148.3(18)
N(1)-H(1A)...O(5)	0.918(15)	1.875(16)	2.760(2)	161.4(18)
O(6)-H(6)...O(2)	0.848(15)	1.785(15)	2.6263(15)	171(2)
N(1)-H(1B)...O(5)#1	0.904(15)	2.490(19)	2.970(2)	113.6(14)
N(1)-H(1C)...O(6)#2	0.924(15)	1.837(15)	2.743(2)	165.9(17)
O(4)-H(4A)...O(1)#3	0.871(16)	1.759(16)	2.6262(17)	174(2)
O(5)-H(5A)...O(2)#4	0.854(16)	1.943(16)	2.7890(19)	171(2)
O(5)-H(5B)...O(3)#5	0.841(16)	1.950(16)	2.7868(18)	173(2)

Symmetry transformations used to generate equivalent atoms:

#1 -x+1,y,-z+1/2 #2 x+1/2,y+1/2,z #3 x,-y+1,z-1/2

#4 x+1/2,y-1/2,z #5 -x+1,-y+1,-z

4.5 Synthesis of potassium 7-carboxy-2,1,3-benzothiadiazole-4-carboxylate

2,1,3-benzothiadiazole-4,7-dicarboxylic acid was dissolved in methanol and aqueous potassium hydroxide was added and stirred for an hour to dissolve, filtered, solvents were removed from the filtrate through rotatory evaporation to dryness, the solid residue was dissolved in hot water which gave the brown needle crystal, which was confirmed by IR and NMR, further with X-ray crystallography.

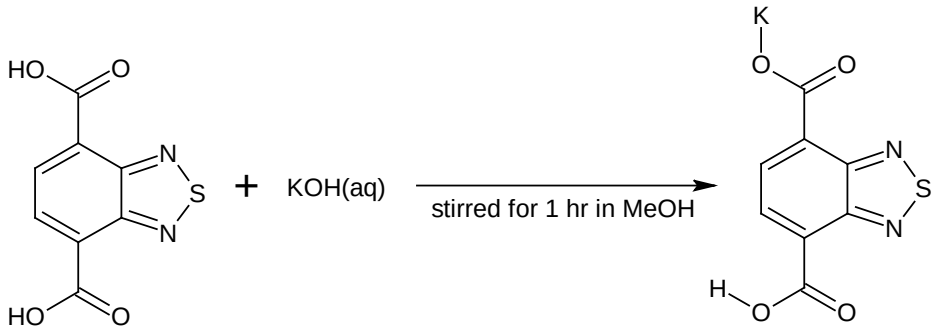

Scheme 4.3 Synthesis of potassium 7-carboxy-2,1,3-benzothiadiazole-4-carboxylate

4.5.1 IR and NMR of potassium 7-carboxy-2,1,3-benzothiadiazole-4-carboxylate

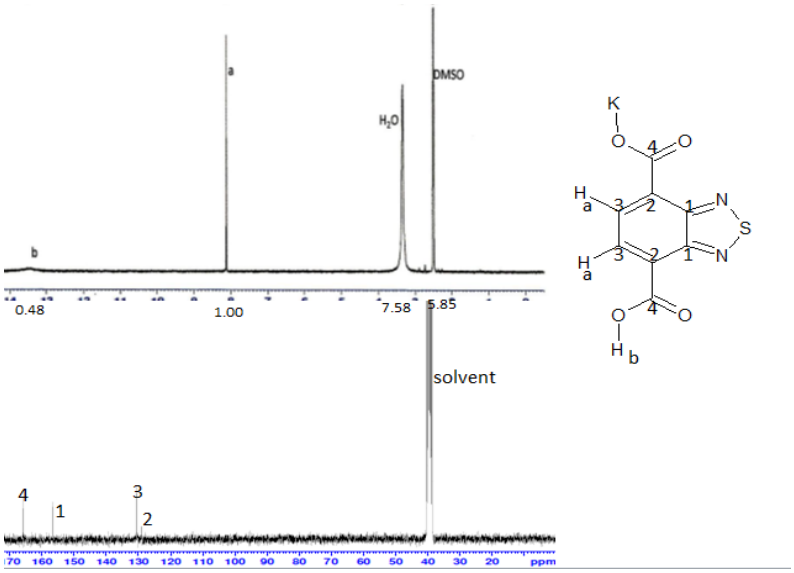

Figure 4.8 Showing the ^{1}H and ^{13}C NMR of potassium 7-carboxy-2,1,3-benzothiadiazole-4-carboxylate

In the IR there are three bonds of interest, the carbonyl (C=O) stretching vibration bands observed at 1676 cm^{-1}, the O-H stretching vibration band is observed at 3424 cm^{-1} (w) coming from the water molecules[9] coordinated to the K^{+} ion and the free OH of the acid with a broad band at between 1800 and 3500 cm^{-1} The ^{1}H NMR shows the benzene protons at 8.12 ppm with a slightly higher frequency than the equivalent protons in the starting acid (see Section 4.2.1) which resonate at 8.33 ppm. Furthermore, the acid proton which appears as a broad hump at 13.52 ppm indicative of strong hydrogen bonding in solution, while the ^{1}H signal of the water molecules which are coordinated to the K^{+} is observed at 3.338 ppm. The ^{13}C NMR spectrum has four distinct peaks at 165.82, 156.77, 130.71 and 129.06 ppm, all very similar in comparison to its parent compound.

4.5.2 X-Ray Crystal Structure of potassium 7-carboxy-2,1,3-benzothiadiazole-4-carboxylate tetrahydrate.

On the crystal structure, it crystallized in the triclinic crystal system and space group of P-1 with Z = 2. Potassium had been said to have affinity in coordination to acetate and was described as having four-fold distribution of water molecules surrounding the K^+ ion[10], with the carbonyl in the di-acid behaving like the acetate. The K^+ is exhibiting a coordination number of eight in this salt, it is coordinated to four oxygen atoms of (bridging) water molecules O5 and O6, to one nitrogen ring of the thiadiazole and to three oxygens of the carboxyl groups, O3 (the deprotonated acid), O1 (a C=O group) and O2 (an OH oxygen). The bond distances of K-O of water are between 2.703(1) – 3.097(9) Å, that of K-N as 2.827(9) Å and that of K-O of the carboxyl groups at 2.671(7) – 2.844(7) Å. The potassium ions form a centrosymmetric dimer in which the K-K distance is 3.664(4) Å, with all the bond angles around the K^+ sphere less than 90.

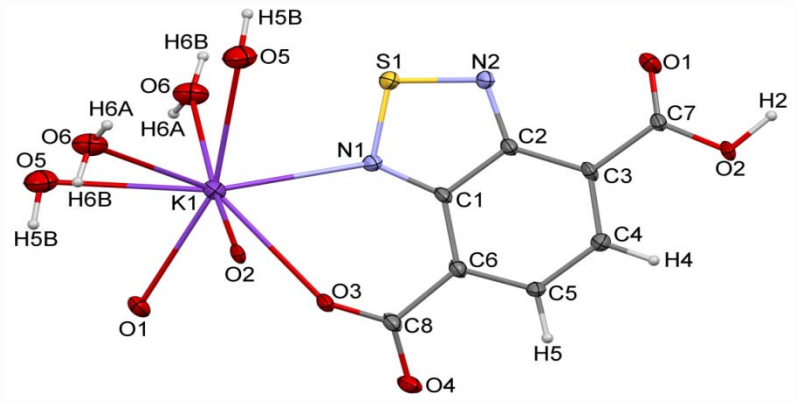

Figure 4.9 A view of the asymmetric unit in the crystal structure of potassium 7-carboxy-2,1,3-benzothiadiazole-4-carboxylate tetrahydrate showing the atom numbering scheme. Four extra oxygen atoms are shown in order to complete the coordination sphere of the K^+ ion.

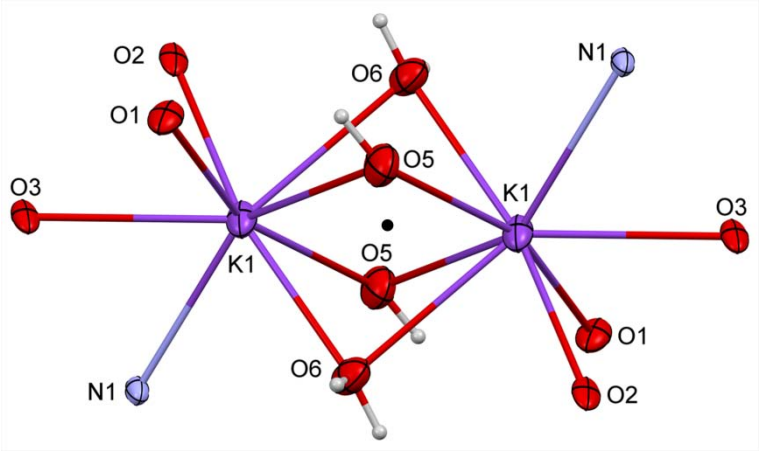

Figure 4.10 The centrosymmetric dimeric bridging potassium ions which link the anions into a double-layer network. The location of the inversion centre is indicated by the black dot.

Table 4.10 Crystal data and structure refinement of potassium 7-carboxy-2,1,3-benzothiadiazole-4-carboxylate

Empirical formula	$C_8\ H_{6.70}\ K\ N_2\ O_6\ S$	
Formula weight	298.01	
Temperature	173(2) K	
Crystal system	Triclinic	
Space group	P -1	
Unit cell dimensions	a = 7.205(3) Å	α = 80.801(5)°
	b = 8.700(4) Å	β = 72.647(5)°
	c = 9.753(4) Å	γ = 66.454(5)°
Z	2	
Final R indices [I>2sigma(I)]	R1 = 0.0828, wR2 = 0.2209	
R indices (all data)	R1 = 0.1213, wR2 = 0.2456	

Table 4.11 Selected bond distances (Å) and angles in (°) of potassium 7-carboxy-2,1,3-benzothiadiazole-4-carboxylate tetrahydrate.

S1-N2	1.600(5)	S1-N1	1.602(5)
S1-K1	3.740(2)	N1-C1	1.335(7)
N1-K1	2.830(5)	N2-C2	1.348(7)
O1-C7	1.197(7)	O1-K1	2.672(4)
O2-C7	1.318(7)	O2-K1	2.815(5)
O3-C8	1.251(7)	O3-K1	2.846(4)
O4-C8	1.252(7)	C1-C6	1.438(7)
C2-C3	1.424(7)	C3-C4	1.368(7)
C3-C7	1.493(7)	C4-C5	1.411(7)
N2-S1-N1	101.10(2)	N2-S1-K1	143.00(18)
N1-S1-K1	44.55(17)	C1-N1-S1	107.00(4)
C1-N1-K1	138.00(4)	S1-N1-K1	112.00(2)
C2-N2-S1	106.60(4)	C7-O1-K1	129.20(4)
C7-O2-K1	120.50(4)	C8-O3-K1	146.10(4)
N1-C1-C6	126.90(5)	N1-C1-C2	112.80(5)
C6-C1-C2	120.30(5)	N2-C2-C3	126.50(5)
N2-C2-C1	112.60(5)	C3-C2-C1	120.90(5)

4.6 Synthesis of cadmium acetate complex of N,N'-bis-(1-pyridin-2-yl-ethylidene)-ethane-1,2-diamine

The ligand N,N'-bis-(1-pyridin-2-yl-ethylidene)-ethane-1,2-diamine was prepared according to a literature procedure.[11] The idea behind this reaction was to replace the acetate groups on Cd with deprotonated 7-carboxy-2,1,3-benzothiadiazole-4-carboxylate so as to form hopefully a dicadmium complex bridged by the thiadiazole and "end-

capped" with the imino-pyridine chelating groups. Thus, in a first attempt, hot methanolic solution of this ligand and a methanolic solution of $Cd(OAc)_2.2H_2O$ was stirred for 30 minutes, whereafter a solution of 7-carboxy-2,1,3-benzothiadiazole-4-carboxylate was added and the resulting solution was filtered hot and allowed the filtrate to stand in the fume hood at room temperature for two days to yield light yellow plate-like crystals. That the reaction was unsuccessful and that the title product formed with acetates in place at Cd was confirmed by melting point, IR, NMR and further with X-ray crystallography as the structure reported in Figure 4.12. This reaction was then repeated without BTD, using the same parameters and quantitative values of the other reagents but with a reagent grade methanol as solvent. This resulted in pure crystals of the same Cd complex but this time with four molecules of water of hydration, a lower melting point, and a lower yield, details are reported in the experimental section and the crystal structure is reported in Figure 4.13 below.

4.6.1 IR and NMR of cadmium acetate complex

In the IR spectrum, the presence of water in the lattice can be noticed, broad bands at 3470 cm^{-1}, the carboxylate bands due to $CH_3CO_2^-$ band at 1556 and 1402 cm^{-1}.[7]

The ^1H NMR in $CDCl_3$ has eight proton signal peaks as reported in Figure 4.11, based on symmetry through the molecule, with TMS and the solvent ($CDCl_3$) peaks at 0.00 and 7.270 ppm respectively. The (^1H) proton (H1) δ 9.1 ppm coupled to 2, 3 and 4 giving doublet of doublet of doublet, the coupling to 4 is very small, other peaks are at δ 7.9, 7.8, 7.5, 4.05, 2.5, 2.24 and 1.7, the signal at 2.24 ppm is attributed to the presence of

water in the solution. The ^{13}C NMR spectrum has ten distinct signals attributed to ten different carbon atoms in Figure 4.11, with details in the experimental section.

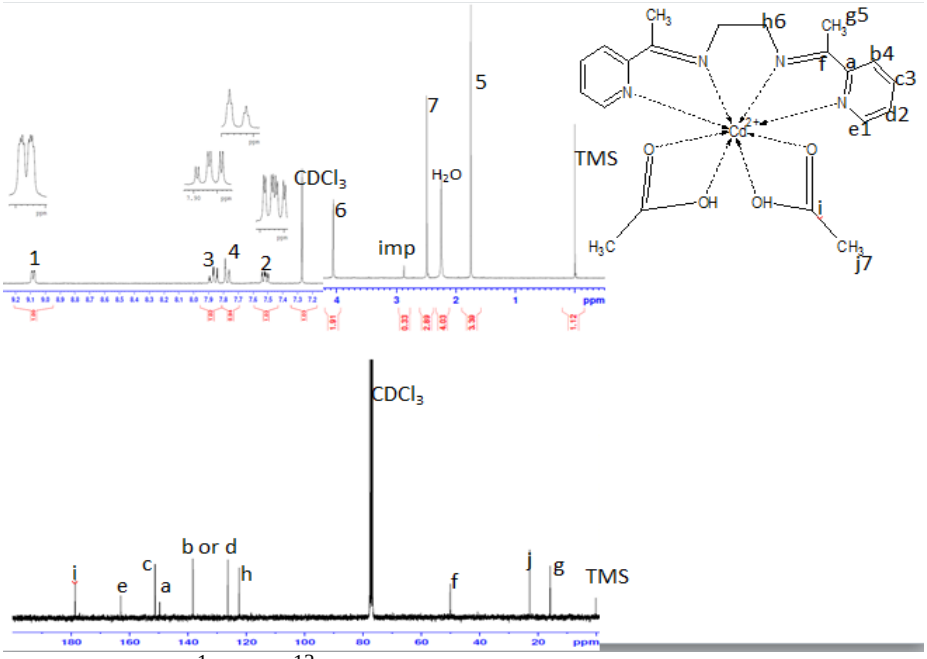

Figure 4.11 Showing ^{1}H and ^{13}C NMR spectra of Cd complex in $CDCl_3$

4.6.2 X-Ray Crystal Structures of cadmium acetate complexes

The X-ray structure determination (Figure 4.5) of the dihydrate structure shows that the N,N-bis-(1-pyridin-2-yl-ethylidene)-ethane-1,2-diamine ligand is coordinated through four almost co-planar nitrogen atoms (two pyridine and two imine donors) to the central Cd^{2+} ion. All four Cd–N distances are statistically indistinguishable with an average value of 2.400(2) Å, but they are arrayed mostly along one side of the metal ion. These Cd-N distances are very similar to those in a closely related (N,N'-bis(2-pyridinecarboxalidene)-1,2-cyclohexanediamine cadmium acetate complex [12] but larger than to those in an aminopyridine complex.[13] Perhaps cadmium is too large to fit comfortably within the chelate ring. The two acetate groups are fairly symmetrically located above and below the CdN_4 plane, with one oxygen of each acetate (O1 and O4)

occupying the axial sites and the second (i.e. O2 and O3) angled down about 40° from vertical, in the direction of the open face of the CdN_4 group. The Cd^{2+} thus has coordination number of eight; this element is well recognized for exhibiting high coordination number.[14,15] The bond angles around Cd^{2+} are all less than 90°, the largest is N3-Cd-O1 87.05(5)° and the smallest is, as expected, the internal acetate O-C-O bond angles of the two oxygen with which it coordinate to the cadmium. There is a significant variation in Cd-O bond distances, ranging from 2.415(1) to 2.590(1) Å. Two water molecules are found in the lattice and are hydrogen bonded to acetate oxygen atoms O1, O2 and O4. The hydrogen bond network in the lattice is unremarkable. However, an important feature of this structure is that the C7-C8 ethylene bridge is disordered by a minor component with the opposite twist of the chelate ring; the refined occupancy of the minor component is only 8%.

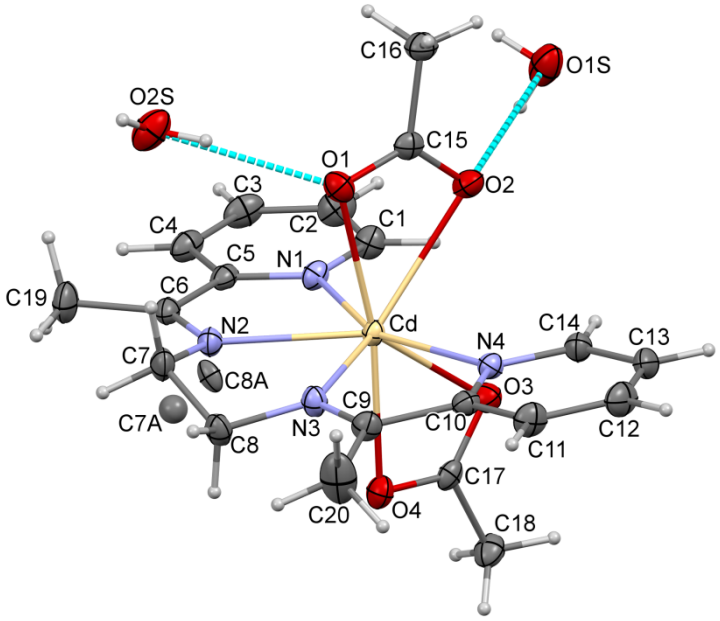

Figure 4.12 Thermal ellipsoids plot (40% probability) of the molecular structure of the cadmium acetate complex showing the atom numbering scheme and the hydrogen-bonded waters of crystallization. Hydrogen atoms belonging to the minor CH_2CH_2 disorder component have been omitted.

Table 4.12 Crystal data and structure refinement of the cadmium acetate dihydrate

Empirical formula	$C_{20}H_{28}CdN_4O_8$	
Formula weight	532.86	
Temperature	173(2) K	
Crystal system	Monoclinic	
Space group	P 2_1/c	
Unit cell dimensions	a = 17.5502(10) Å	α = 90°
	b = 8.6503(5) Å	β = 116.4890(10)°
	c = 16.1548(9) Å	γ = 90°
Z	4	
D_{calc}	1.612 g/cm^3	
Final R indices [I>2sigma(I)]	R1 = 0.0196, wR2 = 0.0448	
R indices (all data)	R1 = 0.0252, wR2 = 0.0472	

Table 4.13 Selected bond distances (Å) and angles in (°) of cadmium acetate dihydrate

Cd-N1	2.3965(14)	O1-C15	1.259(2)	O2-C16	1.254(2)
Cd-N2	2.3999(14)	O3-C17	1.252(2)	O4-C17	1.267(2)
Cd-N3	2.4009(14)	N1-C1	1.330(2)	N1-C5	1.347(2)
Cd-N4	2.4018(14)	N2-C6	1.272(2)	N2-C7	1.461(2)
Cd-O1	2.4148(13)	N2-C(7A)	1.57(3)	N3-C9	1.267(2)
Cd-O3	2.4301(13)	N3-C(8A)	1.58(2)	N4-C14	1.332(2)
Cd-O4	2.4578(13)	N4-C10	1.347(2)	C1-C2	1.393(3)
Cd-O2	2.5899(13)	C2-C3	1.381(3)	C3-C4	1.384(3)
C4-C5	1.397(2)	C5-C6	1.495(3)	C6-C19	1.501(2)
C7-C8	1.519(3)	C(7A)-C(8A)	1.45(3)	C9-C10	1.495(2)
C9-C20	1.498(3)	C10-C11	1.395(2)	C11-C12	1.383(3)
C12-C13	1.375(3)	C13-C14	1.392(2)	C15-C16	1.514(2)
N1-Cd-N2	67.43(5)	N1-Cd-N3	137.82(5)	N2-Cd-N3	70.40(5)
N1-Cd-N4	154.95(5)	N2-Cd-N4	137.51(5)	N3-Cd-N4	67.21(5)
N2-Cd-O1	82.20(5)	N1-Cd-O1	88.39(5)	N3-Cd-O1	87.05(5)
N4-Cd-O1	92.81(5)	N1-Cd-O3	80.73(5)	N2-Cd-O3	128.26(5)
N3-Cd-O3	127.02(5)	N4-Cd-O3	81.77(5)	O1-Cd-O3	138.14(4)
N1-Cd-O4	94.30(5)	N2-Cd-O4	88.18(5)	N3-Cd-O4	83.21(5)
N4-Cd-O4	89.63(4)	O1-Cd-O4	168.16(4)	O3-Cd-O4	53.69(4)
N1-Cd-O2	81.26(5)	N2-Cd-O2	125.23(4)	N3-Cd-O2	125.99(5)
N4-Cd-O2	79.82(4)	O1-Cd-O2	52.12(4)	O3-Cd-O2	86.19(4)
O4-Cd-O2	139.70(4)	C15-O1-Cd	96.70(10)	C15-O2-Cd	88.64(10)
C17-O3-Cd	92.75(11)	C17-O4-Cd	91.11(10)	C1-N1-C5	119.25(15)
C1-N1-Cd	122.14(12)	C5-N1-Cd	118.61(12)	C6-N2-C7	121.42(16)
C6-N2-C(7A)	127.50(9)	C6-N2-Cd	120.94(12)	C7-N2-Cd	116.10(11)
C(7A)-N2-Cd	109.90(9)	C9-N3-C8	121.63(16)	C9-N3-C(8A)	123.60(8)
C9-N3-Cd	129.33(12)	C8-N3-Cd	115.84(11)	C(8A)-N3-Cd	111.10(8)
C14-N4-C10	119.16(15)	C14-N4-Cd	122.26(12)	C10-N4-Cd	118.57(11)

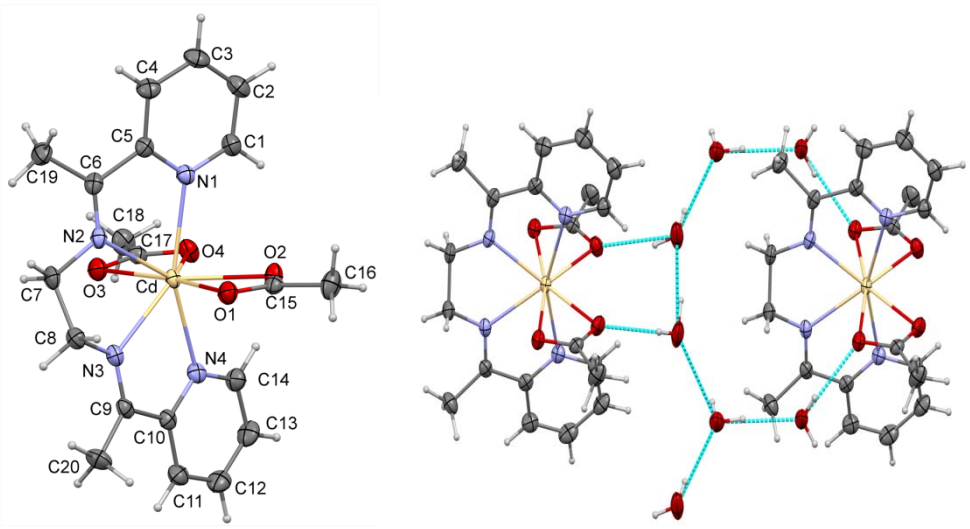

(a) (b)

Figure 4.13 Thermal ellipsoids plot (40% probability) of cadmium acetate dehydrate, (a) the molecular structure of the complex without water, and (b) the H-bonding network with water in the lattice.

Table 4.14 Crystal data and structure refinement of the cadmium acetate complex tetrahydrate

Empirical formula	$C_{20}H_{32}CdN_4O_8$	
Formula weight	568.89	
Temperature	173(2) K	
Crystal system	Triclinic	
Space group	P -1	
Unit cell dimensions	a = 7.9580(16) Å	α = 89.442(2)°
	b = 10.514(2) Å	β = 89.314(2)°
	c = 15.288(3) Å	γ = 88.950(2)°
Z	2	
D_{calc}	1.477 g/cm^3	
Final R indices [I>2sigma(I)]	R1 = 0.0368, wR2 = 0.0944	
R indices (all data)	R1 = 0.0408, wR2 = 0.0965	

Table 4.15 Selected bond distances (Å) and angles in (°) of cadmium acetate tetrahydrate

Cd- N2	2.372(2)	Cd-O1	2.581(2)	Cd-O2	2.352(2)
Cd-N3	2.376(2)	Cd-O4	2.369(2)	Cd-O3	2.547(2)
Cd-N1	2.446(2)	Cd-N4	2.446(2)	O2-C15	1.255(4)
O1-C15	1.257(4)	C15-C16	1.504(5)	O4-C17	1.255(4)
O3-C17	1.260(4)	C17-C18	1.507(5)	N1-C1	1.330(4)
N1-C5	1.346(4)	N2-C7	1.454(4)	N2-C6	1.273(4)
N3-C9	1.273(4)	N3-C8	1.455(4)	C10-N4	1.349(4)
N4-C14	1.335(4)	N3-Cd-N4	66.86(8)	N3-Cd-N2	71.73(8)
N2-Cd-N1	66.97(8)	O3-Cd-O4	52.85(7)	O2-Cd-O4	88.83(8)
O2-Cd-O1	52.49(7)	O1-Cd-N2	85.29(7)	N1-Cd-O1	86.05(7)
N1-Cd-O2	80.36(8)	N1-Cd-O3	96.34(7)	O3-Cd-N4	86.45(7)
N3-Cd-O1	82.94(8)	N4-Cd-O1	97.18(7)	O2-Cd-N4	82.13(8)
Cd-N2-C6	122.40(2)	Cd-N1-C5	117.60(2)	Cd-N2-C7	114.2(2)
Cd-N3-C8	114.10(2)	Cd-N3-C9	122.30(2)	Cd-N4-C10	117.60(2)
O4-Cd-O2	88.83(8)	O1-C15-O2	121.40(3)	O3-C17-O4	121.40(3)

The crystal structure of the tetrahydrate (Fig. 4.13) has an extremely similar coordination complex geometry to that of the dihydrate, but a more complex hydrogen-bonded array of water molecules that bridge two complexes *via* their acetate oxygens (Fig. 4.13b). In this structure, there is no evidence of disorder in the CH_2CH_2 bridge of the diimine, and also there is a now a statistically significant difference in the Cd-N_{imine}, 2.374(3), and Cd-$N_{pyridine}$, 2.446(2) Å, distances with the mean values indicated. Other structural features are very similar to that found in the dihydrate. There are four waters of crystallization in the lattice which form an H-bonded ring linking two complexes together. The crystal lattice has a significantly lower density on account of the more extensive hydrogen-bonded water content.

4.7 Synthesis of cadmium dichloride complex of 2-{(*E*)-[1-(pyridin-2-yl) ethylidene]amino}ethanamine

(N,N'-bis-(1-pyridin-2-yl-ethylidene)-ethane-1,2-diamine) (ligand) and $CdCl_2 \cdot 2.5H_2O$ were measured into an RBF, refluxed in ethanol for an hour, the resulting solution was filtered hot and allowed the filtrate to stand in the fume hood at room temperature for two days to yield light yellow plate-like crystals. The formation of this product was confirmed by melting point, IR, NMR and further with X-ray crystallography as the structure reported in Figure 4.15.

4.7.1 IR and NMR of cadmium dichloride complex

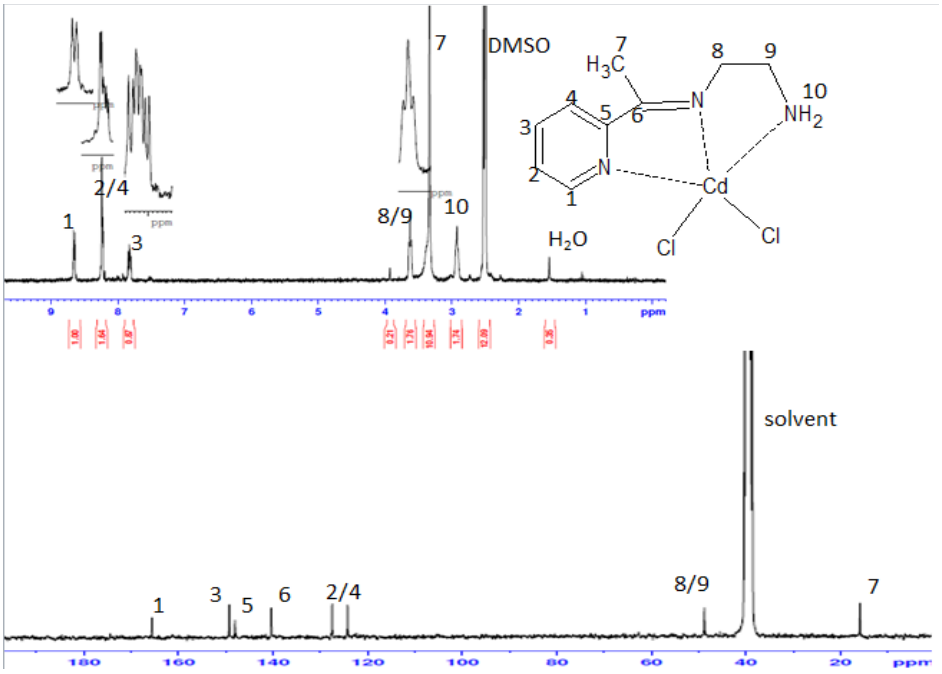

Figure 4.14 Plots of the ^{1}H and ^{13}C NMR spectra of the cadmium complex in DMSO

The IR of this compound has two N-H vibration bands at 3299 and 3252 cm^{-1}, two for C-H of the pyridine ring at 3166 and 2959 cm^{-1}. NMR of this structure has eight distinct proton peaks, the proton in position one appeared at 8.652 ppm and split into two having only one neighbour with a coupling constant of 4.8 Hz, the protons at positions two and

four seemed to overlap with each other and appeared as doublet of doublet of doublet at 8.23 pm, the proton at position three directly across from the nitrogen in the pyridine ring appeared at 7.82 ppm is a multiplet, the two equivalent protons at position six and seven each coupled to each other and appeared at position 3.625 and 2.932 ppm respectively, split into triplet, the methyl proton appeared as a single peak at 2.526 ppm, almost overlapping with the solvent (DMSO) protons. ppm, while the amine proton has a broad peak at 3.341 ppm overlapping with the peak of water protons.[16] The carbon NMR has eight distinct peaks with C in position eight and nine overlapping with each other at 48.81ppm.

4.7.2 X-Ray crystal structure of cadmium dichloride complex of 2-{(*E*)-[1-(pyridin-2-yl) ethylidene]amino}ethanamine

The molecular geometry of this compound is not completely flat due to the chlorine atoms that are out of plane, the ethylene group attached to nitrogen at both ends is also slightly twisted out of plane. The cadmium is coordinated to the ligand through three nitrogen atoms and to its two chlorine atoms possessing a coordination of five, the Cd-Cl bond distance is between 2.317 and 2.392 Å, with an angle of 68.29(5)° for N1-Cd-N2 and 78.83(6)° for N2-Cd-N3. There are short contacts between the amine hydrogen and chlorine which stands at 2.567(2) and 2.891(7) Å, the crystals are connected through short contacts to form a network structure as shown in Figure 4.15b. On the packing mode, two crystals are arranged adjacent to each other, then two adjacent pair are placed in a pattern where two different end are placed parallel to each other in the unit cell.

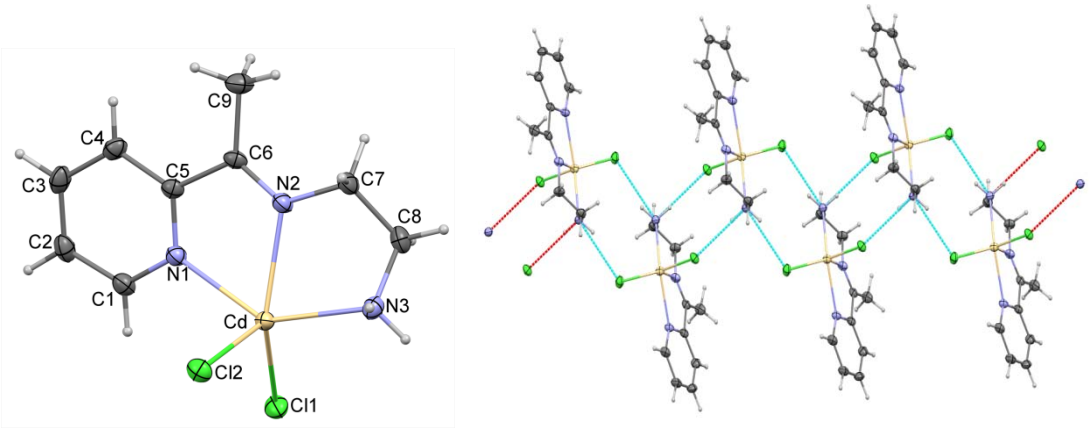

(a) (b)

Figure 4.15 (a) Thermal ellipsoids plot of the molecule within the lattice showing the atom numbering scheme. (b) Chlorine to NH hydrogen bonding network in the lattice.

Table 4.16 Crystal data and structure refinement of cadmium dichloride complex of 2-{(*E*)-[1-(pyridin-2-yl)-ethylidene]amino}ethanamine

Empirical formula	$C_9H_{13}CdCl_2N_3$	
Formula weight	346.52	
Temperature	173(2) K	
Crystal system	Monoclinic	
Space group	$P2_1/n$	
Unit cell dimensions	a = 8.721(3) Å	α = 90°
	b = 15.149(5) Å	β = 97.803(4)°
	c = 9.458(3) Å	γ = 90°
Z	4	
D_{calc}	1.859 g/cm^3	
Final R indices [I>2sigma(I)]	R1 = 0.0326, wR2 = 0.0561	
R indices (all data)	R1 = 0.0377, wR2 = 0.0578	

Table 4.17 Selected bond distances (Å) and angles in (°) of cadmium dichloride complex of 2-{(*E*)-[1-(pyridin-2-yl) ethylidene]amino}ethanamine

Cd-N2	2.315(2)	Cd-N3	2.334(2	C7-C8	1.513(4)
Cd-N1	2.391(2)	Cd-Cl1	2.4405(9)	C6-C9	1.505(3)
Cd-Cl2	2.4884(8)	N1-C1	1.341(3)	C5-C6	1.508(3)
N1-C5	1.349(3)	N2-C6	1.269(3)	C3-C4	1.392(4)
N2-C7	1.470(3)	N3-C8	1.486(3)	C4-C5	1.387(4)
C1-C2	1.382(4)	C2-C3	1.378(4)	N2-Cd-N3	73.90(7)
C7-N2-Cd	115.03(15)	C8-N3-Cd	107.28(13)	N1-C1-C2	122.80(2)
C3-C2-C1	118.40(2)	C2-C3-C4	119.40(2)	C5-C4-C3	119.00(2)
N1-C5-C4	121.40(2)	N1-C5-C6	115.20(2)	C4-C5-C6	123.30(2)
N2-Cd-N1	68.24(7)	N3-Cd-N1	141-41(7)	N2-C6-C9	124.80(2)
N2-Cd-Cl1	136.34(6)	N3-Cd-Cl1	107.10(7)	N2-C5-C5	115.90(2)
N1-Cd-Cl1	95.45(5)	N2-Cd-Cl2	112.72(2)	C9-C6-C5	119.20(2)
N3-Cd-Cl2	100.30(6)	N1-Cd-Cl2	100.80(5)	N2-C7-C8	108.30(2)
Cl1-Cd-Cl2	109.99(3)	C1-N1-C5	118.90(2)	N3-C8-C7	110.50(2)
C1-N1-Cd	123.86(16)	C5-N1-Cd	115.69(14)	C6-N2-Cd	121.63(16)
C6-N2-C7	122.90(2)				

4.8 Synthesis of 4,7-dibromo-5,6-dinitro-2,1,3-benzochalcogeniadiazole

Fuming nitric acid, oleum and 4,7-dibromo2,1,3-benzothiadiazole was stirred for 72 hours. 4,7-dibromo-2,1,3-benzothiadiazole gradually dissolved in the colorless mixtures

of the acids, on completion of the reaction, the reaction mixture was poured into an ice-water and allowed to cool to RT and filtered under vacuum, dried in a desiccator and recrystallized in 95 % ethanol to obtained pale yellow needle crystal. The ^{13}C NMR was as reported in literature[17] and the selenium analogue was also prepared in the same manner, the IR, NMR and melting points were used to confirm that these compounds were made, further confirmation from the X-ray crystallography which was used to ascertain the structures. On physical appearance the selenium analogue has a more bright yellow color then the sulfur.

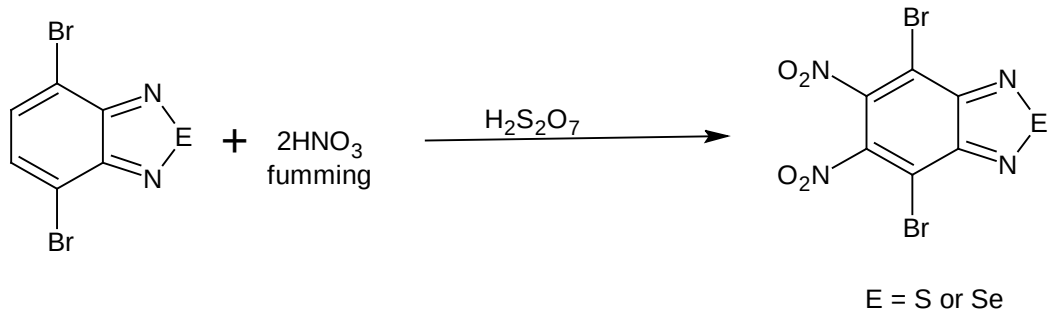

Scheme 4.4 Synthesis of 4,7 dibromo-5,6-dinitro-2,1,3-benzochalcogeniadiazole

4.8.1 IR and NMR of 4,7 dibromo-5,6-dinitro-2,1,3-benzochalcogeniadiazole

On the IR there are only two of vibration bands of interest, the symmetrical NO_2 vibration at 1335 cm^{-1} for the selenadiazole and 1336 cm^{-1} for the thiadiazole, the C=N stretching vibration occur at 883 cm^{-1} for the selenium and 885 for the thiadiazole analogue respectively. The ^{13}C NMR for both compounds is shown in Figure 4.16 below.

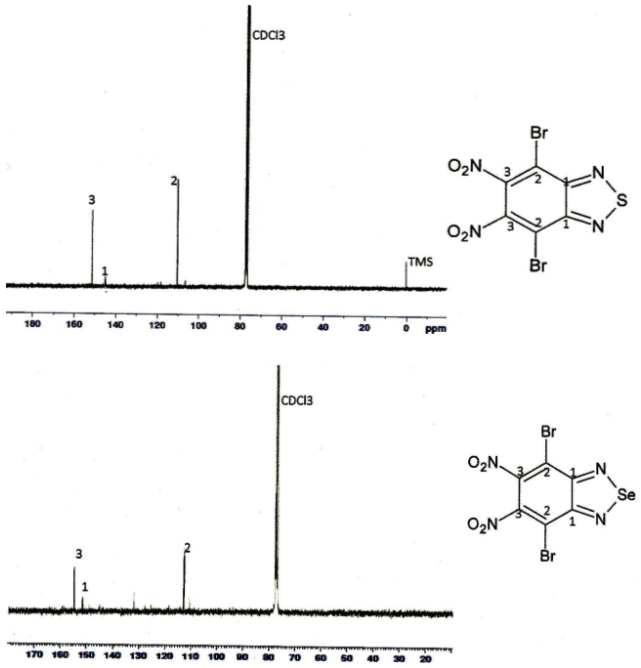

Figure 4.16 Showing the ^{13}C NMR for 4,7-dibromo-5,6-dinitro-2,1,3-benzothiadiazole and selenadiazole

4.8.2 X-Ray Crystal Structure of 4,7-dibromo-5,6-dinitro-2,1,3-benzothiadiazole and selenadiazole

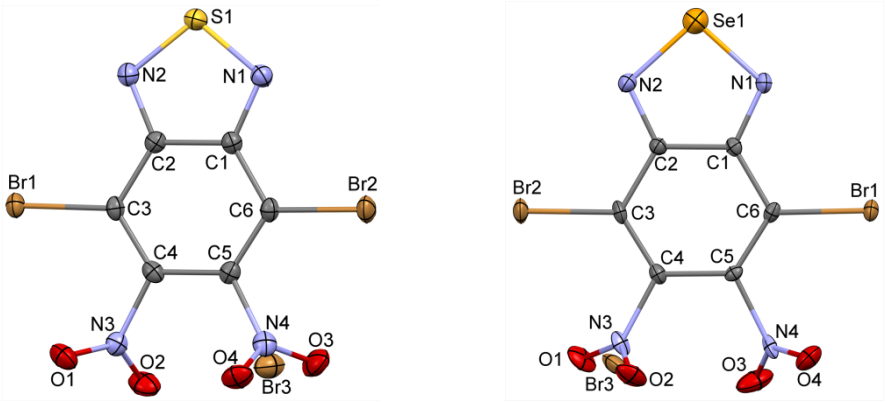

(a) (b)

Figure 4.17 Thermal ellipsoids plots (40% probability) of (a) 4,7-dibromo-5,6-dinitro-2,1,3-benzothiadiazole, and (b) 4,7-dibromo-5,6-dinitro-2,1,3-benzoseleniadiazole as found within the crystal lattices.

These compounds have no protons in them hence only ^{13}C NMR is considered, each with three distinct peaks, the benzothiadiazole analogue has peaks at 151.55, 145.13, and

110.49 ppm, those of the selenadiazole is of the average of 2.50 ppm lower in frequency than those of the thiadiazole. On the crystal structures, the compounds crystallized in an orthorhombic crystal system and in space group of $P2_12_12_1$, on the bond lengths and angles, it is only on the chalcogenadiazole ring that we observed some differences arising from the differences on the atomic size of sulfur and selenium, the N-S bond lengths are 1.615(2) and 1.613(2) Å, while that of N-Se are 1.736(6) and 1.740(6) Å. Short intermolecular contacts in the thiadiazole are Br1-Br2 = 3.5102(3), S1-O4 = 3.104(1) and O3-O4 = 2.904(2) Å, whereas those of seleniadiazole which are as expected longer at Br1-Br2 = 3.541(1), Se1-O3 = 3.026(7) and O1-O2 = 2.93(1) Å. The internal bond angles at the chalcogen are N-Se-N = 95.56(3)° and N-S-N 101.47(8)° for the selenadiazole and thiadiazole, respectively.

4.9 Discussion

2,1,3-benzothiadiazole-4,7-dicarboxylic acid has been successful prepared and characterized, but making a complex of it has not yet been possible because the condition for this specific reaction has not been found. Examining related compounds particularly benzene-1,4-dicarboxylic acid in literature, we found that making MOFs of them involves hydrothermal reaction at varying temperatures. Another process is the use of co-ligand as a capping ligand to create a discrete molecular complex, without co-ligand the complex could result to a continuous polymer. There is also the process where the dicarboxylate had been deprotonated to form a salt of the acid,[11] before subjecting the salt of the acid (ligand) to complex formation with a desired metal salt.

Most of the ligands used in the MOFs in literature have two coordination sites that made it easy and possible for those reactions. In the case of terephthalate, the presence of two

potentially coordinating oxygen atoms in the carboxylic acid group make it very robust for MOF. Like 2,1,3-benzothiadiazole-4,7-dicarboxylic acid, but the latter has two other coordinating sites, which are the 2N on the thiadiazole ring. These diverse aspects of the structural chemistry of 2,1,3-benzothiadiazole-4,7-dicarboxylic acid ligand are markedly sensitive to synthesis conditions requiring a more systematic of the influence of each individual factors, such a temperature, pH and solvent for the reaction.[18] Another issue is the coordination modes and protonation state of the ligand, which are necessary information, especially valuable because once the conditions for the formation of the desired building block are identified, it may become possible to make other modifications as might be required. Such as increasing the length of the ligand thereby increasing the pore size, but this condition as for this reaction are not met yet. Wu Hua and co-worker suggested the use of N donor ligands as co-ligand,[19,11] the use of hydrothermal conditions and the length of the ligand as it affect recrystallization. According to Batten,[20] long ligands will lead to larger voids that may result in high fold interpenetrating structure, however extending the length of the ligand may lead to difficulty in crystallization of the complex.

Examining the geometry of 2,1,3-benzothiadiazole-4,7-dicarboxylic acid, it has four coordination sites as a ligand, which is the first confronting problem making it difficult to only use two, without the rest competing for coordination. Extending the length of the ligand could not have made much difference, since the N of the ring thiadiazole as electron donating group is mid-way between the two carboxylate group.

Another issue is the conditions for de-protonation of the acid hydroxyl group through acid-based reactions, in our case this was tried with KOH, resulting in only mono

potassium salt of the acid as reported in section 4.5. In the asymmetric unit, the potassium is coordinated by a chelate from the carbonyl oxygen and one of the ring thiadiazole N. We did not continue to obtain the di-potassium salt, which we know can be obtained, if the conditions for that reaction are fulfilled. Another issue we looked at, is the survival of this ligand with other reactants in a reaction mixture at a high temperature. For example, we found that this compound is easily desulfurized giving rise to the formation 2,3-di-amino benzene-1,4-dicarboxylic acid. Subjecting 2,1,3-benzothiadiazole-4,7-dicarboxylic acid to similar reaction of benzene-1,4-dicarboxylic acid without a way to protect the thiadiazole ring, and preventing it from partaking in the coordination reaction will not give a meaningful result.

The use of cadmium acetate and cadmium chloride was tried separately with a co-ligand (N,N-bis-(1-pyridin-2-yl-ethylidene)-ethane-1,2-diamine) to make an end-capped complex of 2,1,3-benzothiadiazole-4,7-dicarboxylic acid. In both cases we did not obtain our expected result of the complex, but instead obtained cadmium acetate and a cadmium dichloride complex of the co-ligand as reported in session 4.6 and 4.7. Showing that the co-ligand with 4 electron donating N, two from pyridine and two from amine are better electron donating than carboxylate oxygen of 2,1,3-benzothiadiazole-4,7-dicarboxylic acid, even than the 2N of the thiadiazole ring.

It was decided not to go further with the characterization of the 4,7-dibromo-5,6-dinitro-2,1,3-benzothiadiazole and 4,7-dibromo-5,6-dinitro-2,1,3-benzoselenadiazole because these compounds have been reported in literature,[21] except their X-ray crystal structure which are presented here.

5.10 References

1. Rosi, N. L.; Eckert, J.; Eddaoudi, M.; Vodak, D. T.; Kim, J.; O'Keeffe, M.; Yaghi, O. M., *Science* **2003**, *300*, 1127-1129.
2. Silverstein, R. M.; Webster, F. X. *Spectrometric Identification of Organic Compounds*. Sixth ed.; John Wiley & Sons, Inc.: New York, 1998; p 95.
3. Wheelock, T. *Chem. Eng. Commun.* **1981**, *12*, 137-159.
4. Friedman, S.; Lacount, R. B.; Warzinski, R. P. *J. Am. Chem. Soc.* **1977**, *64*, 164-172.
5. Mukherjee, S.; Mahiuddin, S.; Borthakur, P., *Energy & fuels* **2001**, *15*, 1418-1424.
6. Li, W.; Cho, E. H. *Energy & fuels* **2005**, *19*, 499-507.
7. Silverstein, R. M.; Webster, F. X. *Spectrometric Identification of Organic Compounds*. Sixth ed.; John Wiley & Sons, Inc.: New York, 1998; p 97.
8. Allen, F. H.; Olga. K.; Watson, D. G.; Brammer, L. A.; Orpen, G.; Taylor, R. *J. Chem. Soc. Perkin Trans. II* **1987**, *2*, S1 - S19.
9. Poonia, N. S., *J. Am. Chem. Soc.* **1974**, *96*, 1012-1019.
10. Bolligarlaa, R.; Tripuramallua, B. K.; Sreenivasulub, V.; Dasa, S. K., *Indian J. Chem., Sect. A: Inorg., Bio-inorg., Phys., Theor. Anal. Chem.* **2011**, *50A*, 1410-1417.
11. Banerjee, S.; Lassahn, P.-G.; Janiak, C.; Ghosh, A., *Polyhedron* **2005**, *24*, 2963-2971.
12. Hakimi, M.; Moeini, K.; Mardani, Z.; Khorrami, F., *J. Korean Chem. Soc.* **2013**, *57*.
13. Baruah, A. M.; Karmakar, A.; Baruah, J. B., *Open Inorg. Chem. J.* **2008**, *2*, 62 - 68.
14. Cai, L.-Z.; Wang, M.-S.; Zhang, M.-J.; Wang, G.-E.; Guo, G.-C.; Huang, J.-S., *CrystEngComm* **2012**, *14*, 6196-6200.
15. Raos, A. M. a. N., *Acta Chim. Slov.* **2010**, 866 - 871.
16. ACD/C+H NMR Prectors 2012(v.14.00), A. C. D., Inc., *8 King street East, Suite 107, Toronto, Ontario, Canada M5C IB5*.
17. Wang, E.; Hou, L.; Wang, Z.; Hellström, S.; Mammo, W.; Zhang, F.; Inganäs, O.; Andersson, M. R., *Org. Lett.* **2010**, *12*, 4470-4473.
18. Go, Y. B.; Wang, X.; Anokhina, E. V.; Jacobson, A. J., *Inorg. Chem.* **2005**, *44*, 8265-8271.
19. Wu, H.; Yang, J.; Su, Z. M.; Batten, S. R.; Ma, J. F. *J. Am. Chem. Soc.* **2011**, *133*, 11406-11409.
20. Batten, S. R.; Robson, R., *Angew. Chem., Int. Ed.* **1998**, *37*, 1460-1494.
21. Chem, G. Y. *Polym. Adv. Technol.* **2006**, *47*, 4261-4268.

CHAPTER 5: CONCLUSIONS

5.1 Conclusions

The major objective of this thesis was to synthesize a benzothiadiazole dicarboxylate through a series of intermediate compounds. The chemistry of these ligands were to be investigated and then it was intended to convert the di-acid dicarboxylate into metal organic frame works (MOFs). While preparing the di-acid dicarboxylate was only feasible thus far on a small scale, the conditions for making MOFs with it have not yet been determined. With the understanding of the various applications of MOFs, we investigated the characteristic properties of the ligand metal complexes if they possess those characters of our expected MOFs. While these goals are not just as simple as it is on paper, it was found that accomplishing them turned out to be more challenging than envisaged. Notwithstanding, a lot of significant steps have been made towards accomplishing these objectives and lots was accomplished with the intermediate products. This thesis has pioneered coordination polymers with silver (I) using both the dinitrile and di-ester. Thus the intermediates on the way to the synthesis of the di-acid ligand have been shown to be very useful ligands to coordination polymers in their own right.

The synthesis of 2,1,3-benzothiadiazole-4,7-dicarbonitrile (DCBTD) was very challenging, despite the fact that this compound had previously been reported. The synthesis is cumbersome as removing the by-product ($CuBr_2$) with the use of concentrated HCl and H_2O_2,[1] affects not only the yield but the chemistry of the expected product. A comparative study of the electrochemical properties of the ligand was also

investigated where we observed two electron transfer reversible processes.[2] The EPR spectra are closely similar to those reported in literature. Five new metal (Ag^+) complexes were also reported for this ligand, the structures of these complexes were investigated, the Ag^+ exhibited a coordination from three to six with different geometrical spheres, the C≡N vibration band of the complexes are larger than that of the dinitrile ligand.

In the process of synthesizing the diethyl 2,1,3-benzothiadiazole-4,7-dicarboxylate (DEBTD) from 2,1,3-benzothiadiazole-4,7-dicarbonitrile through 2,1,3-benzothiadiazole-4,7-dicarbonyl dichloride as intermediate. The crystal structure is reported and the electrochemical properties of this ligand were investigated. Two reversible reductive electron transfer processes were observed, with the electrochemical window smaller than that of the 4,7-dinitrile-2,1,3-benzothiadiazole. The EPR splitting is more complex than those of the dinitrile due to differences in the active nuclei in the compounds. We also made five new metal (Ag^+) complexes of this ester ligand, in which we examined the electrochemical properties of one of the complexes and observed three reversible one electron reduction process in each, the third which made this difference is the reduction of Ag^+ to metallic silver and re-oxidation of metallic silver to Ag^+. Since the potentials are not quite distinct from the potentials of the ligand, we concluded that the Ag^+ does not bind with the ligand in solution, hence there is no change in potentials.

The synthesis of 2,1,3-benzothiadiazole-4,7-dicarboxylic acid was successful, and we report the crystal structure. But we could not make any complex of it, hence our aim of making our target metal organic frame work is not yet achieved. In the process of making the target MOFs, we made other compounds as shown in Sections 4.4, 4.5, 4.6 and 4.6 that are new in the chemistry literature, which we also report in this thesis.

5.2 Future work

To continue this work would mean to make metal organic frameworks (MOFs) of the deprotonated 2,1,3-benzothiadiazole-4,7-dicarboxylic acid and study all the possible characteristic of them. On these reported compounds and their complexes, the luminescent properties of the ligand would be interesting to be investigated, as their electrochemistry display two distinct return waves, DFT calculations on these ligands and their complexes can also be studied. Since the electrochemistry of the complexes shows de-complexation reaction in solution, we will therefore recommend solid electrochemistry for these complexes.

Thiadiazole derivatives are inexhaustible as replacement of one substituent in the molecule by an atom, or a molecule or a radical automatically result in the formation of a new thiadiazole derivative that could be more interesting by exhibiting excellent properties than what had been known in literature, but here are a few that catch my attention (Figure 5.1).

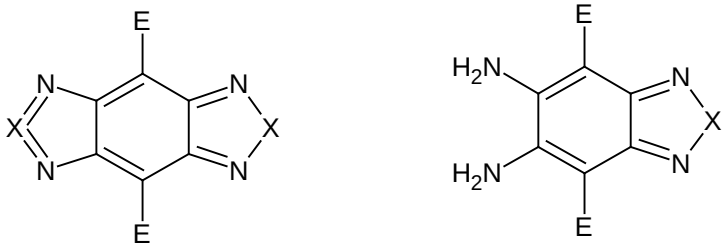

Figure 5.1 E = COOH, COOR, C≡N (where X = S, Se, Te)

The selenium and the tellurium analogue of these compounds are other series that can be made, that of tellurium might be difficult because of the limited numbers of reagents, due to extremely low solubility of its many products and the toxic nature of its compounds. But the electrochemical behavior of these will be quite likely different from those of the thiadiazoles due to differences of the electronic structure of these elements down the

group of the periodic table. Synthesis might also be problematic as the thiadiazole ring will be expanding as the size of the atoms increases from S, Se to Te and molecular weight also increases which are likely to affect the solubility[3] in different solvents, both in synthesis and crystallization of the product if crystals are required. Another series of chalcogeniadiazole compounds of interest that can be investigated are shown the in the figure 5.2 below.

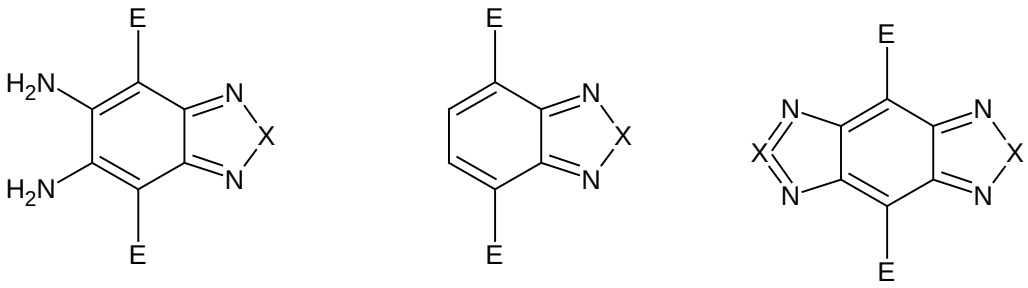

Figure 5.2 X = S, Se, Te. E=-CH_2CN, -$CH_2COOC_2H_5$.

6.3 References

1. Pilgram, K. *J. Heterocycl. Chem.* **1974,** *11*, 835-7.
2. Boeré, R. T.; Roemmele, T. L. *Coord. Chem. Rev.* **2000,** *210*, 369-445.
3. Li, Q.; Ding, Y.; Shao, M.; Wu, J.; Yu, G.; Qian, Y. *Mater. Res. Bull.* **2003,** *38*, 539-543.

CHAPTER 6: EXPERIMENTAL DETAILS

6.1 General procedures

Most of the products of this work were not air or water sensitive, but all chemicals and solvents were reagent grade. Dried toluene was obtained from SPS and methanol was dried with Mg and distilled for some specific use, most of other chemicals purchased were used without further purification. We tried to minimize as much as possible the interference of impurity in all our reaction systems, reagents and products. Samples prepared for the NMR spectroscopy were recorded on a 300 MHz Bruker Avance II spectrometer, but ^{1}H is measured at 300.13 MHz, and ^{13}C NMR at 75.48 MHz, then referenced relative to the residual solvent resonance(s) for ^{1}H and ^{13}C, which was for $CDCl_3$ 7.27 and 77.23 ppm respectively, D_2O 4.8 ppm, DMSO 2.5 and 39.5 ppm. FT-IR spectra were recorded on a Bruker ALPHA FT infrared spectrometer as solids via a diamond ATR sampling accessory. Elemental analyses were performed using an Elementar Americas Vario MicroCube instrument. For the electrochemical experiments, electrochemical grade tetrabutylammonium hexafluorophosphate $[^{n}Bu_4N][PF_6]$ (Fluka) was used for CV experiments as the supporting electrolyte and was kept in a desiccator prior to use. Ferrocene (Fc) was sublimed prior to use, the analytes were pure crystals. Electrospray ionization mass spectrometry instrument used a high resolution mass spectrometer (Thermo Scientific Exactive).

6.1.1 Voltammetry

Square wave and cyclic voltammograms were obtained at room temperature, in CH_3CN and solutions containing 0.1 M $[^{n}Bu_4N][PF_6]$, as the supporting electrolyte. This solution was purged with dry argon for about 10 minutes directly before use, and was kept

saturated with argon during all experiments. Measurements were performed with a Princeton Applied Research PARSTAT 2273 potentiostat. Initial background scans were used to characterize the size of the accessible electrochemical window and provided an estimate of the likely background current limits, the CVs were obtained over a potential range of -2 to +2 volts. The Fc/Fc^{+} redox couple, was used as an internal standard, the 3.0 mm glassy carbon (GC) and the platinum electrodes were used as working electrodes and these were polished with an Al_2O_3 (Buehler, 0.05 μm) slurry on a clean polishing cloth, rinsed with acetone, then distilled water and dried with tissue paper (Kimwipes) before use.

6.1.2 X-ray Crystallography

Suitable crystals are the major prerequisites for this experiment, then growing good quality crystals was required. In theory every soluble pure solid compound can be crystallized to give single crystals suitable for X-ray diffraction studies, and getting a suitable solvent for recrystallization was very necessary. The methods employed in crystal growth for this research work include: cooling, slow evaporation and liquid–liquid diffusion, then crystals are selected, coated in dry Paratone™ oil, mounted on a glass fiber and transferred to a goniometer head on the diffractometer. Diffraction data were collected on a Bruker Apex II diffractometer using monochromated MoKα radiation (λ = 0.71073 Å) and a KRYO-FLEX cold nitrogen gas cooling device at –100°C. The data were corrected for Lorentz and polarization effects, and an empirical absorption correction was applied to the net intensities. The structures were solved by direct, dual-space or Patterson methods, depending on which is best, and refined by least-squares methods on F^2, using the SHELXTL program package. After full-matrix least-squares

refinement of the non-hydrogen atoms with anisotropic thermal parameters, hydrogen atoms were placed in calculated positions (C–H = 0.99 Å). The isotropic thermal parameters of the hydrogen atoms on carbon were fixed at 1.2 times to that of the corresponding carbon. In the final refinements, the hydrogen atoms on carbon were added in a calculated positions and refined using a riding model.

6.2 Materials for synthesis and preparation of starting materials

Most of the materials (o-phenylenediamine, liquid Br_2, thionyl chloride, hydrobromic acid, silver salts) used for this work were purchased from Aldrich; all were used as received. The synthesis of 2,1,3-benzothiadiazole (BTD) (Figure 6.1a) and 4,7-dibromobenzothiadiazole (Figure 6.1b) were carried out according to the literature.[2,3] BTD was prepared by the action of thionyl chloride on o-phenylenediamine using dried toluene from SPS as a solvent through a method of ring-closure, under the protection of $CaCl_2$ drying tube.[4,5,6] Following the idea of Nunn and Ralph who found that boiling the reactants under reflux for 3 hours and distillation of the product gave a high yield of 85% of the heterocycle,[7] we obtained a crude yield of 76.3 %, and pure crystals in 69.2 % yield. 4,7-dibromo-2,1,3-benzothiadiazole is the most commonly used intermediate for the synthesis of BTD containing π-extended compounds, which can easily be prepared from BTD in high yield. We carried out the reaction of BTD with molecular bromine by slow addition in hydrobromic acid (HBr), then refluxed the mixture for 6 hours which gave exclusively 4,7-disubstituted regioisomer,[8,9,10] the first step in this reaction is the electrophilic addition at the position 4 or 7 of the BTD, then the para position. The fast addition of molecular bromine (Br_2) leads to tetrabrominated thiadiazole,[11,12] which was avoided through slow addition, the product was purified by the addition of saturated

sodium bisulphite to remove bromine, washed with water, dried (96.3 % yield) and recrystallized in ethanol to obtained pale yellow needle crystals.

6.2.1 Synthesis of 4,7-dibromo-5,6-dinitro-2,1,3-benzothiadiazole

To 110 mL of fuming nitric acid, was added 110 mL of fuming sulfuric acid in 500 mL two necked RBF containing a magnetic stirrer on ice bath, the temperature was kept below RT, to the mixture was added 22 g (74.8 mmol) of 4,7-dibromo-2,1,3-benzothiadiazole in small portions. Ice was removed and the reaction mixture was allowed to reach RT, and stirred for 72 hours, the reaction mixture poured into ice water (800 mL), the resulting mixture filtered through a Buchner funnel, the residue washed with water and dried, mass 10.64 g (36.7% yield), the crude product recrystallized in 95% ethanol give light yellow plate like crystals. Melting point 194 – 196 °C, (IR) $\nu(cm^{-1})$ 1581 (w), 1542 (vs), 1458 (m), 1385 (m), 1336 (s), 1264 (s), 1246 (m), 1217 (m), 1054 (m), 885 (s), 846 (m),798 (m), 773 (m), 747 (m), 705 (m), 674 (m), 649 (m), 614 (m), 582 (s), 467 (s), 443 (s), 417 (m), ^{13}C (NMR) DMSO δ, 150.38, 142.54, 110.28 ppm. Anal. Calc. For $C_6N_4O_4SBr_2$ with 10% excess Br in the molecule, C 18.60, N 14.10, Found C 18.65, N 14.05. An X-ray crystal was obtained and the structure determined, confirming the presence of co-crystallized tribromide.

6.2.2 Synthesis of 4,7-dibromo-5,6-dinitro-2,1,3-benzoseleniadiazole

Into a two-necked 100 mL RBF containing a magnetic stir bar was placed 21 mL fuming nitric acid, 21 mL fuming sulfuric acid was slowing added on an ice bath to keep the temperature below RT, followed by the addition of 5.0 g of 4,7-dibromo-2,1,3-benzoseleniadiazole, ice was removed. The mixture was stirred for 24 hours, poured into an ice water and allowed to cool to RT, filtered through a Buchner funnel, residue dried

in a dessicator and recrystallized in 95 % ethanol to obtain bright yellow crystals, 2.3 g (36.4 %) yield. Melting point 208 - 210°C, (IR) ν(cm^{-1}) 1576 (m), 1541 (vs), 1457 (m), 1374 (m),1335 (s), 1265 (m), 1218 (m), 1048 (m), 1011(m), 934 (w), 883 (s), 845 (m), 770 (m), 738 (s), 675 (m), 538 (m), 571 (m), 465 (s), 425 (s). Anal. Calc. For $C_6N_4O_4SeBr_2$, with 5% of extra Br in the molecule, C 16.60, N 12.88. Found C 17.19, N 12.81. An X-ray crystal was obtained and the structure determined, confirming the presence of co-crystallized tribromide.

6.3 Synthesis of 2,1,3-benzothiadiazole-4,7-dicarbonitrile and silver complexes

6.3.1 Synthesis of 2,1,3-benzothiadiazole-4,7-dicarbonitrile (DCBTD)

14.7 g (0.05 mole) of 4,7-dibromo-2,1,3-benzothiadiazole and 10.0 g of copper cyanide in 150 mL of DMF was refluxed in 250 mL RBF for 12 hours, on heating the reaction mixture, the color changes through light green, to brown then black. Cool to room temperature and concentrated to about 25% by volume of the solvent, 25 mL concentrated solution of hydrochloric acid added to the black residue, 12.5 mL of 30% hydrogen peroxide added drop wise in an ice bath to keep the temperature between 30 - 40°C.[15a] Removing the solvent completely results in the formation of tar (emulsion) as experienced by earlier chemists like B.N. Schrauzer and S. Eichler,[17] on the addition of concentrated HCl and then H_2O_2. The mixture was stirred for 3 hours and filtered, both the residue and the filtrate were extracted with 450 mL of benzene, the combined orange color extracts were washed with water in a separating funnel and dried over $MgSO_4$, concentrated through rotatory evaporator to give 7.20 g (77.2% yield), the crude was recrystallized from 95% ethanol to give plate like yellow crystals: melting point (mp)

189–190 °C, (Lit. 189 –191°C, recrystallized from benzene).[18] IR ν(cm^{-1}) 456 (m), 515 (m), 627 (s), 869 (vs), 1131 (m), 1291 (m), 1344 (m), 1375 (m), 1580 (m), 2234 (s), 3055 (m), ^{1}H NMR 300 MHz, $CDCl_3$, RT, TMS, δ 8.158 ppm, ^{13}C NMR δ 152.48, 134.62, 113.97, 110.71 ppm. Anal. Cald. For $C_8H_2N_4S$: C, 51.60; H, 1.1; N, 30.10. Found: C, 51.5; H, 1.11; N, 30.00. X-ray crystal structure obtained.

6.3.2 Synthesis of 4,7-dinitrile-2,1,3-benzothiadiazole complex of $AgBF_4$

$[Ag_4(DCBTD)_5][(BF_4)_4]$

46.5 mg (0.25 mmol) of 4,7-dinitrile-2,1,3-benzothiadiazole was dissolved in 8.0 mL of CH_2Cl_2, layered with 39.0 mg (0.2 mmol) of $AgBF_4$ dissolved in 5.0 mL of warm benzene in a crystallization tube, with 1.0 mL of benzene placed between the layers to prevent instant mixing of the two layers. Plate like brown colored crystals, were harvested after 3 days, mass 34 mg (47.5 % yield), melting point 286 -288 ^{0}C, IR ν (cm^{-1}) 3107 (w), 2985 (w), 2254 (w), 1698 (m), 1558 (w), 1375 (w), 1276 (m), 1264 (m), 1191 (m), 1099 (s), 1027 (vs), 902 (m), 878 (s), 754 (m), 629 (s), 517 (m), 463 (m), 384 (s). Anal. Cald. For $C_{40}H_{10}Ag_4B_4F_{16}N_{20}S_5$: C, 28.10; H, 0.59; N, 16.38. Found: C, 31.66; H, 0.73; N, 18.43. X-ray crystal structure obtained.

6.3.3 Another Complex of 4,7-dinitrile-2,1,3-benzothiadiazole and $AgBF_4$,

$[Ag(DCBTD)_2]BF_4$

18.6 mg (0.1 mmol) of 4,7-dinitrile-2,1,3-benzothiadiazole was dissolved in 5.0 mL of CH_2Cl_2, layered with 9.7 mg (0.05 mmol) of $AgBF_4$ dissolved in 14.0 mL of benzene at room temperature in a crystallization tube, plate like brown colored crystals, were harvested after one week, mixed with non-crystalline materials. X-ray quality crystals were sorted used for crystallography and IR and melting point, mass 7 mg (24.7 % yield),

melting point 212 -214 $^{\circ}$C, IR ν (cm^{-1}) 3108 (w), 3082 (w), 3059 (w), 2254 (m), 1548 (m), 1382 (m), 1335 (w), 1289 (w), 1256 (w), 1131 (m), 1101 (vs), 1049 (vs), 1029 (vs), 878 (vs), 854 (s), 766 (m), 631 (vs), 518 (s), 463 (s), 385 (vs). Anal. Cald. For $C_{16}H_4AgBF_4N_8S_2$ C; 33.89, H; 0.71, N; 19.76. X-ray crystal structure was obtained.

6.3.4 Synthesis of 4,7-dinitrile-2,1,3-benzothiadiazole complex of $AgSbF_6$ benzene solvated $[AgDCBTD][(SbF_6)_2.2C_6H_6]$

18.6 mg (0.1 mmol) of 4,7-dinitrile-2,1,3-benzothiadiazole and 68.7 mg (0.2 mmol) of $AgSbF_6$ were both dissolved in warm benzene with vigorous stirring for 30 minute in 50 mL RBF, cool to RT, precipitate formed on cooling, filtered and recrystallized in methanol, filtered and dried to obtained yellow plate crystals, X-ray crystals were selected from the mixture of crystals and powder, mass 42.0 g (48 % yield), melting point 243 – 245 ^{0}C, IR ν (cm^{-1}) 3120 (w), 3069 (w), 2268 (w), 1557 (w), 1342 (w), 1290 (w), 1136 (w), 914 (w), 893 (w), 860 (m), 652 (s), 630 (vs), 514 (m), 465 (m), 423 (w). The EA did not give good report due to de-solvated solvent in the lattice, with two molecules of benzene in the lattice, Anal. Calc., C 23.3, H 1.36, N 5.44. Found C 17.96, H 0.64, N 10.32. To explain the large difference in the results, we found that a fraction of the benzene in the lattice is lost, so we try the Calc. with only one molecule of benzene which gives C 17.68, H 0.84, a much closer fit, meaning that benzene is gradually removed from the lattice over time. X-ray crystal structure was obtained.

6.3.5 Synthesis of 4,7-dinitrile-2,1,3-benzothiadiazole complex of $AgClO_4$ $[Ag_4(DCBTD)_5][ClO_4]_4$

43.7 mg (0.235 mmol) of 4,7-dinitrile-2,1,3-benzothiadiazole and 39.0 mg (0.188 mmol) were dissolved in 5.0 mL of benzene separately, solution put together and stirred for 30 minute, precipitate obtained was filtered in a Buchner funnel and dried. The dried solid precipitate was recrystallized in warm methanol which on cooling gave light yellow rod like crystals filtered and dried, X-ray quality crystal were selected from the bulk, mass 58 mg (71.0 % yield), melting point 245–247 ^{0}C, IR ν (cm^{-1}) 3056 (w), 2247 (w), 1552 (w), 1385 (w), 1346 (w), 1293 (w), 1259 (w), 1081(s), 1020 (s), 788 (s), 695 (m), 615 (vs), 540 (m), 512 (m). Anal. Calc. for this complex: C, 27.30; H, 0.57; N, 15.91; Found: C, 27.46; H, 0.60; N, 15.96, Mass spectrum (m/z) on negative ion mode 82.95 (ClO_3^- for ^{35}Cl, 100%), 98.95 (ClO_4^- for ^{35}Cl, 75.62%). On the positive ion mode 106.90 (Ag^+, 100%), 147.93 ($[Ag(CH_3CN)]^+$, 14.49%), 188.96 ($[Ag(CH_3CN)_2]^+$, 60.80%) X-ray crystal structure was obtained.

6.3.6 Synthesis of 4,7-dinitrile-2,1,3-benzothiadiazole complex of $AgPF_6$ benzene solvate $[AgDCBTD]PF_6.C_6H_6$

18.6 mg (0.1 mmol) 0f 4,7-dinitrile-2,1,3-benzothiadiazole was in 5.0 mL of CH_2Cl_2 layered with 20.0 mg (0.08 mmol) of $AgPF_6$ in 4 mL of benzene, 1.0 mL of benzene placed between the layers to prevent instant mixing of the two solutions, small pale yellow flake crystals was harvested after 5 days, mass 46.0 mg (89 % yield), melting point 238 – 240 ^{0}C, IR ν (cm^{-1}) 2260 (w), 1554 (w), 1458 (w), 1385 (w), 1289 (w), 1134 (w), 898 (w), 829 (w), 670 (w), 633 (w), 555 (w), 463 (w), 379 (w). Anal. Calc. For $C_{14}H_8AgF_6N_4PS$ with benzene in the lattice (solvated), C 32.52, H 1.56, N 10.83, without benzene in the lattice (de-solvated), C 21.89, H 0.46, N 12.76, Found C 22.37, H 0.87, N

13.00, the differences might arise from the difference of benzene lost or remaining in the lattice. X-ray crystal structure was obtained.

6.4 Synthesis of diethyl-2,1,3-benzothiadiazole -4,7-dicarboxylate and silver complexes

6.4.1 Synthesis of diethyl-2,1,3-benzothiadiazole -4,7-dicarboxylate (DEBTD)

5.0 g (26.88 mmol) of 4,7-dinitrile-2,1,3-benzothiadiazole (pure crystals) and excess 25 % aqueous sodium hydroxide (80 mL) in 250 mL RBF was heated to refluxed for 15 hours,[19] until evolution of ammonia stopped, this was monitored and checked with moist litmus paper. *Note;* The reaction started with 50.0 mL of 25 % $NaOH_{(aq)}$ on heating, the reaction mixture turned to gel, then solid, to avoid this, extra 30.0 mL was added at 5.0 mL interval until the reaction mixture stabilized. Cooled to room temperature and acidified with concentrated hydrochloric acid, filtered in a Buchner funnel and air dried to obtain a brown solid, (10.5 g) impure product (actual mass obtained = 10.5g, theoretical mass = 6.02g), which we could not be purified because of the very close solubility of the impurity (NaCl) and that of the product.

10.0 g of the crude acid and 30.0 mL of thionyl chloride was refluxed for 15 hours in 100 mL RBF, cooled and filtered. The filtrate was evaporated in a rotatory evaporator to obtain crude 2,1,3-benzothiadiazole-4,7-dicarbonyl dichloride (11.8 g) (actual mass obtained = 11.8g, theoretical mass = 6.68 g).

8.0 g (30.6 mmol) of the crude 2,1,3-benzothiadiazole-4,7-dicarbonyl dichloride was added to 5.0 mL of pyridine in 80.0 mL of 96 % ethanol, the mixture was refluxed in 250 mL RBF for 2 hours, cooled to RT and poured into water, the product was filtered with a Buchner funnel and dried to give orange coloured solid, 8.2 g (29.3 mmol) 96 % crude

yield. Recrystallization from hexane with the aid of activated charcoal gave a pale yellow weak crystalline solid 2.496 g (8.91 mmol), 51% overall yield. Mp 66-67 °C, IR ν (cm^{-1}) 2981 (w), 1735 (m), 1702 (s), 1587 (w), 1551 (m), 1471 (w), 1447 (w),1369 (m), 1274 (s), 1172 (vs), 1021 (s), 861 (m), 829)m), 756 (s), 670 (w), 532 (m), 484 (m),393 (w), ^{1}H NMR (300 MHz), $CDCl_3$, RT, TMS, δ 8.390, 4.565, 1.496 ppm, ^{13}C (NMR) δ 164.10, 152.95, 131.91, 127.36, 62.33, 14.52 ppm. Anal. Calc. for $C_{12}H_{12}N_2O_4S$, C 51.42, H 4.31, N 10.00, Found C 51.47, H 4.05, N 10.31. X-ray crystal structure was obtained.

6.4.2 Synthesis of diethyl-2,1,3-benzothiadiazole-4,7-dicarboxylate complex of $AgClO_4$ [AgDEBTD]ClO_4

56.0 mg (0.2 mmol) of diethyl-2,1,3-benzothiadiazole-4,7-dicarboxylate was dissolved in 8.0 mL of CH_2Cl_2, layered with 41.5 mg (0.2 mmol) of $AgClO_4$ in 5.0 mL of benzene, 1.0 mL placed between the layers to prevent turbulence, then instant mixing of the two solutions, small yellow needle crystals were harvested after 3 days, mass 60.0 mg (62 % yield), melting point 227 - 229 °C, IR ν (cm^{-1}) 2986 (w), 2940 (w), 1698 (s), 1560 (w), 1468 (w), 1449 (w), 1374 (w), 1392 (w), 1265 (s), 1192 (s), 1170 (m), 1118 (s), 1096 (s),1047 (s), 1019 (vs), 975 (s), 875 (m), 837 (m), 754 (s), 617 (s), 575 (m), 531 (m), 482 (m), 419 (m). E. Anal. Calc. for this complex, C, 27.30; H, 0.57; N, 15.91. Found, C, 27.46; H, 0.60; N, 15.96. Mass spectrum (m/z) 106.905 (Ag^+ 100%), 147.93165 ([$(AgCH_3CN)]^+$ 6.1%), 188.958 ([$Ag(2CH_3CN)]^+$, 11.5%), 235.01775 ([L - OEt]$^+$, 2.4%), 386.95690 ([L, Ag]+, 11.6%), 427.98345 ([L,Ag,CH_3CN]+,7.7%), 667.00870 ([2L, Ag]$^+$, 3.0). X-ray crystal structure was obtained.

6.4.3 Synthesis of diethyl-2,1,3-benzothiadiazole-4,7-dicarboxylate complex of $AgClO_4$ benzene solvate [AgDEBTD]ClO_4.C_6H_6

14.0 mg (0.05 mmol) of diethyl-2,1,3-benzothiadiazole-4,7-dicarboxylate and 0.01 mg (0.05 mmol) of $AgClO_4$ were dissolved in warmed benzene with stirring for 30 minutes, on cooling precipitate was formed, filtered in a Buchner funnel and dried, solid recrystallized in methanol to obtained yellow needle crystal, X-ray quality were sorted from the bulk, mass 16 mg (57 % yield), melting point 216 – 218 °C, IR ν (cm^{-1}) 2983 (w), 2941 (w), 1695 (m), 1676 (m), 1559 (m), 1471 (w), 1395 (w), 1280 (s), 1198 (s), 1092 (s), 1049 (s), 1023 (vs), 906 (m), 876 (m), 835 (m), 756 (s), 619 (vs), 454 (m), 384 (m). E.A. Calc. for this complex. With benzene in the lattice, C, 38.2; H, 3.20; N, 4.95, when de-solvated completely C, 29.56; H, 2.48; N, 5.74. Found, C, 31.99; H, 2.66; N, 6.23. The difference was found to be gradual loss of benzene from the lattice which invariably raised the mass of N. On calculation, we found that the loss in mass in the C and H is the exact ratio of C:H as it is in benzene. Mass spectrum (m/z) 106.905 (Ag^+ 100%), 147.93165 ($[(AgCH_3CN)]^+$ 8.1%), 188.958 ($[Ag(2CH_3CN)]^+$, 11.5%), 235.01775 ($[L - OEt]^+$, 2.4%), 386.95690 ([L, Ag]+, 11.6%), 427.98345 ([L,Ag,CH_3CN]+,1.3%), 667.00870 ($[2L, Ag]^+$, 3.0). X-ray crystal structure was obtained.

6.4.4 Synthesis of diethyl-2,1,3-benzothiadiazole-4,7-dicarboxylate complex of $AgBF_4$ hydrate [AgDEBTD]$BF_4.H_2O$

56.0 mg (0.2 mmol) of diethyl-2,1,3-benzothiadiazole-4,7-dicarboxylate and 38.8 mg (0,2 mmol) of $AgBF_4$ were measured separately into 50.0 mL RBF, 8.0 mL of benzene was measured and added to the mixture, stirred for 30 minute and warmed gently to dissolve. On cooling precipitate was formed, filtered and dried, solid recrystallized in methanol which gave yellow needle crystals through slow evaporation of the solvent. X-ray quality crystal was sorted from the bulk mixed with powder, mass 78.0 mg (82 % yield), melting

point 247 – 249 °C, IR ν (cm^{-1}) 3566 (w), 3483 (w), 2999 (w), 1697 (s), 1653 (m), 1558 (m), 1473 (m), 1376 (m), 1281 (s), 1200 (s), 1047 (s), 1017 (vs), 906 (s), 877 (s), 833 (m), 762 (s), 575 (m), 519 (s),478 (s), 419 (s). E. Anal. Cald. for this complex $C_{12}H_{14}AgN_2O_5SBF_4$, C, 29.2; H, 2.9; N, 5.7. Found. C, 29.2; H, 2.8; N, 5.7, Mass spectrum (m/z) 106.905 (Ag^+ 100%), 147.93165 ($[(AgCH_3CN)]^+$ 9.7%), 188.958 ($[Ag(2CH_3CN)]^+$, 4.0%), 235.01775 ([L - OEt]$^+$, 2.0%), 386.95690 ([L, Ag]+, 8.1%), 427.98345 ([L,Ag,CH_3CN]+,10.4%), 667.00870 ([2L, Ag]$^+$, 2.1). X-ray crystal structure was obtained.

6.4.5 Synthesis of diethyl-2,1,3-benzothiadiazole-4,7-dicarboxylate complex of $AgPF_6$ benzene solvate [AgDEBTD]$PF_6.C_6H_6$

14.0 mg (0.05 mmol) of diethyl-2,1,3-benzothiadiazole-4,7-dicarboxylate was dissolved in 6.0 mL of CH_2Cl_2 layered with 12.64 mg (0.05 mmol) of $AgPF_6$ dissolved in 5.0 mL of benzene with 1.0 mL of benzene place between the layers to prevent instant mixing of the solution and turbulence that could generate precipitation in the crystallization tube, colorless needle X-ray crystals were harvested after 3 days, mass, (50 % yield), melting point 207-209 °C, IR ν (cm^{-1}) 1690 (s), 1554 (m), 1475 (w), 1450 (w), 1445 (m), 1410 (w), 1277 (s), 1198 (m), 1125 (m), 1050 (s), 1023 (s), 871 (s), 761 (s), 692 (vs), 555 (m), 476 (s), 443 (s), 390 (m). Anal. Calc. C, 21.89, H, 0.46, N, 12.76, Found, C, 22.37, H, 0.87, N, 13.00, the result shows addition materials (impurities). Mass spectrum (m/z) 106.905 (Ag^+ 100%), 147.93165 ($[(AgCH_3CN)]^+$ 7.9%), 188.958 ($[Ag(2CH_3CN)]^+$, 2.5%), 235.01775 ([L - OEt]$^+$, 3.0%), 386.95690 ([L, Ag]+, 7.1%), 427.98345 ([L,Ag,CH_3CN]+,7.1%), 667.00870 ([2L, Ag]$^+$, 1.0). X-ray crystal structure was obtained.

6.4.6 Synthesis of diethyl-2,1,3-benzothiadiazole-4,7-dicarboxylate complex of $AgSbF_6$ benzene solvate $[AgDEBTD]SbF_6.C_6H_6$

56.0 mg (0.2 mmol) of diethyl-2,1,3-benzothiadiazole-4,7-dicarboxylate was dissolved in 8.0 mL of CH_2Cl_2 layered with 68.7 mg (0.2 mmol) dissolved in 5.0 mL of benzene, with 1.0 mL placed between the solutions to prevent turbulence and instant mixing that could result in precipitation, the set up was kept in the fume hood, yellow needle crystals were harvested after 3 days, mass 62 mg, (49.7 % yield), melting point 296 – 298 °C, IR ν (cm^{-1}) 2982 (w), 2945 (w), 1687 (s), 1557 (m), 1474 (m),1397 (w), 1374 (m), 1274 (s), 1199 (m), 1123 (m), 1050 (m), 1024 (m), 914 (m), 886 (m), 836 (m), 761 (m), 695 (s), 653 (vs), 574 (m), 477 (m), 419 (w). Anal. Calc. for this complex: C, 30.80; H, 2.58; N, 3.99. Found: C, 30.85; H, 2.43; N, 4.15, Mass spectrum (m/z) 106.905 (Ag^+ 99.6%), 147.93165 ($[(AgCH_3CN)]^+$ 10.7%), 188.958 ($[Ag(2CH_3CN)]^+$, 7.5%), 235.01775 ($[L\text{-}OEt]^+$,10.0%), 281.05963 ($[LH]^+$, 2.2%) 386.95690 ([L, Ag]+, 5.8%), 427.98345 ([L,Ag,CH_3CN]+,11.9%), 667.00870 ($[2L, Ag]^+$, 2.5). X-ray crystal structure was obtained.

6.5 Synthesis of 2,1,3-benzothiadiazole-4,7-di carboxylic acid and derivatives

6.5.1 Synthesis of 2,1,3-benzothiadiazole-4,7-dicarboxylic acid

3.0 g (10.7 mmol) of pure diethyl-2,1,3-benzothiadiazole-4,7-dicarboxylate and 1.4 g (25.0 mmol) of potassium hydroxide in a mixture of 30.0 mL of ethanol and 1.2 mL of water (25:1 ratio) was refluxed for 12 hours, cooled to RT, concentrated to dry solid on a rotatory evaporator. Solid dissolved in 40.0 mL of water and acidified with 0.62 mL of concentrated hydrochloric acid (25.0 mmol), precipitate was formed during acidification,

filtered and dried to obtained tan solid 2.20 g, 92 % yield, solid recrystallized in water to give pale yellow solid. Melting point 322-323 °C, IR ν (cm^{-1}) 3424 (m), 3402 (m), 3124 (m), 3066 (m), 2385 (m), 2195 (m), 1893 (w), 1867 (w), 1682 (s), 1623 (m), 1589 (m), 1554 (m), 1500 (m), 1400 (m), 1381 (m), 1336 (m), 1288 (s), 1230 (s), 1175 (s), 1099 (m), 1021 (m), 991 (m), 980 (m), 967 (m), 883 (s), 865 (s), 830 (s), 788 (m), 753 (vs), 695 (s), 584 (s), 562 (s), 548 (s), 458 (s), 415 (s), 401 (s), 380 (s), ^{1}H NMR (300 MHz), DMSO RT, TMS, δ 8.155 ppm, ^{13}C (NMR) δ 165.22, 152.24, 131.70, 127.55 ppm. Anal. Calc. for C 39.67, H 2.49, N 11.57, Found C 39.59, H 2.44, N 11.77. X-ray crystal structure was obtained.

6.5.2 Synthesis of potassium 7-carboxyl-2,1,3-benzothiadiazole-4-carboxylate

28.0 mg (0.1 mmol) of 2,1,3-benzothiadiazole-4,7-dicarboxylate was dissolved in 8.5 mL of methanol, 14.0 mg (0.25 mmol) of aqueous potassium hydroxide was added in 50 mL RBF, stirred and refluxed for I hour, cooled to RT, filtered and dried, dried solid dissolved in hot water and recrystallized on cooling, mass 19.0 mg pure crystals (58 % yield), melting point 348-349 °C, IR ν (cm^{-1}) 3424 (w), 2888 (w), 2454 (w), 1731 (m), 1708 (m), 1676 (s), 1590 (m),1539 (m),1485 (m), 1394 (s), 1357 (m), 1290 (m), 1244 (s), 1181 (s), 1000 (m),870 (m),788 (m), 755 (vs), 729 (s), 666 (m), 618 (m), 556 (s), 452 (s), 414 (s), ^{1}H NMR (300 MHz), DMSO RT 8.122 ppm, ^{13}C (NMR) δ 165.82, 156.77, 130.71, 129.06 ppm. Anal. Calc. For C 32.51, H 2.27, N 9.40. Found C 32.50, H 2.31, N 9.43. X-ray crystal structure was obtained.

6.6 Synthesis of desulfurized 2,3-diaminobenzene-1,4-dicarboxylic acid

5.0 g (26.9 mmol) of 4,7-dinitrile-2,1,3-benzothiadiazole and 100 mL of 25 % aqueous solution of sodium hydroxide was heated to reflux, on heating the solution was turning gel and water was added in 5.0 mL portion until it stabilised, a total of 75 mL of water was added, refluxed for 15 hours, until evolution of ammonia stopped, this was confirmed by placing moist red litmus on the mouth of the reaction vessel, cooled to RT, the brown solution was acidified with concentrated hydrochloric acid which gave pale green precipitate, filtered and dried, recrystallized in water to obtained 4.2 g (79.8 % yield), mp 286-290 °C, IR ν (cm^{-1}) 3442 (m), 3346 (m), 1676 (m), 1638 (m), 1602 (s), 1513 (m), 1463 (m), 1414 (m), 1326 (m), 1289 (m), 1213 (s), 1165 (s), 1086 (m), 907 (s), 779 (s), 739 (s, 618 (s), 557 (s), 495 (s), 474 (vs), 424 (vs), ^{1}H NMR (300 MHz), DMSO RT, TMS, δ 8.615, 6.999, 3.345 ppm, ^{13}C (NMR) δ 170.07, 140.65, 116.20, 110.69 ppm. Anal. Calc. for C 43.05, H 4.96. N 12.55. Found, C 42.79, H 4.70, N 12.39. X-ray crystal was obtained.

6.7 Synthesis of N,N'-bis-(1-pyridin-2-yl-ethylidene)-ethane-1,2-diamine and its cadmium complexes

6.7.1 Synthesis of N,N'-bis-(1-pyridin-2-yl-ethylidene)-ethane-1,2-diamine

The ligand N,N'-bis-(1-pyridin-2-yl-ethylidene)-ethane-1,2-diamine, was prepared by refluxing 0.9 g (15.0 mmol – 1mL) of ethylenediamine and 3.639 g (30.0 mmol) of 2-acetyl-pyridine in 30 mL of dry methanol for two hours, cool to RT and concentrated in a rotavap, the crude product recrystallized in hexane to obtain pale yellow microcrystalline solid. Mass of product 2.417, yield 61%, IR ν (cm^{-1}) 3304(w), 3052(w), 3006(w), 2917(m), 2896(m), 2830(w), 1665(w), 1641(s), 1630(s), 1584(s), 1562(s), 1465(s),

1435(s), 1357(s), 1298(s), 1278(s), 1242(m), 1182(w), 1153(w), 1106(m), 1090(m), 1044(m), 992(m), 964(m), 925(m), 897(m), 820(m), 789(vs), 768(vs), 741(s), 655(s), 621(s), 573(vs), 402(vs), IR was used to confirm the result with C=N vibration band that absorb near 1640 - 1690 cm^{-1}.[20, 23]

6.7.2 Synthesis of cadmium acetate complex of N,N'-bis-(1-pyridin-2-yl-ethylidene)-ethane-1,2-diamine dihydrate

A hot methanolic (dried with Mg and distilled) solution of 0.53 mg (0.2 mmol) of N,N'-bis-(1-pyridin-2-yl-ethylidene)-ethane-1,2-diamine and a methanolic solution of 53.2 mg (0.2 mmol) of $Cd(OAc)_2.2H_2O$ were both added to an aqueous solution of 26.8 mg (0.1 mmol) of disodium 2,1,3-benzothiadiazole-4,7-dicarboxylate with constant stirring for 30 minutes, the resulting solution was filtered hot and allow the filtrate to stand in the fume hood at room temperature for two days to yield light yellow plate-like crystals, mass 67 mg (63.4 % yield). Note; on analysis it was found that disodium 2,1,3-benzothiadiazole-4,7-dicarboxylate did not react, instead a complex of the ligand reacted solely with $Cd(OAC)_2.2H_2O$ which gave the reported result, very similar to some well-known cadmium complexes.[21,22,20] Melting point 277-280 °C, IR ν (cm^{-1}) 3355 (m), 3272 (m), 3064 (w), 2935 (w), 1654 (m), 1578 (s), 1552 (vs), 1475 (m), 1403 (vs), 1451 (m), 1310 (s), 1250 (m), 1217 (m), 1155 (m), 1047 (m), 1009 (m), 925 (m), 907 (w), 786 (s), 749 (m), 665 (s), 625 (s), 581 (s), 524 (s), 409 (s). ^{1}H NMR (300 MHz), $CDCl_3$ RT, TMS, δ 9.10, 7.90, 7.86, 7.52, 4.06, 2.49, 2.35 ppm, ^{13}C NMR 178.54, 163.69, 151.39, 149.67, 135.25, 126.32, 122.45, 50.14, 22.89, 15.92 ppm. Anal. Calc. for C 33.84, H 4.46, N 8.47. Found C 34. 42, H 4.34, N 8.41. Mass spectrum (m/z) 379.05 ($[C_{16}H_{18}CdN_4 + H]^+$,

22.75%), 439.072 ($[C_{18}H_{22}CdN_4O_2]^+$ 100%), 499.140 ($[C_{20}H_{24}CdN_4O_4 + H]^+$, 5.89%), 133.0768 ($[C_8H_9N_2]^+$, 46.36%). X-ray crystal was obtained.

6.7.3 Synthesis of cadmium acetate complex of N,N'-bis-(1-pyridin-2-yl-ethylidene)-ethane-1,2-diamine tetra hydrate

A hot solution of *N*,*N*'-bis[(1*E*)-1-(pyridin-2-yl)ethylidene]ethane-1,2-diamine containing 53.2 mg (0.2 mmol) in a wet methanol and a methanolic solution of 53.2 mg (0.2 mmol) of $Cd(OAc)_2.2H_2O$ was refluxed with constant stirring for 30 minutes, the resulting solution was filtered hot, the filtrate was kept in the fume hood at room temperature for a week before the crystal was harvested, to yield pale yellow plate-like crystals, mass 67 mg (59 % yield). Melting point 166–168 °C, FT-IR ν (cm^{-1}) 3376(m), 3251(m), 3067(m), 2935(w), 1653(m), 1580(s), 1553(s), 1475(m), 1422(s) 1408(s), 1380(s), 1310(s), 1252(m), 1218(m), 1134(m), 1102(m),1087(m), 1048(s), 936(m), 906(m), 786(s), 750(m), 668(s), 656(s), 624(vs), 581(s), 553(s), 408(s). ^{1}H NMR (300 MHz), $CDCl_3$ RT, TMS, δ 9.10 (ddd, *J* = 4.8, 1.0, Hz, 2H), 7.90 (td, *J* = 8.1, 7.8, 1.8 Hz, 2H) 7.86 (dt, 7.8, 1.0 Hz, 2H) , 7.52 (dt, 7.5, 4.8,1.2 Hz, 2H), 4.06, 2.49, 2.35, 1.75 ppm, ^{13}C NMR 178.54, 163.69, 151.39, 149.67, 135.25, 126.32, 122.45, 50.14, 22.89, 15.92 ppm. Anal. Calc. for C; 42.22, H; 5.67, N; 9.84. Found, C; 42.08, H; 4.87, N; 8.75. X-ray crystal was obtained.

6.7.4 Synthesis of cadmium chloride complex of N,N'-bis-(1-pyridin-2-yl-ethylidene)-ethane-1,2-diamine

53.27 mg (0.2 mmol) of *N*,*N*'-bis[(1*E*)-1-(pyridin-2-yl)ethylidene]ethane-1,2-diamine was dissolved in hot methanol and a hot methanol solution of $CdCl_2.2.5H_2O$ was added and refluxed for an hour and filtered, white residue was collected and light yellow filtrate

which was kept for 3 days, the solvent dried up without yielding a crystal to yellow deposit. I concluded that the $CdCl_2$ did not react because of its very low solubility or due to low boiling point of the solvent (methanol).

Then it was repeated with 53.27 mg (0.2 mmol) of *N*,*N*'-bis[(1*E*)-1-(pyridin-2-yl)ethylidene]ethane-1,2-diamine and a 45.7 mg (0.2 mmol) of $CdCl_2.2.5H_2O$ were measured into 30 mL of ethanol and refluxed for an hour and filtered, yellow filtrate and dirty white (brown) residue, the filtrate was kept in the fume hood, crystal grown after 2 days, but filtered on the 4 day to give white crystals, mass 117 mg (42 % yield), melting point 301-303 °C, FT-IR ν (cm^{-1}) 3299(m), 3252(m), 3166(w), 2959(w), 1655(m), 1610(w), 1589(m), 1472(w), 1464(m), 1438(m), 1476(m), 1354(m), 1307(s), 1274(m), 1254(m), 1166(m), 1140(w), 1103(m), 1066(s), 1009(m), 994(m), 970(m), 894(m), 843(m), 789(vs), 764(m), 748(m), 653(m), 630(m), 588(m), 577(m), 511(m), 441(w), 411(m), 388(m). ^{1}H NMR (300 MHz), DMSO, RT, δ 8.65 (d, *J* =4.8 Hz), 8.23 (dt, *J* = 1.2 Hz, 2H), 7.82 (m, *J* = 2.7 Hz), 3.63 (t, *J* = 5.4 Hz, 2H), 3.34 (s), 2.92 ppm. ^{13}C NMR 165.63, 149.30, 148.06, 140.43, 127.54, 124.22, 48.81, 15.91 ppm. Anal. Calc. for C; 31.19, H; 3.78, N; 12.12. X-ray crystal was obtained.

6.8 References

1. Wang, M.; Hu, X.; Liu, P.; Li, W.; Gong, X.; Huang, F.; Cao, Y. *J. Am. Chem. Soc.* **2011,** *133*, 9638-9641.
2. Smith, W. T., Jr.; Chen, W. Y. *J. Org. Chem.* **1962,** *27*, 676-8.
3. Heitkaemper, P. Preparation of 2,1,3-benzothiadiazoles from o-phenylenediamines. DE19652222A1, 1998.
4. Mikroyannidis, J. A.; Tsagkournos, D. V.; Sharma, S. S.; Vijay, Y. K.; Sharma, G. D. *J. Mater. Chem.* **2011,** *21*, 4679-4688.
5. Xu, S.; Liu, Y.; Li, J.; Wang, Y.; Cao, S. *Polym. Adv. Technol.* **2010,** *21*, 663-668.
6. Beecken, H.; Darstellung, E. V. *Chem. Ber.* **1967,** *100*, 2164-2169.
7. Nunn, A. J.; Ralph, J. T. *J. Chem. Soc.* **1965**, 6769-6777.
8. Misra, R.; Gautam, P.; Jadhav, T.; Mobin, S. M. *J. Org. Chem.* **2013,** *78*, 4940-4948.
9. Neto, B. A. D.; Correa, J. R.; Silva, R. G. *RSC Adv.* **2013,** *3*, 5291-5301.
10. Neto, B. A. D.; Lapis, A. A. M.; Da-Silva, E. N., Jr.; Dupont, J. *Eur. J. Org. Chem.* **2013,** *2013*, 228-255.
11. Sun, X.; Zhuang, X.; Ren, Y. *Adv. Mater. Res. (Durnten-Zurich, Switz.)* **2012,** *482-484*, 1221-1224.
12. Cozzolino, A. F.; Vargas-Baca, I.; Mansour, S.; Mahmoudkhani, A. H., *J. Am. Chem. Soc.* **2005,** *127*, 3184-3190.
13. Schieferstein, R. H.; Pilgram, K. *J. Agric. Food Chem.* **1975,** *23*, 392-5.
14. Vanelle, P.; Liegeois, C. T.; Meuche, J.; Maldonado, J.; Crozet, M. P. *Heterocycles* **1997,** *45*, 955-962.
15. Pilgram, K.; Skiles, R. D. *J. Heterocycl. Chem.* **1974,** *11*, 777-780; Garo, F.; Häner, R., *Eur. J. Org. Chem.* **2012,** *2012*, 2801-2808.
16. Koopman, H.; van Daalen, J. J.; Daams, J. *Weed Research* **1967,** *7*, 200-207.
17. Schrauzer, G. M.; Eichler, S. *Chemische Berichte* **1962,** *95*, 260-267.
18. Pilgram, K.; Skiles, R. D. *J. Heterocycl. Chem.* **1974,** *11*, 777-80.
19. Pesin, V. G.; D'Yachenko, E. K. Synthesis of 4-carboxy- or 4,7-dicarboxy-2,1,3-benzothiadiazole. SU176588, 1965.
20. Banerjee, S.; Lassahn, P. G.; Janiak, C.; Ghosh, A. *Polyhedron* **2005,** *24*, 2963-2971.
21. Banerjee, S.; Ghosh, A.; Wu, B.; Lassahn, P. G.; Janiak, C. *Polyhedron* **2005,** *24*, 593-599.
22. Ratilainen, J.; Airola, K.; Fröhlich, R.; Nieger, M.; Rissanen, K., *Polyhedron* **1999,** *18*, 2265-2273.
23 Pavia, D. L.; Lampman, G. M.; Kriz, G. S. Introduction to spectroscopy, Brooks-Cole, 2001, pp 77-78.